

## ABSTRACT

Title of Dissertation:                   COMPARATIVE PROTEOMICS STUDIES OF  
  SOLUBLE NUCLEAR PROTEINS OF DRUG  
  SUSCEPTIBLE AND RESISTANT HUMAN  
  BREAST CANCER MCF-7 CELLS

Zongming Fu, Doctor of Philosophy, 2004

Dissertation Directed By:           Professor Catherine Fenselau  
  Department of Chemistry and Biochemistry

Drug resistance is a major obstacle in cancer chemotherapy. Better understanding of the mechanisms of the drug resistance can help to improve clinical treatment and develop new drugs. Since most anticancer drugs target the nuclei of the cancer cells, differential expression of nuclear proteins may play crucial roles as cancer cells acquire drug resistance. Thus I have carried out a comparative proteomics research project to study differential expression of nuclear proteins in drug resistant human breast cancer MCF-7 cells. Two dimensional gel electrophoresis and stable isotope labeling by amino acids in cell culture are used to conduct the study. Protein identification is acquired by peptide fingerprinting or microsequencing. Relative quantitation of the proteins is derived from gel comparisons and from ratios of labeled and unlabeled peptide pairs. A drug susceptible MCF-7 cell line and four drug

resistant MCF-7 cell lines were examined. The drug resistant cell lines are resistant to different chemotherapeutic drugs and are well characterized. The known mechanisms of drug resistance can not satisfactorily answer how the drug resistance is conferred.

One hundred and twenty proteins have been identified from the nuclear protein mixture of MCF-7 cells, from which more than 90% are classically categorized as nuclear proteins. Fourteen proteins are found to be significantly less or more abundant ( $\cdot 2$  fold) in MCF-7 breast cancer cell lines resistant to etoposide, mitoxantrone, adriamycin in the presence of verapamil by both gel comparisons and isotope labeling. Abundances of cytoskeleton proteins, such as cytokeratin 8, cytokeratin 19, septin 2, and alpha tropomyosin, are altered in common across the three resistant cell lines. MCF-7 cell lines resistant to etoposide and mitoxantrone are more similar in protein abundance changes. Some of the proteins whose abundances are altered have also been reported to play important roles in resisting genotoxic stress in other normal and cancer cells. Their potential mechanistic contributions to drug resistance and implications for genetic regulation are discussed.

COMPARATIVE PROTEOMICS STUDIES OF SOLUBLE  
NUCLEAR PROTEINS OF DRUG SUSCEPTIBLE AND RESISTANT  
HUMAN BREAST CANCER MCF-7 CELLS

By

Zongming Fu

Dissertation submitted to the Faculty of the Graduate School of the  
University of Maryland, College Park in partial fulfillment  
of the requirements for the degree of  
Doctor of Philosophy  
2004

Advisory Committee:  
Dr. Catherine Fenselau, Chair  
Dr. Elisabeth Gantt  
Dr. Peter Gutierrez  
Dr. Douglas Julin  
Dr. Cheng Lee

© Copyright by

Zongming Fu

2004

## Dedication

This dissertation is dedicated to my father, Guoxin Fu,  
an elementary school teacher who worked hard to bring up his children.

## Acknowledgements

First of all, I would like to thank my advisor and mentor Dr. Catherine Fenselau for giving me the opportunity to study in her lab. I have learned a lot about how to be a scientist by working with her. I would also like to thank all her lab members, especially Dr. Yetrib Hathout, Kevin Shefcheck, and Andrei Chertov for their support and friendship.

I would like to thank Dr. Elisabeth Gantt, our former program director, especially for her encouragement and guidance when I started my graduate study. I would like to thank all my other committee members, Dr. Peter Guterieez, Dr. Douglas Julin, Dr. Cheng Lee, Dr. Wengxia Song, Dr. Eric Baehrecke, Dr. Ian Mather and Dr. Jonathan Arias for their invaluable time and advice.

I would like to thank Ms. Damali Martin for her help with my fluorescence microscope work.

Finally, I would like to thank my family for their support. My wife not only takes all responsibility of taking care of our kids on the weekends, she also provides computer support for my research. My brothers have been taking care of my mother for my share since I came to study in US. My in-laws visited and helped us look after our kids. My daughter and son allowed me to do some work on the weekends. My graduate study would have been impossible without their support.

# Table of Contents

Dedication .....	ii
Acknowledgements.....	iii
Table of Contents .....	iv
List of Tables .....	vi
List of Figures .....	vi
List of Figures .....	vii
Chapter 1: Overview .....	1
Chapter 2: Introduction .....	6
Breast cancer and chemotherapy .....	6
Drug resistance and its known mechanisms .....	7
Model organisms.....	11
Drug susceptible MCF-7 cells (control) .....	11
MCF-7 cells resistant to VP-16 (MCF-7/VP).....	11
MCF-7 cells resistant to mitoxantrone (MCF-7/MX).....	12
MCF-7 cells resistant to adriamycin in the presents of verapamil (MCF-7/AdrVp) .....	13
MCF-7 cells resistant to adriamycin (MCF-7/Adr) .....	14
Proteomics and comparative proteomics .....	19
Two-dimensional gel electrophoresis .....	20
Mass spectrometry .....	22
Protein identification.....	27
Stable isotope labeling by amino acids in cell culture.....	28
Chapter 3: Materials and methods .....	30
Materials .....	30
Cell culture.....	30
Isolation of nuclei and preparation of nuclear proteins .....	31
Protein assay .....	32
2-D gel electrophoresis .....	32
Analysis of gel images.....	33
In-gel tryptic digestion and peptide desalting.....	35
Mass spectrometry analysis and protein identification.....	36
Stable isotope labeling analysis .....	42

Chapter 4: Results .....	43
Nuclei isolation and protein extraction .....	43
2-D gel electrophoresis and protein identification .....	45
Evaluation of <sup>13</sup> C <sub>6</sub> -arginine and <sup>13</sup> C <sub>6</sub> -lysine metabolic labeling .....	51
Nuclear protein expression profile of MCF-7/VP cells .....	55
Nuclear protein expression profile of MCF-7/MX cells .....	65
Nuclear protein expression profile of MCF-7/AdrVp cells .....	70
Nuclear protein expression profile of MCF-7/Adr cells .....	76
Chapter 5: Discussion .....	80
2-D gel electrophoresis and protein identification .....	80
Densitometry vs. isotope labeling .....	80
Biological implications of abundance changes .....	81
Lower abundance of poly [ADP-ribose] polymerase (PARP)-1 .....	83
Lower abundance of cytoskeletal proteins .....	84
Higher abundance of nucleolin .....	85
Higher abundance of high mobility group protein-1(HMG-1) .....	86
Higher abundance of 40S ribosomal protein SA .....	87
Higher abundance of prohibitin .....	87
Higher abundance of mitotic checkpoint protein BUB 3 .....	88
Higher abundance of the 70 kDa glucose-regulated protein (GRP78) .....	89
Higher abundance of cyclophilin B .....	89
Summary and prospectus .....	90
References .....	92



## List of Tables

1. Proteins identified from nuclear extraction of control MCF-7 cell.....	47
2. Relative abundance of nuclear proteins from MCF-7/VP cells .....	62
3. Relative abundance of nuclear proteins from MCF-7/MX cells.....	69
4. Relative abundance of nuclear proteins from MCF-7/AdrVp cells.....	74
5. Nuclear proteins having abundance changes in MCF-7/Adr cells.....	79
6. Summary of abundance change in three drug resistant MCF-7 cell lines.....	82

.

## List of Figures

1. Schematic of gel images comparison to identify differentially expressed proteins.....	4
2. Schematic of metabolic labeling for analysis differentially expressed proteins by isotope ratios with massspectrometry .....	5
3. Known mechanisms of drug resistance related to nuclear proteins.....	10
4. Chemical structure of etoposide.....	15
5. Chemical structure of mitoxantrone.....	16
6. Chemical structure of adriamycin.....	17
7. Chemical structure of verapamil.....	18
8. Schematic of peptide fragmentation by low collision energy CID.....	26
9. Schematic of gel image comparison by densitometry.....	34
10. Schematic of protein identification by peptide mass fingerprinting.....	40
11. Schematic of protein identification by peptide microsequencing.....	41
12. Nuclei of control MCF-7 cells stained with propodium iodide.....	44
13. Annotated 2-D gel map of nuclear proteins of control MCF-7 cells.....	46
14. 2-D gel map of nuclear proteins from control MCF-7 cells in regular media.....	52
15. 2-D gel map of nuclear proteins from control MCF-7 cells in $^{13}\text{C}_6$ - arginine and $^{13}\text{C}_6$ -lysine media.....	53
16. Evaluation of isotope $^{13}\text{C}_6$ incorporation in nucleophosmin.....	54
17. 2-D gel map of nuclear proteins of MCF-7/VP cells.....	56
18. 2-D gel map of nuclear proteins MCF-7/VP cells and labeled control MCF-7 cells.....	57
19. Densitometric comparison of 2-D gels of nuclear proteins: control vs. MCF-7/VP cells.....	58
20. Nucleophosmin has no change in abundance in MCF-7/VP cells.....	59

21. Nucleolin has a higher abundance in MCF-7/VP cells.....	60
22. Septin 2 has a lower abundance in MCF-7/VP cells.....	61
23. 2-D gel map of nuclear proteins of MCF-7/MX cells.....	66
24. 2-D gel map of nuclear proteins from MCF-7/MX cells and isotope labeled control MCF-7 cell mixture.....	67
25. Densitometric comparison of 2-D gels of nuclear proteins: control vs. MCF-7/MX cells.....	68
26. 2-D gel map of nuclear proteins from MCF-7/AdrVp cells.....	71
27. 2-D gel map of nuclear proteins from MCF-7/AdrVp cells and isotope labeled control MCF-7 cell mixture.....	72
28. Densitometric comparison of 2-D gels of nuclear proteins: control vs. MCF- 7/AdrVp cells.....	73
29. 2-D gel map of nuclear proteins from MCF-7/Adr cells.....	77
30. Densitometric comparison of 2-D gels of nuclear proteins: control vs. MCF-7/Adr cells.....	78

## **Chapter 1: Overview**

Chemotherapy is widely used to treat cancers. Drug resistance is a major cause of chemotherapy failure. It is important to understand the mechanisms of the drug resistance to improve clinical treatments. Many chemotherapy drugs target nuclear proteins in cancer cells. Their ultimate objective is to selectively kill the cancer cells while minimizing the damage to healthy cells. Nuclear proteins may play important roles in the development of drug resistance in cancer cells. Identification and characterization of differential abundance of nuclear proteins in association with drug resistance may provide clues for better understanding of the mechanisms of the acquired drug resistance in cancer cells.

The primary objective of this research is to contribute to the understanding of the mechanisms of the acquired drug resistance conferred by nuclear proteins. Our specific aims are 1) Develop and evaluate methods to isolate nuclei and extract nuclear proteins of MCF-7 cells; 2) Compare expression profiles of nuclear proteins of drug-susceptible and drug-resistant MCF-7 cells; 3) Identify proteins whose expressions are up or down regulated in drug-resistant MCF-7 breast cancer cells; 4) According to the functions of the proteins whose abundances are changed, consider possible mechanisms of drug resistance.

Two-dimension gel electrophoresis is used to provide comparative proteomics studies. Nuclei are isolated and nuclear proteins are extracted from cultured drug susceptible and resistant MCF-7 cells, respectively. The nuclear proteins are then

subjected to 2-D gel electrophoresis and the gels are visualized. Parallel gels are analyzed by Compugen software and protein expression levels are compared according to the densitometry of the protein spots in the gels. The spots are then cut out and digested by trypsin. The digestion products are then analyzed by matrix-assisted laser desorption/ionization (MALDI) and electrospray mass spectrometers. Protein identifications are obtained using protein peptide fingerprinting or microsequencing and bioinformatics. An illustration of the strategy is depicted in Figure 1.

In addition, isotope labeling is also used to confirm the expression changes detected by gel comparison.  $C^{13}$  - Labeled lysine and arginine are introduced into the media in which drug susceptible cells are cultured. The labeled cells are mixed with drug resistant cells cultured in non-labeled media. Then nuclei are isolated and nuclear proteins are extracted. The protein mixture is subjected to 2-D gel electrophoresis and mass spectrometry analysis. Changes in protein abundance are determined by isotope ratios of labeled and unlabeled counterpart peptides. An illustration of the strategy of isotope labeling is depicted in Figure 2.

Chapter 2 introduces the background and significance of this research. Chemotherapy and acquired drug resistance are briefly introduced. Known mechanisms of drug resistance are summarized. Also I will discuss the characterization of the model organisms and the advantages of proteomics approach. Application of Mass spectrometry is briefly introduced.

Chapter 3 presents materials and methods. Methods are described in detail. The methods include cell culture, nuclei isolation, protein extraction, 2-D gel electrophoresis, gel image comparison, MALDI mass spectrometry, electrospray mass spectrometry,

tandem mass spectrometry, protein identification and determination of peptide isotope ratio.

Chapter 4 gives results of the experiments. It shows a 2-D gel map of control MCF-7 nuclear proteins and the proteins identified. Differentially expressed proteins detected by both strategies in four drug resistant MCF-7 cell lines are summarized.

Chapter 5 mainly discusses biological implications of the changes found. For example, the up-regulation of nucleolin and down-regulation of PARP 1 are probably involved in repression of apoptosis, their potential roles in drug resistance are discussed. The pros and cons of both strategies are illustrated. Finally, a future perspective for this research is also presented.

## Scheme 1: Densitometric Comparison of gel images

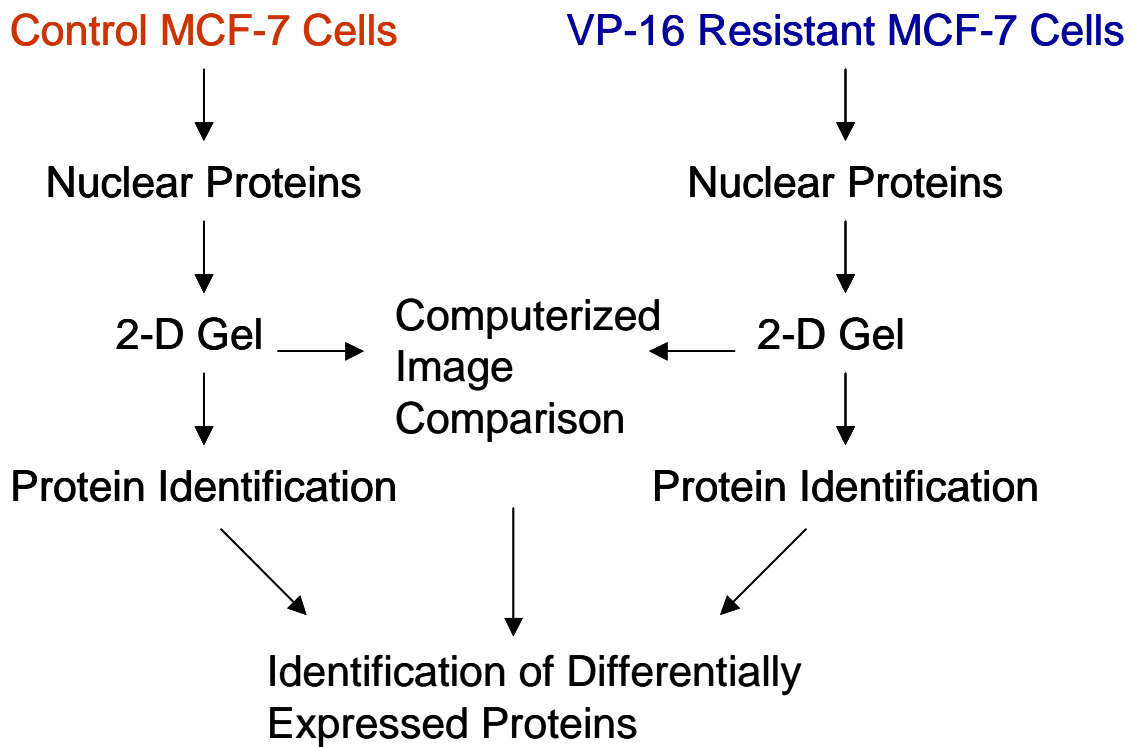


Figure1: Schematic of gel images comparison to identify differentially expressed proteins.

## Scheme 2: Metabolic Stable Isotope Labeling

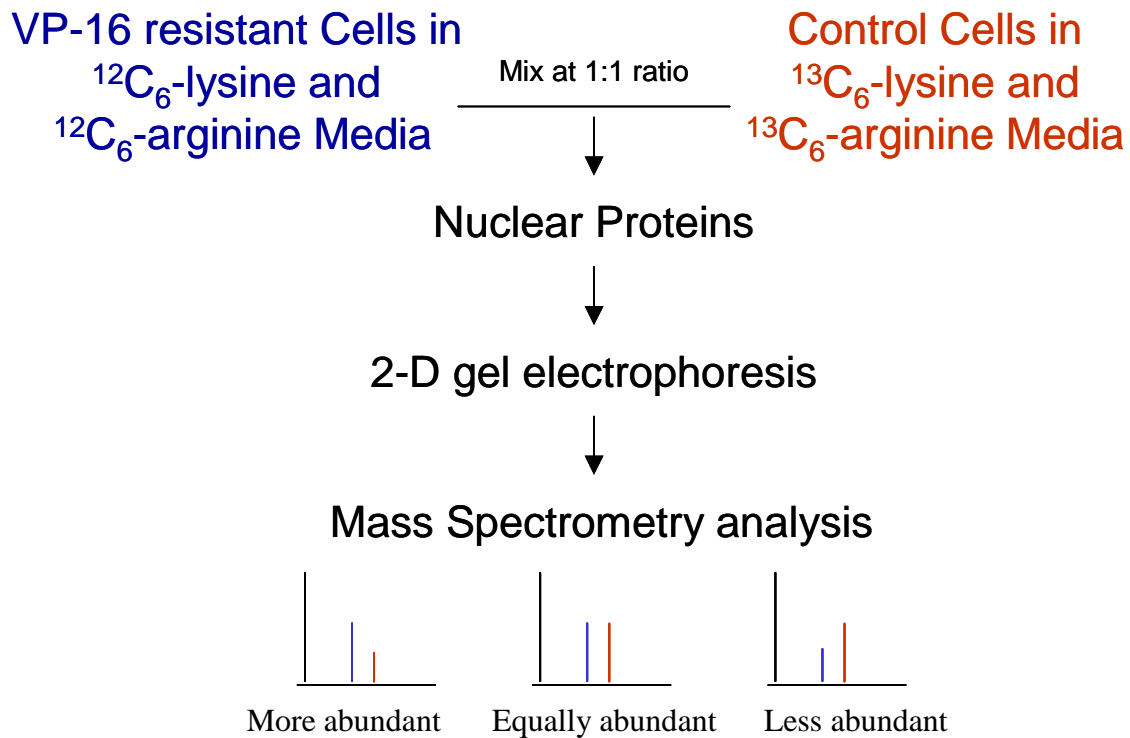


Figure 2: Schematic of metabolic labeling for analysis of differentially expressed proteins with mass spectrometry.



## **Chapter 2: Introduction**

### **Breast cancer and chemotherapy**

Breast cancer is the most common type of cancer among women in the US and many other countries. According to the American cancer society, there were about 212,600 new cases of breast cancer diagnosed in women in the US alone in 2003. Approximately 40,000 of these cases resulted in death (1). Many breast cancer deaths could be avoided by early detection and improved treatment.

Chemotherapy is the treatment of cancer with anticancer drugs that can kill cancer cells. It is sometimes the first or even the only choice to treat many cancers. More often, however, it is used in addition to surgery, radiation therapy and immunotherapy.

Chemotherapy differs from surgery and radiation in that it is a systemic treatment, which means that the drugs can travel throughout the whole body or system instead of being confined or localized to one area or organ such as breast, lung, or brain. This is very important because chemotherapy can reach cancer cells that may have spread to other parts of the body. In most cases, anticancer drugs are often given in combination. The drugs are often administered as a pill or by injection into a vein (IV). Either way, the drugs enter the bloodstream and travel throughout the body. Since anticancer drugs are also toxic to healthy cells, their dose that can be administered to patients is limited (2).

More than 50 chemotherapeutic drugs are available to treat cancers now, and many more are being developed and tested in clinical trials. Most chemotherapeutic drugs interfere with the ability of cells to grow or multiply. Based on how they work,

chemotherapeutic drugs are classified as the following main types: covalent DNA binding drugs, antimetabolites, noncovalent DNA binding drugs, inhibitors of chromatin function, and drugs affecting endocrine function. They often target DNA and act in the nuclei of the cancer cells. Many anticancer drugs have proven to be highly effective chemotherapeutic agents for treating a variety of types of cancers, including breast cancer. However, eventually they all stimulate acquired drug resistance (3-6).

### **Drug resistance and its known mechanisms**

Drug resistance occurs when a particular drug does not affect the cancer cells. There are primarily two types of resistance: intrinsic and acquired resistance. Intrinsic resistance occurs when the drug does not affect cells the very first time they are treated with it. Acquired resistance occurs after a period of anticancer drug treatment. A few cells that are not responsive to the drug treatment survive and multiply until most of the cell population becomes insensitive to the drug. Resistance occurs not only to the drug in use, but cross-resistance also may be acquired to other drugs, especially to the drugs having structural analogs or similar mechanisms of action (6).

Drug resistance is a major obstacle in cancer chemotherapy. It accounts for the failure of chemotherapy to cure the majority of cancer patients and has been described as the single most common reason for discontinuation of a drug. It is important to understand the mechanisms of the drug resistance to improve clinical treatment and develop new drugs. Efforts have been made to study the mechanisms over the past three decades. The main known mechanisms at the molecular and cellular levels include increased drug efflux (7-11), decreased drug uptake (10-11), enhanced intracellular detoxification (12-15), up-regulation of DNA repair system (15-17), inadequate drug activation (13), and

blocking of programmed cell death (apoptosis) (19-20). P-glycoprotein is the most intensively studied single protein involved in drug resistance. It is a membrane protein encoded by the MDR I gene, and its overexpression is believed to be mainly responsible for multiple drug resistance (MDR). The role of P-glycoprotein is to activate an efflux pump that allows less accumulation of chemotherapy drugs in cancer cells (7). Its discovery has led to development of strategies to overcome drug resistance caused by its effect. New drugs (a third generation of P-glycoprotein inhibitors) continue to be developed based on this finding (21). However, the mechanisms of drug resistance are not well understood. It is widely accepted that the mechanisms are multifactorial and no single protein expression is solely responsible for acquired drug resistance (22-27). To overcome drug resistance, different strategies need to be adopted for drug resistance conferred by different mechanisms (28-32). Better understanding of the mechanisms is necessary to achieve the goals of overcoming drug resistance and improving chemotherapy.

The availability of rough human genome information and the recent development of mass spectrometry have greatly facilitated the proteomics approach as a powerful tool to study drug resistance in human cells (33-38). In this study, I have compared nuclear proteins of drug susceptible and resistant human breast cancer MCF-7 cells using proteomics techniques. The nucleus, which is the largest organelle in the MCF-7 cell, is the control center of the cell. Its many important functions, such as RNA transcription and processing, DNA replication and repair, are closely related to cell growth and death (39-40). Most chemotherapy drugs, such as alkylating agents, cross-linking agents, intercalating agents and topoisomerase inhibitors, target DNA or enzymes closely related

to DNA, and therefore act in the nucleus of the cancer cell (2). Nuclear proteins may play important roles in cancer cells to confer drug resistance. Changes of expression levels of nuclear proteins may well reveal clues about how MCF-7 cells acquire drug resistance (41-42). Figure 3 shows a scheme of known mechanisms of drug resistance related to nuclear proteins. Inhibition of apoptosis and enhancement of DNA repair have been the focuses of the mechanisms of drug resistance related to nuclear proteins. Change of drug targets, such as mutation of topoisomerase I, has also been reported (22). Recently, defect of DNA repair has been linked to drug resistance in *Plasmodium falciparum* (43). This may also apply to drug resistance in cancer cells. The defect of DNA repair may make the cancer cells more tolerable to mutations, which may cause drug resistance.

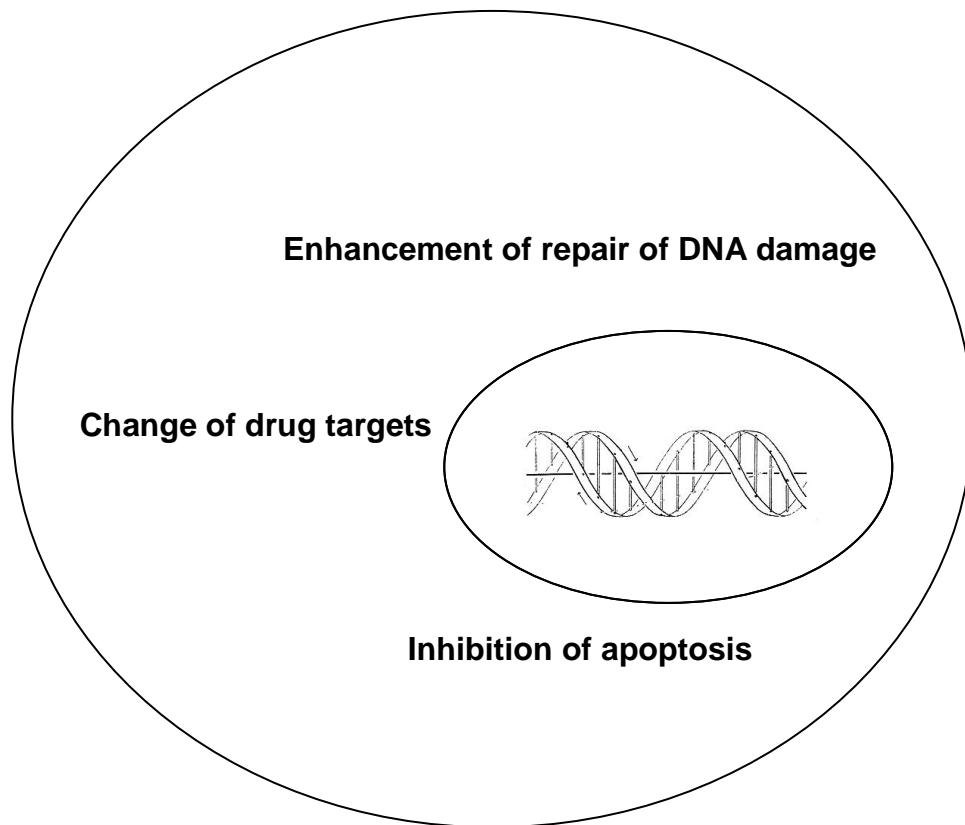


Figure 3: Known mechanisms of drug resistance related to nuclear proteins. Adopted from Dr. Michael M. Gottesman, *Annua. Rev. Med.* 2002. 53:615-27.

## **Model organisms**

### **Drug susceptible MCF-7 cells (control)**

MCF-7 cell lines are used in present research for analysis of their nuclear proteins. Drug- susceptible MCF-7 cell line (MCF-7/WT) is used as the control. Because of its stability, the cell line has been widely used to study the effects of anticancer drugs since it was established from a pleural effusion of patient with metastatic mammary carcinoma in 1973. It tests positive for cytoplasmic estrogen receptors and is capable of forming domes (44). Four drug-resistant MCF-7 cell lines were studied are all derived from this parental cell line.

### **MCF-7 cells resistant to VP-16 (MCF-7/VP)**

The first drug resistant cell line is VP-16 resistant MCF-7 cell line (MCF-7/VP), which was developed in Dr. Ken Cowan's laboratory in NIH by selection during culture in increasing concentrations etoposide. It is reported to be 28-fold resistant to etoposide (VP-16), 21-fold resistant to teniposide and 9-fold resistant to adriamycin (45). The chemical structure of etoposide is shown in Figure 4. Etoposide is clinically used for treatments of small cell lung cell cancer and refractory testicular tumors. Its actions involve locking topoisomerase II in a cleavable complex and activating a Ca/Mg endonuclease to trigger apoptosis. Schneider et al characterized resistance in this VP-16 resistant cell line as multifactorial (45). No overexpression of P-glycoprotein was detected in this cell line. The levels of topoisomerase II and its sequence were similar in both cell lines. However, topoisomeras II from VP-16 resistant cells appeared to be 7-fold less sensitive to drug- induced cleavable complex formation in whole cells and 3-

fold less sensitive in the nuclear extract, compared to control MCF-7 cells. Reduction in intracellular drug concentration as a consequence of overexpression of the multiple drug resistance related protein (MRP) was suggested as a cause of the resistance but the analysis was not conclusive (45-46). This indicates that other proteins might contribute to the insensitivity to the drug in the VP-16 resistant cells. In addition, a study by Marion Gehrman in our lab found no significant expression changes of cytoplasmic proteins in VP-16 resistant cells (unpublished data). These observations led us to focus on the nucleus and other organelles.

### **MCF-7 cells resistant to mitoxantrone (MCF-7/MX)**

A second drug resistant MCF-7 cell line (MCF-7/MX) was also provided by Dr. Ken Cowan. It was isolated by serial passage of the parental control MCF-7 cells in stepwise increasing concentrations of the anthracenedione mitoxantrone. MCF-7/MX cells are approximately 4000-fold resistant to the cytotoxic effects of mitoxantrone, and 50 to 180-fold cross-resistant to analogs of camptothecin, a known topoisomerase I poison. They are also approximately 10-fold cross-resistant to adriamycin and etoposide (47-48). Intracellular accumulation of radio-labeled mitoxantrone was markedly reduced in MCF-7/MX cells relative to that in control MCF-7 cells. This decrease in intracellular drug accumulation can be reversed by sodium azide and 2, 4-dinitrophenol, suggesting an energy-dependent process associated with enhanced drug efflux (49). Mitoxantrone resistance in MCF-7 cells is not mediated by MDRI, MRP. Functional assays and western blot analysis for topoisomerase I and topoisomerase II have revealed no difference in activity or protein levels of topoisomerase I and topoisomerase II in MCF-7/MX cells (46, 48). Recently, A 95 kDa multidrug resistant transporter, encoded by the

mitoxantrone resistance gene, MXR, also termed breast cancer resistant protein (BCRP), was found overexpressed in the cell line (8, 50-55). Mitoxantrone is most commonly used in treatment of leukemia, lymphomas, breast cancer, and ovarian cancer. Figure 5 shows the chemical structure of mitoxantrone. Its action involves inhibiting the strand passing activity of topoisomerase II (47). The mechanisms of drug resistance in this cell line are also considered multifactorial. Chromosome transfer experiments show that at least one genetic event is dominant (59).

### **MCF-7 cells resistant to adriamycin in the presents of verapamil (MCF-7/AdrVp)**

The third drug resistant MCF-7 cell line (MCF-7/AdrVp) was provided by Dr. Douglas Ross from The University of Maryland Medical School. It was isolated by selecting the viable human breast cancer MCF-7 cells with incremental increases of adriamycin (Adr) in the presence of verapamil. It is 900-fold resistant to Adr, does not overexpress Pgp, and does not exhibit decreased accumulation of Adr because of the presence of verapamil (54). BCRP was also found overexpressed in the cell line. It appears to play a major role in the multidrug resistance. However, BCRP overexpressing transfectant MCF-7 cells and MCF-7/AdrVp cells differ in that the degree of drug resistance in the latter is great than in the transfected cells. It is possible that expression of other proteins is required (55-61). Figure 6 shows the chemical structure of adriamycin (Adr). Its generic name is doxorubicin. Adriamycin is a glycoside isolated from culture of *Streptomyces peucetius var. caesius*. It is an anthracycline antibiotic with cytotoxic actions. Several mechanisms have been proposed to explain for the anticancer actions of adriamycin, including free radicals mediated cytotoxicity through redox cycling of Adr semiquinone radical, interaction of DNA, stabilization of topoisomerase



II-DNA complex and inhibition of RNA and protein synthesis. It is well accepted that its ability of generating free radicals is of dominance in its anticancer actions. It is clinically used to treat hematological malignancies such as acute leukemias and lymphomas, and is also used to treat solid tumors including breast, lung, and thyroid cancer. Its clinical use is limited by its cardiotoxicity(54). Verapamil is a calcium channel blocker, which acts to overcome Pgp-mediated drug resistance as a competitive inhibitor of drug binding and efflux (54). Its chemical structure is shown in Figure 7.

### **MCF-7 cells resistant to adriamycin (MCF-7/Adr)**

The fourth drug resistant cell line MCF-7/Adr was first selected in stepwise increasing concentration of adriamycin in 1986 (62). It has been used as a model to study drug resistance in cancer cells. It is 192-fold resistant to adriamycin and has distinctive biochemical characteristics (63-65). A DNA fingerprint study has indicated that this cell line is far apart from the control cell line (64). It has a full-length caspase-3 gene which is missing in control MCF-7 cell line (66). Questions were raised about the identity and origin of the cell line recently (66-68). Study in our lab has shown it has a dramatically different expression profile of cytosolic proteins from that of control MCF-7, MCF-7/VP and MCF-7/AdrVp cell lines (69). This suggested that it was most likely that its expression profile of nuclear proteins was also distinctive. It was used as a possible positive control to analyze changes in abundance of the nuclear proteins. Characterization of its nuclear protein expression profile can also help clarify its identity and origin.

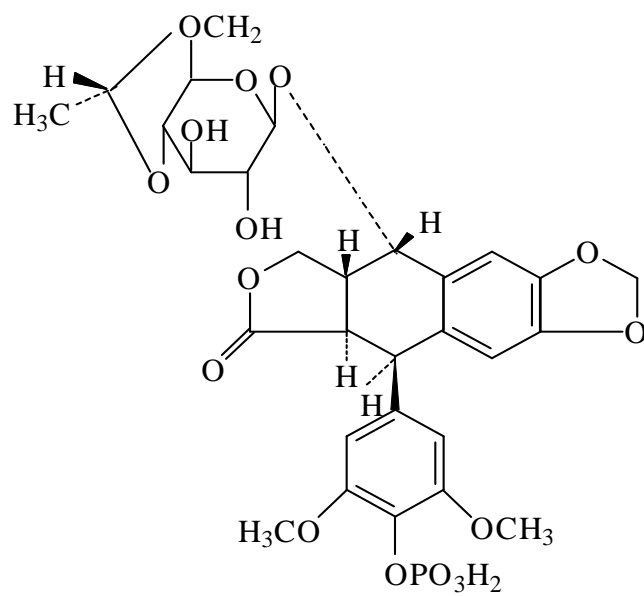


Figure 4: Chemical structure of etoposide

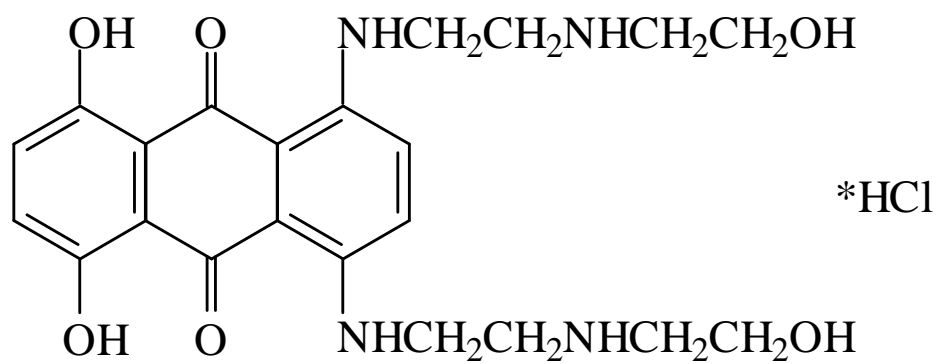


Figure 5: Chemical structure of mitoxantrone.

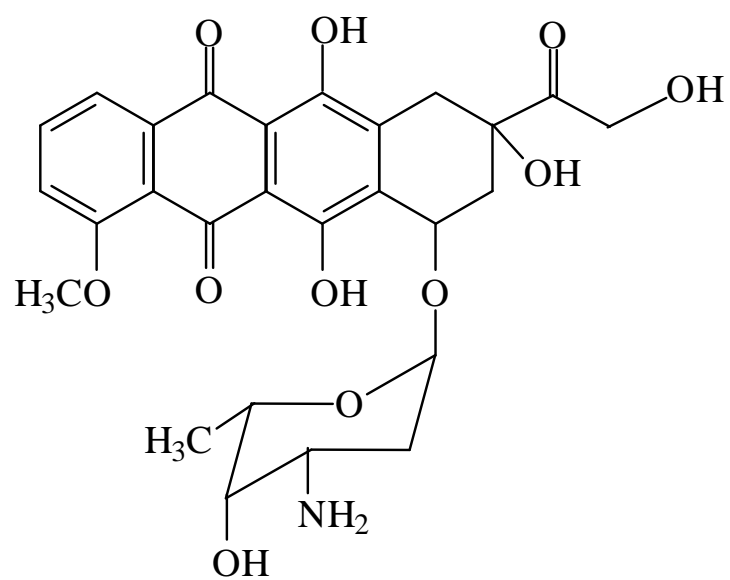


Figure 6: Chemical structure of adriamycin.

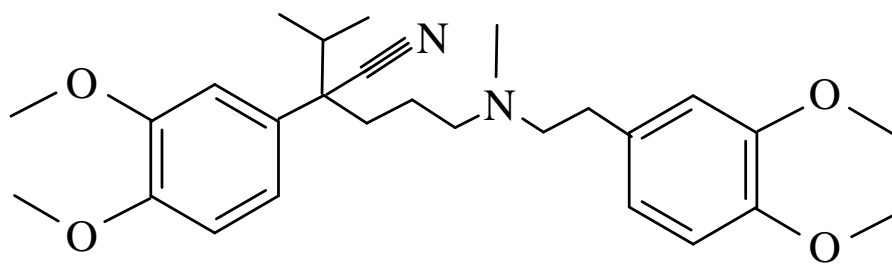


Figure 7: Chemical structure of verapamil.

### **Proteomics and comparative proteomics**

Proteome refers to the entire complement of proteins of a certain type of cell or organism. The term “proteome” was first coined in 1995, as an equivalent to genome (70-71). Proteomics is generally defined as the systematic analysis of complex protein mixtures under certain conditions. Actually, it dates back to the mid 70’s of the last century with the independent introduction of 2-D gel electrophoresis, which separates proteins first by their isoelectric points and then by their sizes. In the beginning, about 300 proteins could be separated by 2-D gel electrophoresis (72-73). Now, with refined techniques, more than 10,000 protein spots can be separated with high reproducibility (74-75). This has the potential to reveal almost all proteins of a specific cell type, its proteome.

The proteomics approach, which directly measures protein expressions, is more meaningful to study biological functions of proteins than the genomic approach (76). Unlike the genome, which is static, proteome is highly dynamic. The genome indicates all the proteins that may be expressed, but not necessarily the proteins that are expressed (77). Proteins undergo posttranslational processing and modification, such as phosphorylation, acetylation, ubiquitination, or glycosylation, which strongly influence their functions but can not be deduced from the DNA or RNA sequence. These modifications may be detected by proteomics techniques (78-80). It has been demonstrated that RNA levels do not always correspond to protein expression levels (81-83). The human genome has about 30,000-40,000 genes, however, the number of proteins

is much larger (33-34). Traditional biological research approaches, which usually study one or a few proteins at a time, can not deal well with complicated mixtures. In the nucleus of MCF-7 cells, there are several thousands of proteins, many of which may be related to drug resistance (37-38). A proteomics approach is the best choice to study it.

Comparative Proteomics analyzes relative protein expression in two or more samples (83-84). The samples are taken from organisms in the control and altered states. In this research, 2-D gel electrophoresis is used in combination with mass spectrometry to identify and analyze differentially expressed nuclear proteins in drug resistant MCF-7 cells. Protein identifications are acquired by peptide mass mapping and sequence tagging. Protein differential expression is determined by contrasting the position and density of spots in two-dimension gels. Stable isotope metabolic labeling is also used to determine protein differential expression, according to the isotope ratios of the labeled and unlabeled peptide pairs from drug susceptible and resistant MCF-7 cells. The results from both gel comparison and metabolic labeling are compared and evaluated.

### **Two-dimensional gel electrophoresis**

Two-dimensional Gel electrophoresis is a combination of two types of gel electrophoresis: isoelectric focusing (IEF) and sodium dodecyl sulfate- polyacrylamide gel electrophoresis (SDS-PAGE) (71-72). IEF separates proteins by their isoelectric points using a pH gradient across a high electric potential. The isoelectric point of a protein is a characteristic pH at which its net charge is zero. The protein sample is dissolved in a small volume of rehydration buffer containing nonionic detergent, DTT and denaturing reagent urea. The rehydration buffer solubilizes, denatures and dissociates all the peptide chains but leave the intrinsic charge of the proteins unchanged. In an

electric field, the protein will move to the position of its isoelectric point in the pH gradient and become immobilized. A pH gradient can be formed with a mixture of ampholytes, which are aliphatic polyaminopolycarboxylic acids with different pIs. Immobilized pH gradient (IPG) gel strips are most commonly used for isoelectric focusing now. IPG gel strips are made from acrylamide derivatives that have different acidic and basic side chains on them. Creating different mixtures of these acrylamide derivatives and polymerizing them can make polyacrylamide gels with different immobilized pH gradient ranges and with resolution of up to 0.01 pI units. They are very reproducible and commercially available (86-89).

The second dimension in 2-D gel electrophoresis is SDS-PAGE. In this step the IPG gel strip containing the separated proteins is subjected to electrophoresis again, but in a direction at right angle to that used in the first dimension. This method separates proteins according to their molecular weights. SDS is a detergent used to denature proteins and eliminate positive charges on proteins. The first dimension gel strips are soaked in SDS and then placed on one edge of a SDS polyacrylamide gel slab, through which each protein migrates to form a discrete spot when a voltage is added (90-93).

As a result, 2-D gel electrophoresis can provide protein mixture as arrays of spots on a polyacrylamide gel. The spots can be visualized by several different gel staining methods. These methods include silver staining, fluorescent staining, and Coomassie blue staining, which is used in this study. Coomassie blue is an organic dye that binds to proteins. Proteins will be stained in proportion to the amount of their basic and aromatic amino acids and the amount of sample in the spot.



Protein quantitation can be determined based on density of the reagents binding to the proteins. Manual or computerized inspection can compare protein differential expressions in parallel gels. Computer software can make digitized images of the gel arrays and evaluate them.

### **Mass spectrometry**

A mass spectrometer is an instrument that measures the mass-to-charge ratio of the ions formed from the sample molecules. It can be described in five parts: inlet, ion source, mass analyzer, detector, and recorder. The inlet is used to introduce sample from room pressure into the ion source under vacuum. The ion source converts the sample molecules into sample ions. The mass analyzer controls the movement of the sample ions and allows them to be separated according to their masses. The detector detects the arrival of mass-separated ions and converts them into a stronger electric signal. The recorder creates the mass spectrum. Different combinations of ion source, mass analyzer and detector can make different types of mass spectrometers (94).

Mass spectrometry has been a powerful analytical technique to identify, quantify compounds and elucidate their structures and chemical properties since it was invented (94-95). However, its application to macromolecules was limited before the two breakthroughs were made in ionization methods: matrix-assisted laser desorption/ionization (MALDI) and electrospray ionization (ESI) (97-99). These methods solved the technical difficulty of generating ions from nonvolatile macromolecules such as proteins or peptides without significant fragmentation for further analysis. They were referred to as “soft” ionization methods because fragmentation is minimal and some noncovalent interactions may be preserved during the ionization process under specific

conditions. These methods rapidly gained popularity and catalyzed the revolution of protein analysis.

MALDI was first developed by two groups, Karas and Hillenkamp from US and Tanaka from Japan in 1987(97-98). This ionization technique is performed by cocrystalizing the sample in a chromaphoric organic matrix and irradiating analyte-matrix crystals with a pulsed UV laser. The matrix has a strong absorbance at the laser wavelength. When the laser strikes the crystals on the target surface, the crystals were electronically exploded. Photo-excited matrix molecules undergo reaction with the analyte in the plume. As a result, the analyte molecules become ionized predominantly by simple protonation, leading to the formation of  $[M+H]^+$  type ions. Sometimes multiply charged ions, dimers and trimers can also be formed. Negative ions are formed from reactions involving deprotonation of the analyte by the matrix to form  $[M-H]^-$  and from interactions with photoelectrons to form the  $[M]^-$  radical molecular ions. The ionized analyte is then pulsed into the mass spectrometer for analysis. MALDI has been used in conjunction with different kinds of mass spectrometers; such as Fourier transform ion cyclotron resonance (FT-ICR), quadrupole ion trap, and time of flight (TOF) mass spectrometers (100). MALDI-TOF is commonly used for protein and peptide analyses (101-102).

ESI was developed into modern-day ionization technique by Fenn in 1980s (99). ESI is performed by spraying the conducting sample solution across a high potential difference from a needle into an orifice in the interface. The sample solution forms a finely charged mist of analyte and solvent and then heat and gas flows are used to desolvate the ions in the sample solution to yield highly charged analyte ions. This

method can produce multiply charged ions with the number of charges tending to increase as the molecular weight increases. Analytes with a mass in excess of the mass range of the mass spectrometry can still be detected since mass spectrometers determine the mass of the sample as a function of mass-to-charge ratio. This method can also be readily coupled to HPLC and other liquid separation techniques. A refined version of electrospray, nanospray, was developed in 1996 (103). It actually is a miniaturized electrospray, which uses a needle with much smaller diameter than that used in electrospray and nL/min flow rates. Nanospray is more sensitive than electrospray since the process is concentration dependent. ESI has been successfully used with a variety of mass spectrometers, including triple quadrupole, quadrupole ion trap and quadrupole time of flight (104).

Tandem mass spectrometry (MSMS) has become available in recent years for the analysis of biological samples (105). A tandem mass spectrometer can be regarded as two mass spectrometers in series connected by a chamber that can be used to activate fragmentation of ions. This chamber is known as a collision cell. A sample can be scanned and sorted in the first mass spectrometer, and then a selected ion of a molecule can be broken into pieces of product ions, which can be analyzed in the second mass spectrometer. For tandem mass spectrometers in conjunction with ESI, fragment ion spectra are generated by collision-induced dissociation (CID). The peptide ion of interest is selected and fragmented in a collision cell and the fragment ion spectra are recorded. Tandem mass spectra generated by the fragment of peptide ions by low collision energy CID are dominantly fragment ions resulting from cleavage at the amide bonds. A schematic of peptide fragmentation by low collision energy CID is shown in Figure 8. If

the positive charge in association with the parent peptide remains on the amino-terminal side of the peptide fragment, it is termed a *b* ion. If the charge remains on the carboxyl-terminal side of the broken amide bond, it is termed a *y* ion. The mass differences between *b* ion series or *y* ion series correspond to the masses of amino acids. A partial or whole amino acid sequence tag of the peptide can be obtained from the mass difference. According to the spectra collected from the parent and product ions, structure information may be revealed about the precursor molecule (105-107).

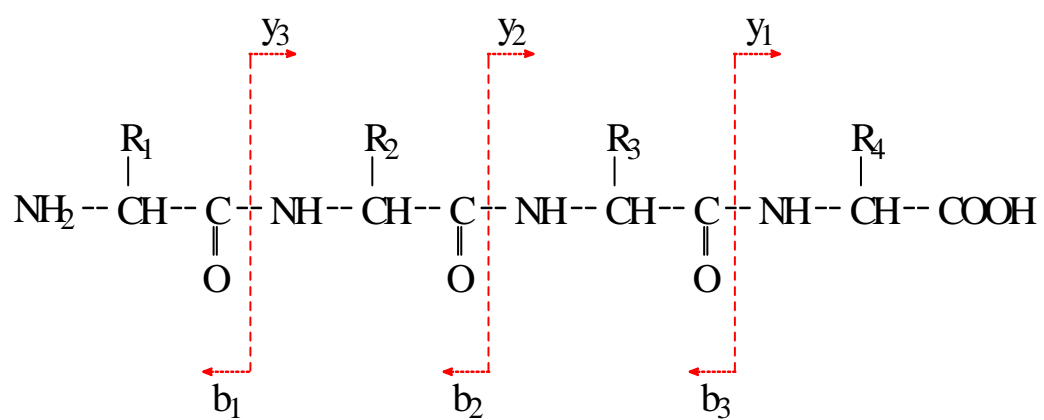


Figure 8: Schematic of peptide fragmentation by low collision energy CID.

### **Protein identification**

Traditionally, proteins have been sequenced and identified most frequently by Edman degradation of the proteins or their peptide fragments. The partial sequences could be used for generation of probes of the gene coding for the protein from a gene library, and sometimes were used to assemble the complete protein sequence from overlapping fragments. After the sequencing of human genome and other genomes, the increasing sequence database made it possible to use short sequences of peptides to identify proteins. This was done by correlating experimental information with sequences in the database using search algorithms. Mass spectrometry was suitable to provide the required data (106).

There are two main strategies to identify proteins by mass spectrometry: peptide mass mapping and microsequencing. Peptide mass mapping is also referred to as peptide mass fingerprinting. Its idea was first introduced by Cleveland in 1977 et al. and was incorporated with mass spectrometry in 1993 (108-109). The principle is that proteins of different amino acid sequence will generate different mixtures of proteolytic peptides, whose masses constitute mass fingerprints unique for specific proteins. A mass spectrum of a mixture of peptides can be generated following site-specific proteolytic cleavage of a protein. Then the masses of the peptides are used for database searching. Each protein in database is theoretically “digested” to produce a list of peptide masses that is compared to the list of experimental masses. A search algorithm is used to compare the set of experimental peptide masses against the sets of theoretical masses in the database. If certain criteria are met to produce qualified matches, a protein can be identified. Many variables such as pI, molecular weight, and post-translational modifications can be taken

into account to help the identification. Peptide mass mapping depends on the correlation of several peptide masses from the protein with corresponding masses calculated from the database. To get a confident identification, enough peptide masses are needed (110-112). This method cannot be used to identify mixtures of proteins. It does not work well with small proteins either, since small proteins may not yield enough peptides for analysis.

The other strategy to identify proteins by mass spectrometry is microsequencing. It depends on tandem mass spectrometry to generate spectra that contain sequence information. This sequence information, in combination with the peptide mass, and the masses before and after the tag, is used to search a database to identify the precursor protein of the peptide (105-107). Other information on the protein, such as post-translational modification, molecular weight, pI etc., can be taken into account of the search algorithm (112-113). A high-quality sequence tag can easily identify the protein confidently. The more sequence tags obtained for a protein, the more confident the identification is. This method can be used to identify a single protein that cannot be identified by peptide mapping, and can also be used to analyze peptides mixture of different proteins.

### **Stable isotope labeling by amino acids in cell culture**

For comparative proteomics, stable isotope labeling by amino acids in cell culture, has become a popular technique to identify differentially expressed proteins. Using metabolic labeling, two sets of cells are grown in amino acid-deficient culture media, supplemented with, for example,  $^{12}\text{C}_6$ - or  $^{13}\text{C}_6$ -labeled amino acids. The proteins in the two sets of cells contain either the light or the heavy isotopes. The two sets of cells can then be mixed in equal ratios and subjected to protein isolation and further analysis. The

mass difference between unlabeled and labeled proteins is expected to have no effect on the sample processing. Upon digestion of the proteins, unlabeled and labeled peptides have the same chemical properties and are supposed to behave identically during extraction, desalting and ionization. The ratio of intensities of the light and heavy peptide pair is measured in mass spectrometry to provide relative abundance information for the peptide pair and their original proteins (114-115).

In the present research,  $^{13}\text{C}_6$ -labeled arginine and  $^{13}\text{C}_6$ -lysine are introduced into the drug susceptible MCF-7 cells, which are mixed in turn with the other three drug resistant cells. Since tryptic digestion of proteins produces arginine and lysine terminating peptides, all peptides except the original C-terminus, are labeled at C-terminus. Thus peptide pairs of 6-dalton difference are generated and are easily detected by mass spectrometry.



## Chapter 3: Materials and methods

### Materials

The protein isoelectric focusing (IEF) cell, Protean II Xi cell, Immobilized pH gradient (IPG) strips (17cm,pH3-10NL), IPG buffer (pH 3-10NL), Protean II ready gels (8-16% Tris-HCl precast gel 193x183x1.0 mm, IPG COMB), microbiospin P6 columns in Tris.HCl buffer and biosafe stain, phosphate buffer saline solution(PBS), were purchased from Bio-Rad (Hercules, CA). Nuclei Pure Prep Nuclei Isolation Kit (Cat No: NUC-201), propidium iodide, micrococcal nuclease, trypan blue, urea, thiourea, CHAPS, ethylenediaminetetraacetic acid (EDTA), dithiothreitol (DTT), CaCl<sub>2</sub>, NH<sub>4</sub>HCO<sub>3</sub>, NaCl, Eagle's minimal media (MEM), fetal bovine serum (FBS), iodoacetamide, TrisBase, sodium dodecylsulfate (SDS), glycerol were from Sigma Co. (St. Louis, MO). Modified porcine trypsin (sequence grade) was purchased from Promega (Madison, WI). ZipTip C<sub>18</sub> is from Millipore (Billerica, MA). <sup>13</sup>C<sub>6</sub>-lysine and <sup>13</sup>C<sub>6</sub>-arginine were purchased from Cambridge Isotope Laboratories (Cambridge, MA).

### Cell culture

MCF-7 cells were cultured in MEM (Sigma, St. Louis, MO) with 10% of FBS (Sigma) and 1% penicillin streptomycin. Isotope labeled control MCF-7 cells were cultured in the same MEM except that the essential amino acids lysine and arginine were replaced with their isotopic <sup>13</sup>C<sub>6</sub> counterparts (U-13C<sub>6</sub>, Cambridge Isotope Laboratories, Cambridge, MA). Dialyzed FBS were used, from which non-labeled lysine and arginines have been removed. Isotope labeled control MCF-7 cells were processed

and checked separately to make sure that isotope labeled amino acids were incorporated into the proteins in the nuclei before mixing with resistant cells. Every 6 months, the drug resistant cell lines were subjected to a reselection cycle of three passages with culture medium containing increased concentrations of the appropriate drugs.

### **Isolation of nuclei and preparation of nuclear proteins**

A nuclei isolation kit (Sigma, Product No. NUC-201) was used to isolate and purify MCF-7 nuclei, according to user instructions with slight modifications. Cultured MCF-7 cells were harvested at 95% confluence. The cultures were treated with trypsin to cleave and centrifuged at 500 g, then washed twice with PBS. The cell pellets were weighed and added to hypotonic lysis buffer in a ratio of 1g cells to 10 ml buffer with 0.5 % Triton X-100. Then they were vortexed for 10 seconds and were set on ice for 5 minutes. The cell lysate was stained with 0.4% trypan blue solutions (Sigma) to monitor if the cells were completely broken. If no intact MCF-7 cell could be observed under a light microscope, then the cell lysate was centrifuged through a sucrose cushion at 30,000g for 45 minutes to purify the nuclei. The nuclei pellets were washed twice with nuclei storage buffer and spun down at 500g. A small sample of the nuclei was observed under a fluorescence microscope stained with propidium iodide, the nuclei were weighed and nuclear protein extraction solutions were added in a ratio of 4ml solution for every 1 gram of nuclei. The nuclei pellets were resuspended in the NaCl buffers described earlier and vortexed vigorously for 15 seconds every 10 minutes, for a total of 40 minutes on ice. Then the suspension was centrifuged at 16000g for 10 minutes. The supernatant fraction was immediately transferred to new pre-chilled tubes and snap-frozen in aliquots with liquid nitrogen and stored at  $-80^{\circ}\text{C}$  (116).

### **Protein assay**

Bio-Rad DC protein Assay kit was used to measure protein concentration of the nuclear protein extract. The DC Protein Assay is compatible with the chemicals used in protein extraction. A modified assay protocol was used to perform the assay. A series of 0, 25, 50, 75, 100, 125 ug/ml sample of bovine serum albumin (BSA) were used to make standard curve. Absorbances were read at 750nm using a Beckman DU 530 life science UV/Vis spectrometer. The protein concentrations of samples were calculated based on their absorbances and dilution fold.

### **2-D gel electrophoresis**

Three hundred and fifty micrograms of proteins was used to conduct 2-D gel electrophoresis. Before loading the first dimension strip, the protein sample was desalted with Biospin-6 spin columns (Biorad, Hercules, CA) and added to three and a half micrograms of micrococcal nuclease and incubated at 37 °C for 30 minutes to eliminate possible DNA or RNA contamination. The sample was then dried by Speed Vac and 320ul of rehydration buffer was added, which contained 7M urea 2M thiourea, 2% chaps 50mM DTT and 1% of IPG buffer (Pharmacia, Piscataway, NJ). The solution was incubated at room temperature for 1 hour. Seventeen cm pH3-10 NL ReadyStrip™ IPG strips (Biorad, Hercules, CA)) were used for the first dimension isoelectric focusing (12 hours rehydration, 60000hv), 193x183x1.0mm, 8-16% Tris-HCl IPG COMB precast gels (Biorad) were used for the second dimension SDS polyacrylamide gel electrophoresis (16 mA for 30 minutes and then 24 mA for 4 hours and 40 minutes). At the end of the run, the gels were removed and soaked in a solution containing acetic acid/methanol/water (5:45:50, v/v/v) for at least 1 hour for fixation, followed by three washes for 5 minutes in

water. Staining was performed with Bio-Safe colloidal Coomassie blue G-250 (Biorad, Hercules, CA) for 2 hours. The gels were then rinsed by water until the desired contrast was achieved for densitometric image analysis.

### **Analysis of gel images**

A GS-800 calibrated densitometer (Biorad, Hercules, CA) was used to visualize Coomassie stained gel slabs. After the gels were scanned, the images were exported as TIFF files. The TIFF files of 2-DE images of control and drug resistant MCF-7 nuclear proteins were compared using Compugen Z3 software (Compugen Ltd., Tel Aviv, Israel). In each gel, the intensity of a spot was measured and recorded. It represents the sum of all pixels in the spot boundary after subtracting the background level values. For comparative analysis, relative intensity of each pair of matching spots was measured and relative abundance and differential abundance values were displayed. The image comparison was checked manually to exclude any error in matching pairs of spots. Spots of interest were also examined using “zoom” images. Figure 9 shows a schematic of gel images comparison using Compugen software.

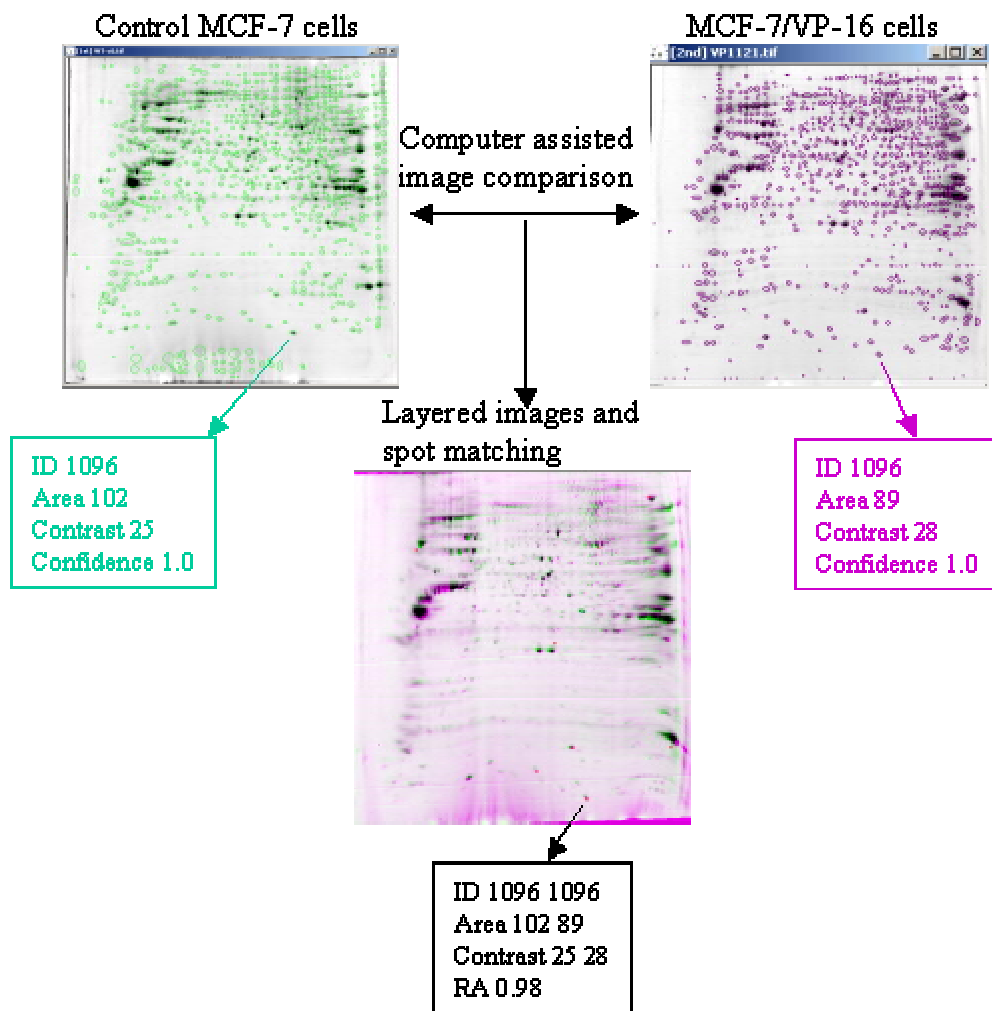


Figure 9: Schematic of gel image comparison by densitometry.

### **In-gel tryptic digestion and peptide desalting**

After gel image analysis, the spots of interest were then excised. The spots could be stored at  $-80^{\circ}\text{C}$  at this time or directly subjected to in-gel digestion. Before digestion, the spots were cut into roughly  $1\text{-mm}^3$  cubes, and transferred to clean 1.5 microfuge tubes. The gel particles were washed with water and water/acetonitrile 1:1 (v/v) (one change, 15 minutes/change). Solvent volumes used in the washing step roughly equaled two times the gel volume. Then all the liquid was removed, and enough acetonitrile was added to cover the gel particles. After the gel pieces shrank, acetonitrile was removed and  $0.1\text{ M NH}_4\text{ HCO}_3$  was added to rehydrate the gel pieces for 5 minutes. Next, an equal volume of acetonitrile was added and incubated for 15 minutes, followed by removing all liquid and drying down the gel particles in a vacuum centrifuge. Afterward  $10\text{ mM DTT}/0.1\text{ M NH}_4\text{ HCO}_3$  was added and incubated for 45 minutes at  $56^{\circ}\text{C}$  to reduce the proteins. After reduction, the tubes were chilled to room temperature, and excess liquid was removed and replaced by roughly same volume of freshly prepared  $55\text{ mM}$  iodoacetamide /  $0.1\text{ M NH}_4\text{ HCO}_3$  for alkylation. The tubes were incubated for 30 minutes at room temperature in the dark followed by removing the iodoacetamide solution. The gel particles were washed with  $0.1\text{ M NH}_4\text{ HCO}_3$  and acetonitrile as described before followed complete drying down in a Speed Vac. Then  $50\text{ mM NH}_4\text{ HCO}_3$ ,  $5\text{ mM CaCl}_2$  and  $12.5\text{ ng/ul}$  sequencing grade modified trypsin ( Promega, Madison, WI) were added to rehydrate the dried gel particles at  $4^{\circ}\text{C}$  (ice bucket). Enough trypsin solution should be added if the initially added volume was absorbed by the gel pieces. After 45 minutes incubation on ice, the remaining enzyme supernatant was removed and replaced with  $5\text{-}20\text{ ul}$  of  $50\text{ mM NH}_4\text{ HCO}_3$ ,  $5\text{ mM CaCl}_2$  depending on the

sizes of the gel spots. The tubes were then incubated at 37 °C in a water bath overnight. After overnight digestion, a sufficient volume of 25 mM NH<sub>4</sub> HCO<sub>3</sub> was added to cover the gel pieces and incubated for 15 minutes, followed by adding the same volume of acetonitrile and incubation for 15 minutes. After the supernatant was recovered, the extraction was repeated two times with 5% formic acid and acetonitrile (1:1, v/v). All the extracts from same gel spot were pooled and dried down in a Speed Vac. The dried extract samples could be stored at -80 °C or redissolved with 10 ul 0.1% TFA water for desalting with ZipTip C<sub>18</sub> pipette tips ( Millipore, Bellerica ) (117-118).

To desalt the peptide extracts, a wetting solution (50% acetonitrile in water) was first aspirated and dispensed into the tips twice, followed by two times of addition and aspiration of equilibration solution ( 0.1 % TFA water). The redissolved peptide extracts were then aspirated into the tips 10 cycles for maximum binding of the complex mixtures. Next, five cycles of wash solution (0.1 % TFA in water) were aspirated into tips and dispensed to waste. Finally 5 ul of 0.1% TFA, 70% acetonitrile was used to elute the peptides. The eluted samples could be used directly for mass spectrometry analysis with an AXIMA-CFR MALDI –TOF (Kratos, Chestnut Ridge, NY) mass spectrometer or would be dried by Speed Vac and redissolved in acetic acid/methanol/water(2:49:49, v/v/v) for analysis using electrospray on a hybrid quadrupole time-of-flight instrument(QSTAR/Pulsar, Applied Biosystem, Foster City, CA).

### **Mass spectrometry analysis and protein identification**

Mass spectra are acquired with an AXIMA-CFR (Kratos, Chestnut Ridge, NY) mass spectrometer and an API QSTAR Pulsar Qq-TOF (Applied Biosystem, Foster City, CA)

instrument. Protein identifications were obtained from peptide mass fingerprinting and microsequencing.

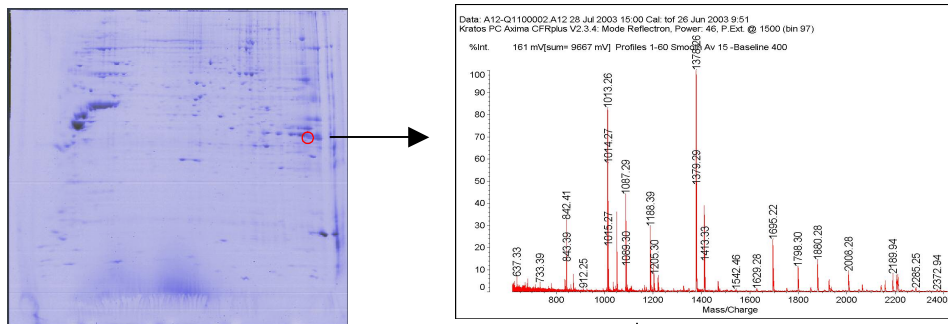
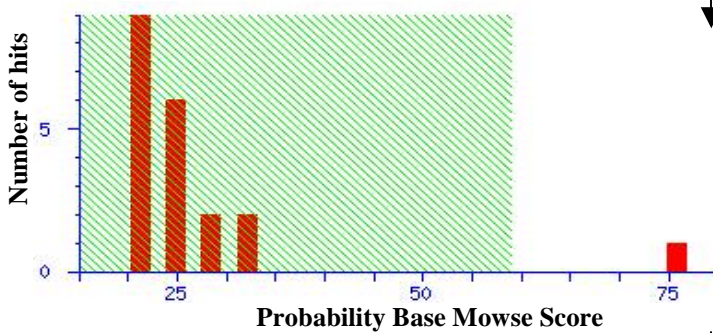
Routinely, the samples were first analyzed using the MALDI mass spectrometer. The instrument was operated in the reflectron positive ion mode. The laser power was set at 45-50 on the manufacturer's scale of 0 to 180. The monoisotopic peaks of trypsin autolysis products,  $m/z$  842.51 and 2211.11, were used for internal calibration of each spectrum. If these trypsin autolysis peaks were not detected, melletin and angiotensin II were used as external calibrants. An aliquot of 0.5ul of sample solution was put on the plate and covered with 0.5 ul of 50 mM alpha-hydroxycinnamic acid in 0.1% TFA, 70% acetonitrile, then dried before being put into the instrument. Spectra were recorded by accumulating 50-100 laser shots, depending on the quality of the sample. The data from the spectra were used to identify proteins by peptide mass fingerprinting. Peptide mass fingerprinting uses residue-specific peptides mass to match against theoretical peptide libraries generated from the human genome to create a list of likely protein identifications. We used Mascot search programs from [www.matrixscience.com](http://www.matrixscience.com) to obtain protein identifications for our experiments. The NCBI and SwissProt databases were searched. If certain criteria were met, the protein was considered to be identified confidently. An illustration of protein identification by peptide mass mapping is depicted in Figure 10. Mascot search results show candidate proteins and scores based on probability analysis. Our identifications were confirmed manually by checking for consistency in the pIs and molecular weight values provided by the 2-D gel array. If no conclusive identification could be acquired, the sample would be analyzed using nanospray tandem mass spectrometry to identify proteins by microsequencing.



Protein identification using microsequencing involves using tandem mass spectrometry to obtain sequence information for one or several peptides of the protein to match against theoretical sequences generated from the protein database. The instrument used for acquiring tandem mass spectrometry was a hybrid quadrupole time-of-flight (TOF) mass spectrometer, API QSTAR Pulsar Qq-TOF. The instrument was operated in two modes. The first was the MS mode, in which ions entered the instrument from the nanospray source and passed through two quadrupoles. The ions were then pulsed into the TOF tube and  $m/z$  values were measured. The resulting mass spectrum showed the mass-to-charge ratios of all the analytes entering the mass spectrometer at that time. Typically, 2  $\mu$ l of the peptide solution in acetic acid/methanol/ water (2:49:49, v/v/v) was loaded into a capillary tip (Protana, Odense, Denmark) and mounted into the nanospray source. Spray voltage was set at 900V. MS scan range is from 350-1200 $m/z$ . The second mode of operation was MS/MS, or collisional activation with a product ion scan. The ions of interest (precursor ions) were isolated by the first quadrupole, and the more abundant ions are automatically selected to pass into the second quadrupole, where they were fragmented by collision with an inert gas such as nitrogen. The fragmented products (product ions) are then pulsed into the TOF analyzer and measured. Product ion spectra are recorded. Under low energy collision, peptide ion fragmentation occurs typically between each amino acid residues, thus generating b-ion and y-ion series. A partial *de novo* sequence can be obtained for each precursor peptide ion, which is used for database search. Again candidate proteins are listed by the bioinformatics program along with probabilities of correct identifications. Multiple microsequences improve the reliability of the protein identification. We usually chose 3-4 doubly charged peptides ions for

sequencing. We used the **BioExplore** program integrated with the instrument to identify proteins using the resulting MS/MS spectra. An illustration of protein identification by microsequencing is depicted in Figure 11. Other database search programs such as TagIdent (<http://www.expasy.ch>) and MS-Blast (<http://www.dove.embl-heidelberg.de/blast2/msblast.html>) were used as necessary.

## Nuclear Proteins of MCF-7

**Probability Based Mowse Score** is score is  $-10 \cdot \log(P)$ , where P is the probability that the observed match is a random event. Protein scores greater than 59 are significant ( $p < 0.05$ ) in the case of a single protein.

**41% sequence coverage**  
Matched peptides shown in **Bold Red**

```

1  MEREKEQFRK LFIGGLSFET TEESLRNYYE QWGKLTDCVV MRDPASKRSR
51  GFGFVTFSSM AEVDAAMAAR PHSIDGRVVE PKRAVAREES GKPGAHVTVK
101 KLVGGIKED TEEHHLRDYF EYGKIDTIE IITDRQSGKK RGFVTFDD
151 HDPVDKIVLQ KYHTINGHNA EVRKALSRQE MQEVQSSRSG RGGNFGFGDS
201 RGGGNFGPG PGSNFRGGSD GYGSGRGFGD GYNGYGGGPG GGNFGGSPGY
251 GGRGGYGGG GPGYGNQGGG YGGGYDNYGG GNYGSGNYND FGNYNQPSN
301 YGPMKSGNFG GSRNMGPGYGGGNYGPGGSG GSGGYGGRSR Y
    
```

Figure 10: Schematic of protein identification by peptide mass fingerprinting.

### Nuclear proteins of MCF-7

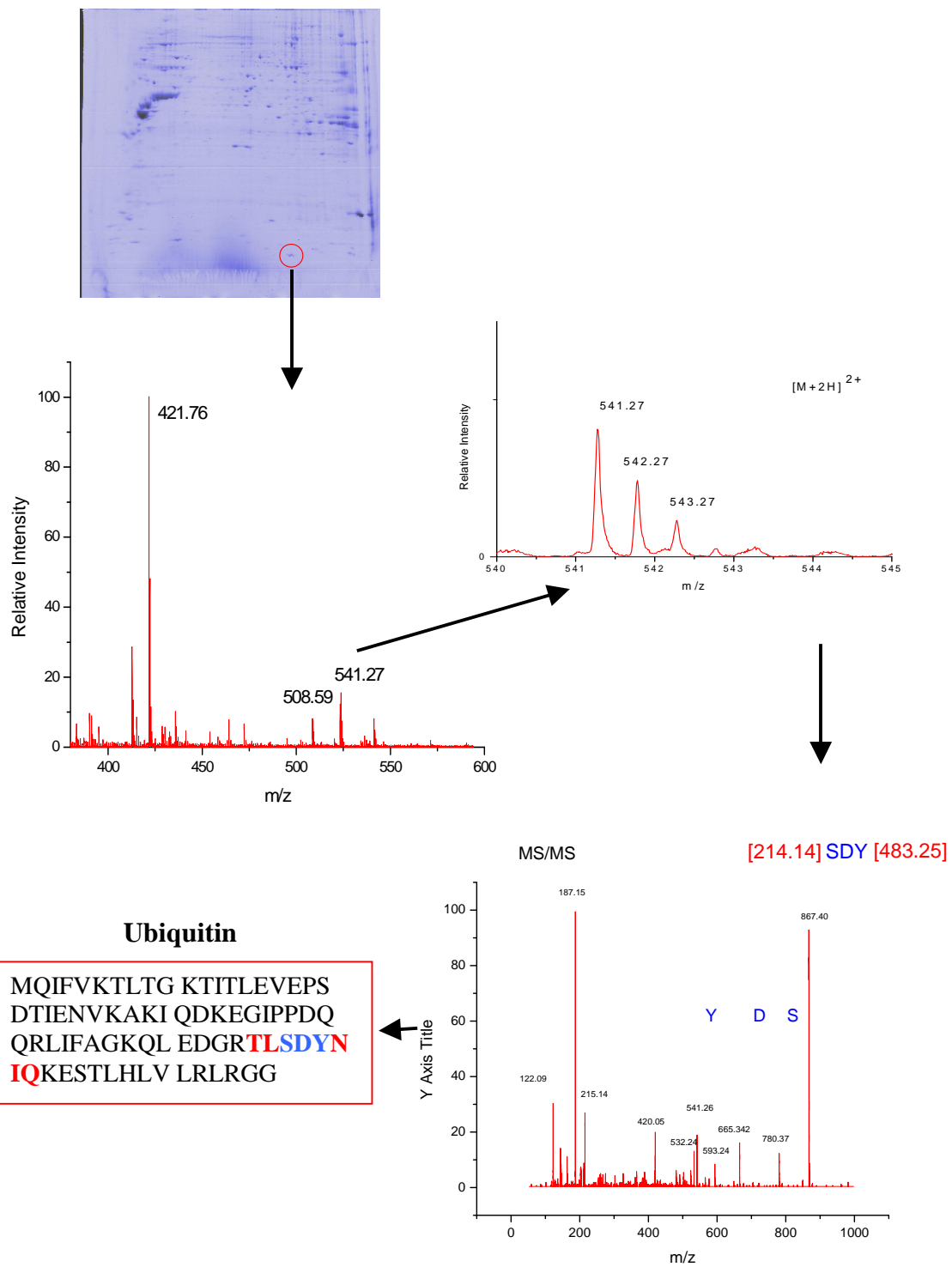


Figure 11: Schematic of protein identification by peptide microsequencing.

### Stable isotope labeling analysis

In our stable isotope labeling experiments,  $^{13}\text{C}_6$ -lysine and  $^{13}\text{C}_6$ -arginine were introduced into the control MCF-7 cells during cell culture, and these were mixed with drug resistant cells in a ratio of approximately 1:1. Incorporation of isotopes was evaluated to quantitate the extent to which of the lysine and arginine were replaced by  $^{13}\text{C}_6$ -lysine and  $^{13}\text{C}_6$ -arginine counterparts in the nuclear proteins of control cells. The nuclear protein expression profile of MCF-7 cells cultured in isotope labeling media was compared using image analysis with that of MCF-7 cells cultured in regular media. Since protein samples were first separated by 2-D gel electrophoresis, six- Dalton -separated peptide pairs were easily obtained in the spectra of the mixture. Peptides from proteins known from 2-D gel images not to be modified were examined to calibrate the mixing ratios of cells. To avoid the effects of overlapped peptides, peaks of ions having no adjacent peaks which were different by around 6 Daltons were chosen to calculate relative abundance. Relative abundance (RA) is defined as peak area of unlabeled peptide over that of labeled peptide. However, isotope incorporation percentage must be taken into account. Supposing the incorporation percentage of  $^{13}\text{C}_6$ -lysine or  $^{13}\text{C}_6$ -arginine in a particular peptide was X%, the revised relative expression was as follows,

$$\text{RA} = [\text{unlabeled peak area} - (100 - X)/X \text{ labeled peak area}] / [100/X \text{ labeled peak area}]$$

For example, if the incorporation percentage of  $^{13}\text{C}_6$ -lysine and  $^{13}\text{C}_6$ -arginine in a protein is 90%. The labeled peak area only represents 90% of the peak area from the label cells. Its revised peak area should be 100/90 labeled peak area. The peak area originated from unlabeled cells should be the unlabeled peak area minus (100-90)/90 labeled peaked area.

## Chapter 4: Results

### *Nuclei isolation and protein extraction*

Reproducible sample preparations are crucial for comparative proteomics studies. We have successfully developed and evaluated methods to isolate nuclei and extract nuclear proteins of MCF-7 cells for subsequent 2-D gel electrophoresis. Figure 12 shows drug susceptible MCF-7 nuclei before and after purification. Under a light microscope and fluorescent microscope the purified nuclei stained with propodium iodide appeared to be free of rough endoplasmic reticulum (ER) and other contaminants, and no difference could be detected between nuclei from drug susceptible and drug resistant MCF-7 cells. MCF-7 cells were harvested at 95% confluence. Typically,  $6-8 \times 10^6$  cells were harvested from a  $150 \text{ cm}^2$  flask. Their total wet weight was 0.17-0.20 gram. 0.17-0.24 gram of nuclei was obtained from 1.0 gram of cell pellet, from which 7.5-9.0 mg of nuclear proteins could be acquired.

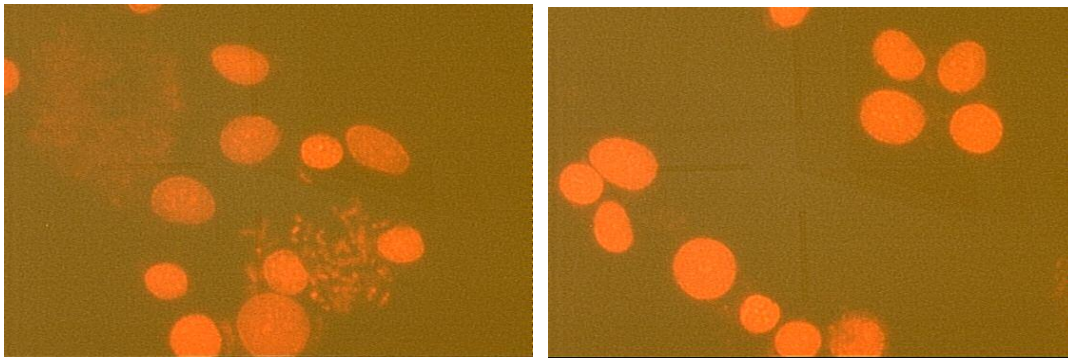


Figure 12: Nuclei of control MCF-7 cells stained with propidium iodide. a: MCF-7 nuclei released from the cells lysate with hypotonic buffer. b: MCF-7 nuclei after centrifugation with sucrose cushion.

## **2-D gel electrophoresis and protein identification**

The protein samples were subjected to 2-D gel electrophoresis after desalting with a spin column P-6 (Biorad, Hercules, CA). The gels were stained with Coomassie blue and visualized. After images were recorded digitally, the spots were excised and digested with trypsin. The digestion products were subjected to mass spectrometry analysis. Protein identifications were acquired based on peptide fingerprinting or microsequencing. The purity of the nuclear protein mixture was evaluated by identification of proteins on the gel. Figure 13 shows an annotated 2-D gel electrophoresis map of nuclear proteins of control MCF-7 cells, proteins identified from which were listed in Table 1. Typically, proteins identified by peptide mass fingerprinting have sequence coverage above 30%. At least two sequence tags were acquired for each protein identified by microsequencing. The mascot scores all exceed the 95% confidence criteria set by the software. In most cases, the molecular weights and pI of each protein fit well with their position in the 2-D gel map. Although 160 spots were identified, only 120 different proteins were identified. Some proteins appeared on more than one spot in the gel. For example, spots 134, 135, 136 and 137 were of same protein hnRNP L. In rare cases, one spot contained more than one single protein, because 2-D gel electrophoresis can not separate proteins with both similar molecular weight and pI. For example, spot 72 were identified to have two proteins, BAF53 (PI 5.39, MW 47430) and hnRNP F (PI 5.38, MW 45985). Proteins having significantly smaller molecular weights than their theoretical values were judged as truncated.



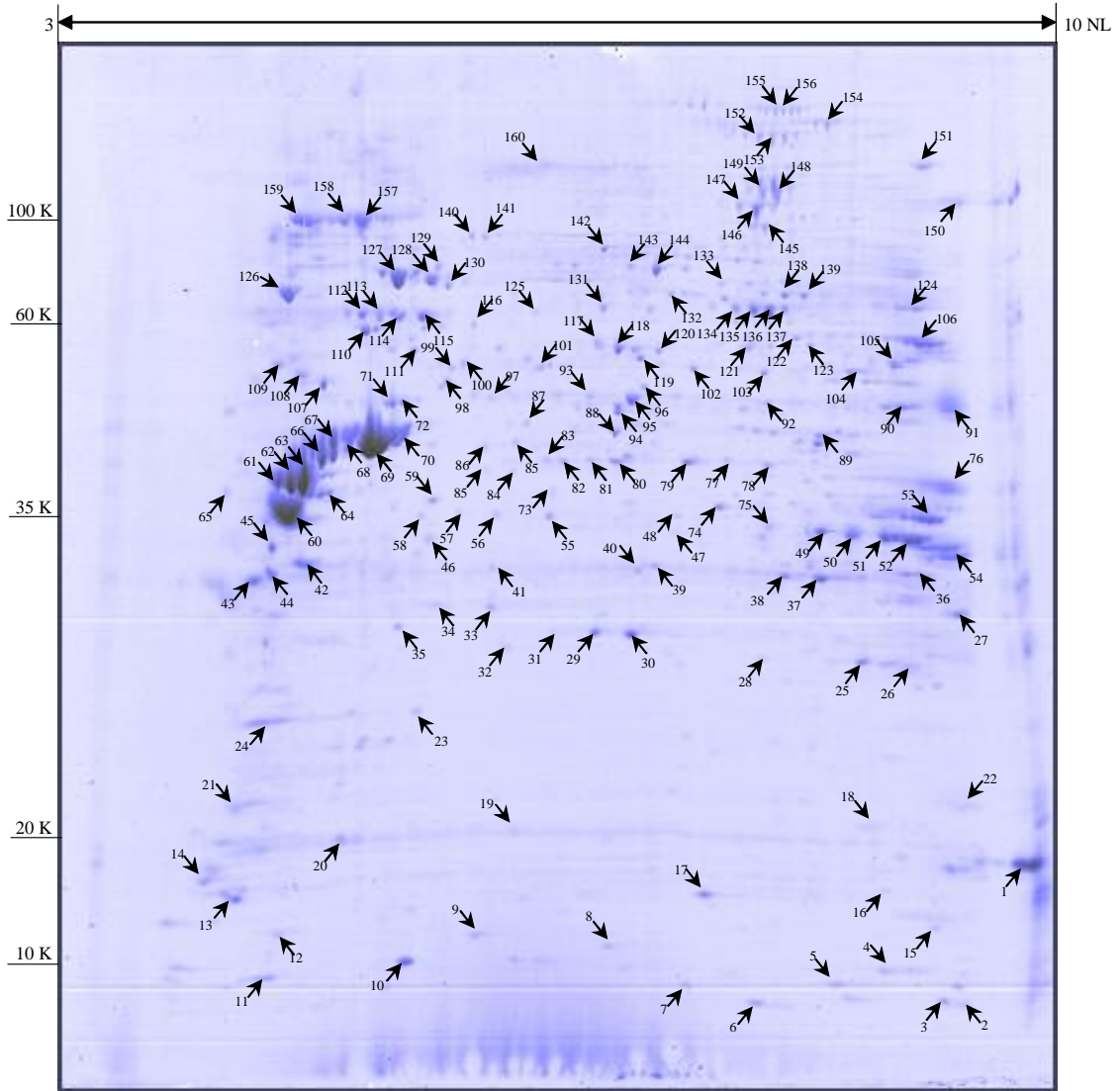


Figure 13: Annotated 2-D gel map of nuclear proteins from control MCF-7 cells.

Table 1: Proteins identified from nuclear extraction of control MCF-7 cell.

Spot NO	Protein ID	PI	MW	Accession NO	Subcellular location
1	Micrococcal Nuclease	9.8	19299	P43209	
2--3	snRNP-G	8.98	8490	Q15357	N
4	Signal recognition particle 9Kd Pro	8.27	9974	P49458	N
5	P10 protein	7.3	11064	P60903	N
6	Ubiquitin	6.56	8560	P02248	N
7	U6 snRNA-associated Sm-like protein LSm2	6.04	10828	Q9Y333	N
8	S100 calcium-binding protein A16	6.28	11794	Q96FQ6	C,N
9	S100 calcium-binding protein A13	5.91	11464	Q99584	C,N
10	Enhancer of rudimentary homolog	5.63	12422	Q14259	N
11	snRNP-F	4.7	9776	P49458	N
12	U6 snRNA-associated Sm-like protein LSm7	5.1	11595	Q9UK45	N
13	60 Sacidic ribosomal protein P2	4.42	11658	P05387	N
14	U6 snRNA-associated Sm-like protein LSm3	4.58	11707	Q9Y4Z1	N
15	NHP-2 like protein 1	8.72	14165	P55769	N
16	Single-stranded DNA-binding protein	9.59	17249	Q04837	N
17	40S ribosomal protein S12	6.36	14728	P25398	C
18	Putative RNA-binding protein 3	8.86	17160	P98179	N
19	VAMP-associated protein	6.85	27211	O95292	MB
20	DIMI protein homolog	5.53	16775	O14834	N
21	60s ribosomal protein L23a	10.44	17684	P29316	N
22	Cyclophilin B	9.33	22785	P23284	E, N
23	NIF3L1BP1 protein	5.69	23039	Q6I9Y2	
24	40S ribosomal protein S7	10.09	22113	P62081	N
25	HMG 2	7.77	24059	P26583	N
26	HMG-4L	8.45	21125	Q9UJ13	N
27	FK506-binding protein 3	9.29	25161	Q00688	N
28	PSA 2	7.12	25865	P25787	N
29-30	HMG-1	5.62	24747	P09429	N
31	HSP 27	5.98	22768	P04792	N
32	eIF4E	5.79	25082	P06730	N
33	40 S ribosomal protein SA	4.79	32833	P08861	N
34	Prohibitin	5.57	29786	P35232	C,MT, N
35	Breast carcinoma amplified sequence 2	5.48	26115	O75934	N
36	U2 small nuclear ribonucleoprotein A'	8.72	28398	P09661	N

37-38	Guanine nucleotide-binding protein beta	7.6	35055	P25388	N
39	PSA 1	6.15	29822	P25786	N
40	Nuclear protein Hcc-1	6.1	23656	P82979	N
41	Annexin IV	5.85	35729	P09525	N
42	Annexin V	4.94	35783	P08758	N
43	Splicing factor SC35	11.88	25560	Q01130	N
44	EF-1-beta	4.5	24617	P24534	C,N
45	Alpha tropomyosin	4.72	32856	P09493	CT
46	Guanine Nucleotide -binding protein	5.6	37307	P11016	N
47-48	hnRNP H3	6.37	36903	P31942	N
49	Annexin II	7.56	38677	P07355	N
50-53	hnRNP A2/B1	8.97	37464	P22622	N
54	hnRNP A1	9.26	37464	P09651	N
55-57	60 S acidic ribosomal protein p0	5.71	34252	P05388	N
58	CapZ alpha-1	5.45	32903	P52907	N
59	eIF-3 beta 2	5.38	36479	Q13347	N
60	Nucleophosmin	4.47	32746	P06748	N
61-63	Cytokeratin 19	5.04	44079	P08727	CT
64	hnRNP C	4.95	33667	P07910	N
65	Set Protein	4.12	32084	Q01105	N
66-68	Cytokeratin 8 (truncated)	4.76	53515	P05787	N
69	Actin beta	5.15	42408	P60709	N
70	Transcription factor NF-AT 45K chain	8.26	44897	gi 1082855	N
71	Elongation initiation factor 4A-1	5.32	46352	P04765	N
72/1	BAF 53	5.39	47430	O96019	N
72/2	hnRNP F	5.38	45985	P52597	N
73	PP1A	5.94	37488	P62136	C
74-75	hnRNP Do	7.62	38581	Q14103	N
76	hnRNPA3	8.74	39947	P51991	N
77	Mitotic checkpoint protein BUB 3	6.36	37131	O43684	N
78-83	hnRNP A/B	6.49	35945	Q99729	N
84	THO complex subunit 3	5.7	38747	Q96J01	N
85-86	Actin gamma	5.31	41766	P02571	CT
87	Calcium-binding transporter	5.31	45790	Q9P129	MB
88	Septin 2	6.25	41689	Q15019	CT
89	Creatine kinase	8.6	47007	P12532	MT

90	Septin 7	8.85	48756	Q16181	N
91	Elongation factor 1-alpha 1	9.1	50451	P04720	C
92	Regulator of chromosome condensation	7.18	44941	P18754	N
93-94	Proliferation-association pro 2G4	6.13	44101	Q9UQ80	N
95	Elongation factor 1-gamma	6.25	50429	P26641	N
96	Cleavage stimulation factor	6.12	48324	Q05048	N
97	DEK oncogene	8.69	42933	P35659	N
98	RUV-like 2	5.49	51125	Q9Y230	N
99-100	HLA-B associated transcript-1	5.44	49416	Q13838	N
101	hnRNP H	5.89	49198	P31943	N
102	Septin 6	6.24	49685	Q14141	N
103	Glutamate dehydrogenase 1	7.66	61359	P00367	CT
104	ATP synthase alpha chain	9.16	59714	P25705	M
105	SRP 54	8.87	55668	P61011	N
106	54 kDa DNA- and RNA-binding Protein	9.01	54066	Q15233	N
107	ATP synthase beta chain	4.64	56525	Q14283	M
108	HAT type B subunit	4.89	48132	Q16576	N
109	CAF-1 subunit	4.74	47911	Q09028	N
110	Splicing factor 3A subunit 3	5.27	58812	Q12874	N
111	hnRNP K (truncated)	5.39	51230	Q07244	N
112-115	hnRNP K	5.39	51230	Q07244	N
116	Copine III	5.6	60947	O75131	N
117	T-complex protein 1, beta	6.01	57452	P78371	N
118	Nuclear matrix pro 200	6.14	55603	Q9UMS4	N
119	RuvB-like 1	6.02	50538	Q9Y265	N
120	Aspartyl-tRNA synthetase	6.11	57100	P14868	C, N
121	Glutamate dehydrogenase 1	7.66	61359	P00367	M
122	U4/U6 sn RNP	7.05	59097	O43172	N
123	Phenylanyl-tRNA synthetase alpha chain	7.46	57396	Q9Y285	C, N
124	Probable RNA-dependent helicase p68	9.06	69105	P17844	N
125	T-complex protein 1, alpha	5.8	60306	P17987	C
126	Nucleolin (76K)	4.41	76224	P19338	N
127	Heat shock cognate 71 kDa	5.37	71082	P11142	C,N
128	HSP 70-1	5.48	70294	P08107	M

129	Stress-70 protein	5.87	73635	P38646	M
130	Annexin VI	5.42	75695	P08133	N
131	Delta coat protein	5.89	57174	P48444	MB
132	Stress-induced-phosphoprotein 1	6.4	63227	P31938	C, N
133	Phenylanyl-tRNA synthetase beta chain	6.4	66088	Q9NSD9	C, N
134-137	hnRNP L	6.65	60719	P14866	N
138-139	hnRNP Q	8.68	69590	O60506	N
140-141	ATP-depended DNA helicase II, 80kDa subunit	5.55	83091	P13010	N
142	liscening factor	6.08	81884	P33993	N
143-144	ATP-depended DNA helicase II, 70kDa subunit	6.23	69953	P12956	N
145	ATP-dependent helicase DDX1	6.81	82380	Q92499	N
146-147	EF-2	6.42	96116	P13639	C
148-149	C1-THF synthase	6.94	101364	P11586	C
150	Splicing factor PQ	9.45	762116	P23246	N
151	PARP-1	8.99	113680	P09874	N
152-153	Structure maintainece of chromosome 3	6.77	141454	Q9UQE7	N
154	Structure maintainece of chromosome 1	7.51	143144	Q14683	N
155-156	Bifunctional aminoacyl-tRNA synthetase	7.77	161923	P07814	N
157-158	TER AtPase	5.14	89950	P55072	N
159	Nucleolin (100K)	4.41	76224	P19388	N
160	hnRNP U	5.76	90423	Q00839	N

N – Nuclear    C – Cytoplasmic    MT – Mitochondria

E – Endoplasmic reticulum    CT-cytoskeleton    MB-membrane

### *Evaluation of $^{13}\text{C}_6$ -arginine and $^{13}\text{C}_6$ -lysine metabolic labeling*

The nuclear protein expression profile of control MCF-7 cells with isotope  $^{13}\text{C}_6$ -arginine and  $^{13}\text{C}_6$ -lysine media was compared with that of control MCF-7 cells cultured in regular media. The MCF-7 cells were cultured in growth media with  $^{13}\text{C}_6$ -arginine and  $^{13}\text{C}_6$ -lysine. After 5 passages, the cells were harvested and nuclear proteins were extracted. The protein sample was subjected to 2-D gel electrophoresis. The gel images were taken and compared with those from control MCF-7 cells cultured in regular media. The spots were excised and digested with trypsin. The subsequent peptides were analyzed with mass spectrometers. The gel image comparison showed that the protein expression profile of control MCF-7 cells with isotope labeling represented that of control MCF-7 cells cultured in regular media. Figure 14 shows a 2-D gel map of nuclear proteins of control MCF-7 cells in regular media. Figure 15 shows a 2-D gel map of nuclear proteins of control MCF-7 cells cultured in  $^{13}\text{C}_6$ -arginine and  $^{13}\text{C}_6$ -lysine media. In addition, mass spectrometry analysis indicated that  $^{13}\text{C}_6$ -arginine and  $^{13}\text{C}_6$ -lysine were incorporated into the proteins at about 90%. Figure 16 shows incorporation of  $^{13}\text{C}_6$ -arginine and  $^{13}\text{C}_6$ -lysine in nucleophosmin.

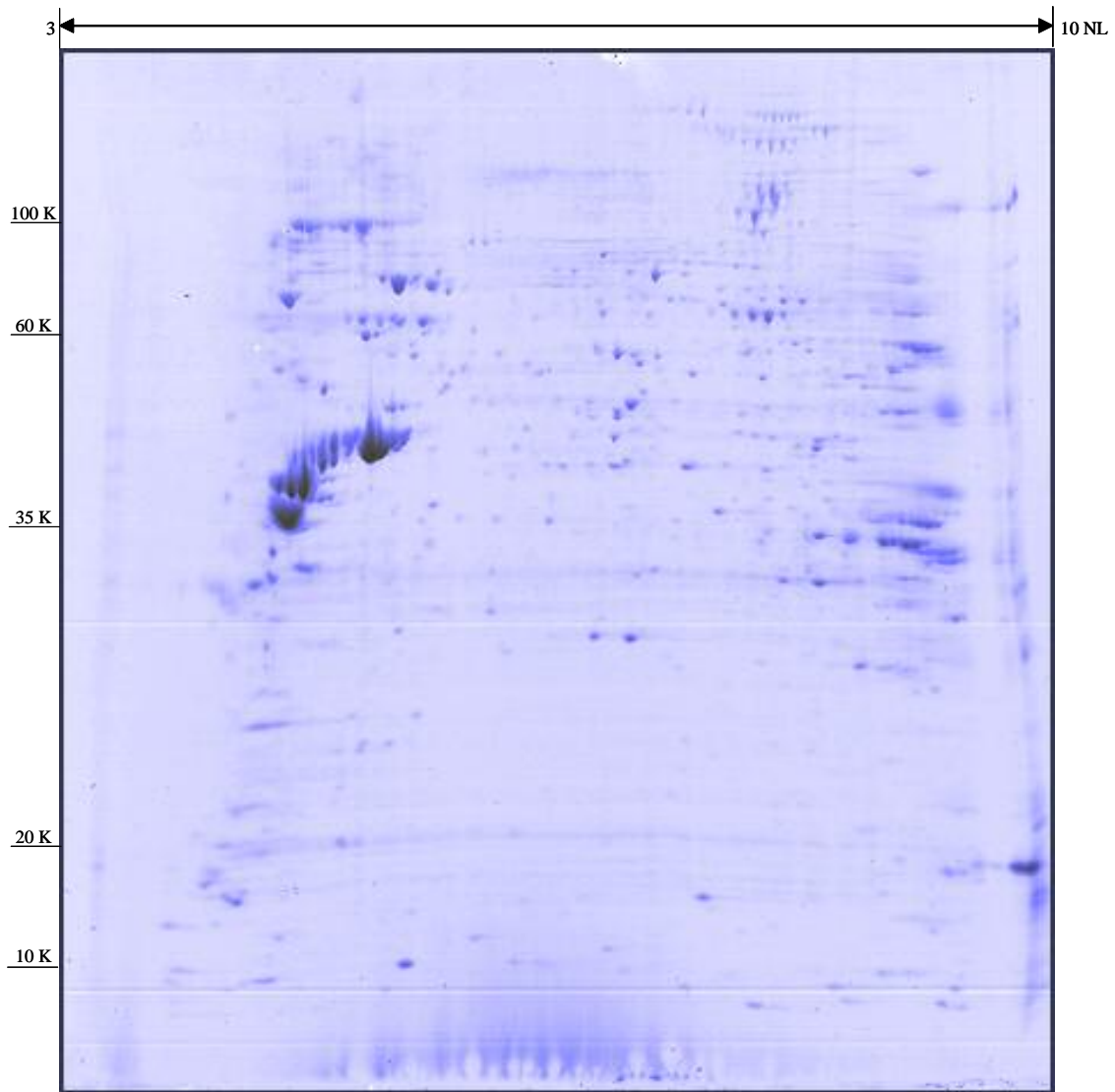


Figure 14: 2-D gel map of nuclear proteins from control MCF-7 cells in regular media.

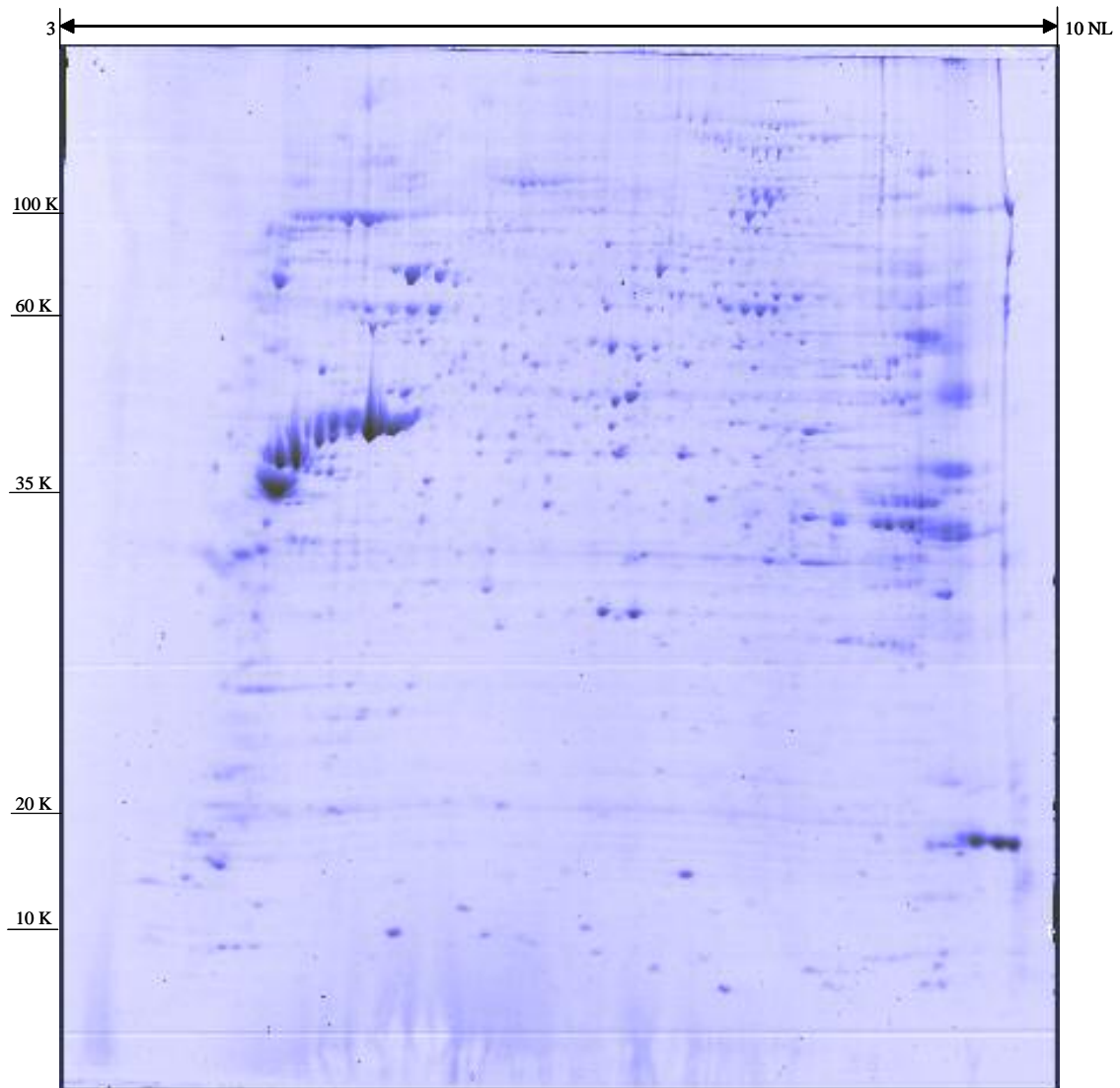
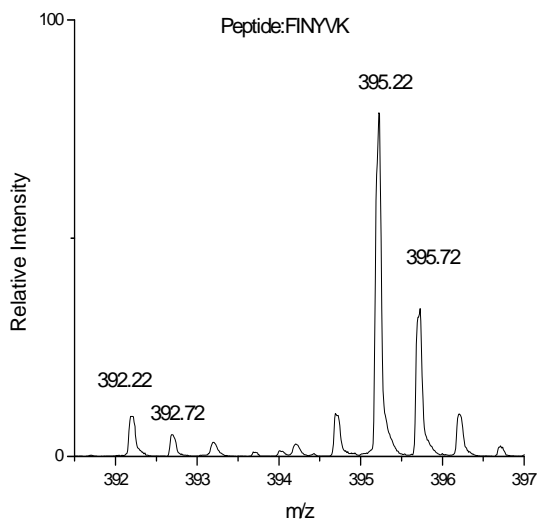
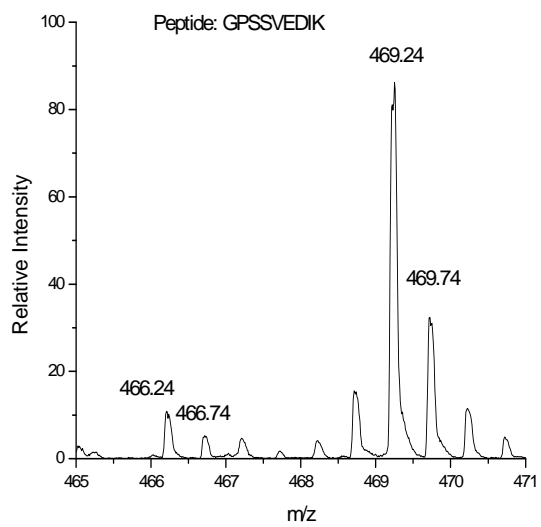


Figure 15: 2-D gel map of nuclear proteins from control MCF-7 cells in  $^{13}\text{C}_6$ -arginine and  $^{13}\text{C}_6$ -lysine media.





Incorporation Percentage: 89



Incorporation Percentage: 90

Figure 16: Evaluation of metabolic incorporation of isotope  $^{13}\text{C}_6$  in nucleophosmin.

### **Nuclear protein expression profile of MCF-7/VP cells**

The expression profile of Vp-16 resistant MCF-7 cells was compared with that of control MCF-7 cells with both densitometric comparison and metabolic labeling methods. Figure 17 shows a 2-D gel map of nuclear proteins from VP-16 resistant MCF-7 cells. Figure 18 shows 2-D gel map of nuclear proteins from VP-16 resistant MCF-7 cells and labeled control MCF-7 cells mixture. Figure 19 shows the results of densitometric comparison of a pair of 2-D gel arrays of nuclear proteins from control and VP-16 resistant MCF-7 cells made using Compugen software. Of the 120 proteins identified, abundances of 9 proteins were found significantly more or less abundant using 2-fold as the threshold. Those are circled in Figure 19. Nucleolin, HMG 1, 40s ribosomal protein SA and cyclophilin B are more abundant. Cytokeratin 8, cytokeatin 19, septin 2, PARP-1 and alpha tropomyosin are less abundant. Figure 20 shows an example of gel arrays and mass spectra of a protein whose abundance levels are the same in the two cell lines. The protein was identified as nuclephosmin. It was subsequently used as a control for cell mixing. Figure 21 shows gel arrays and mass spectra of nucleolin, which reveals that it was more abundant in VP-16 resistant MCF-7 cells. Figure 22 shows gel arrays and mass spectra of septin 2, which was less abundant in VP-16 resistant MCF-7 cells. Table 2 provides the results of protein relative abundance in VP-16 resistant cells with both methods.

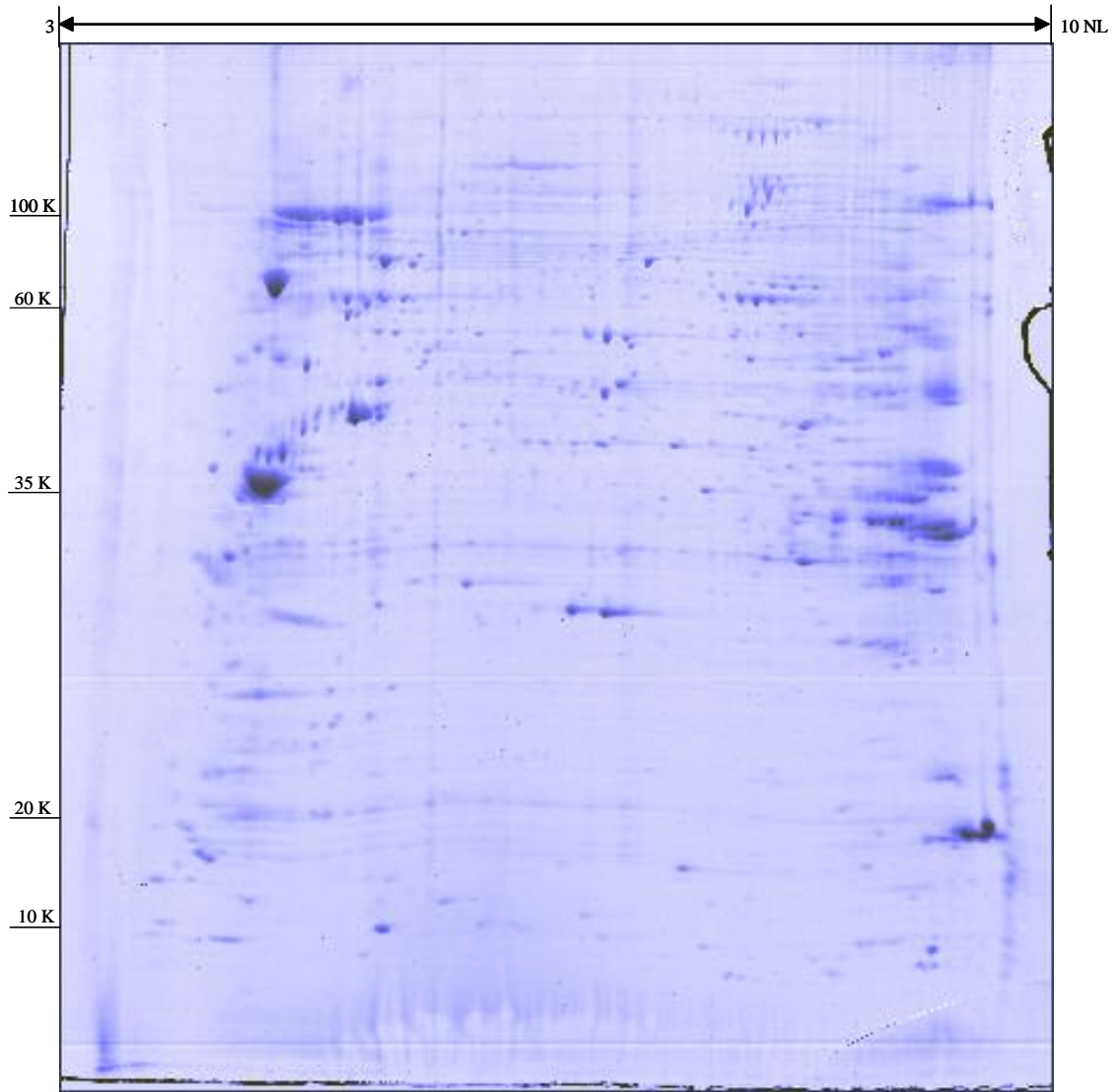


Figure 17: 2-D gel map of nuclear proteins of MCF-7/VP cells.

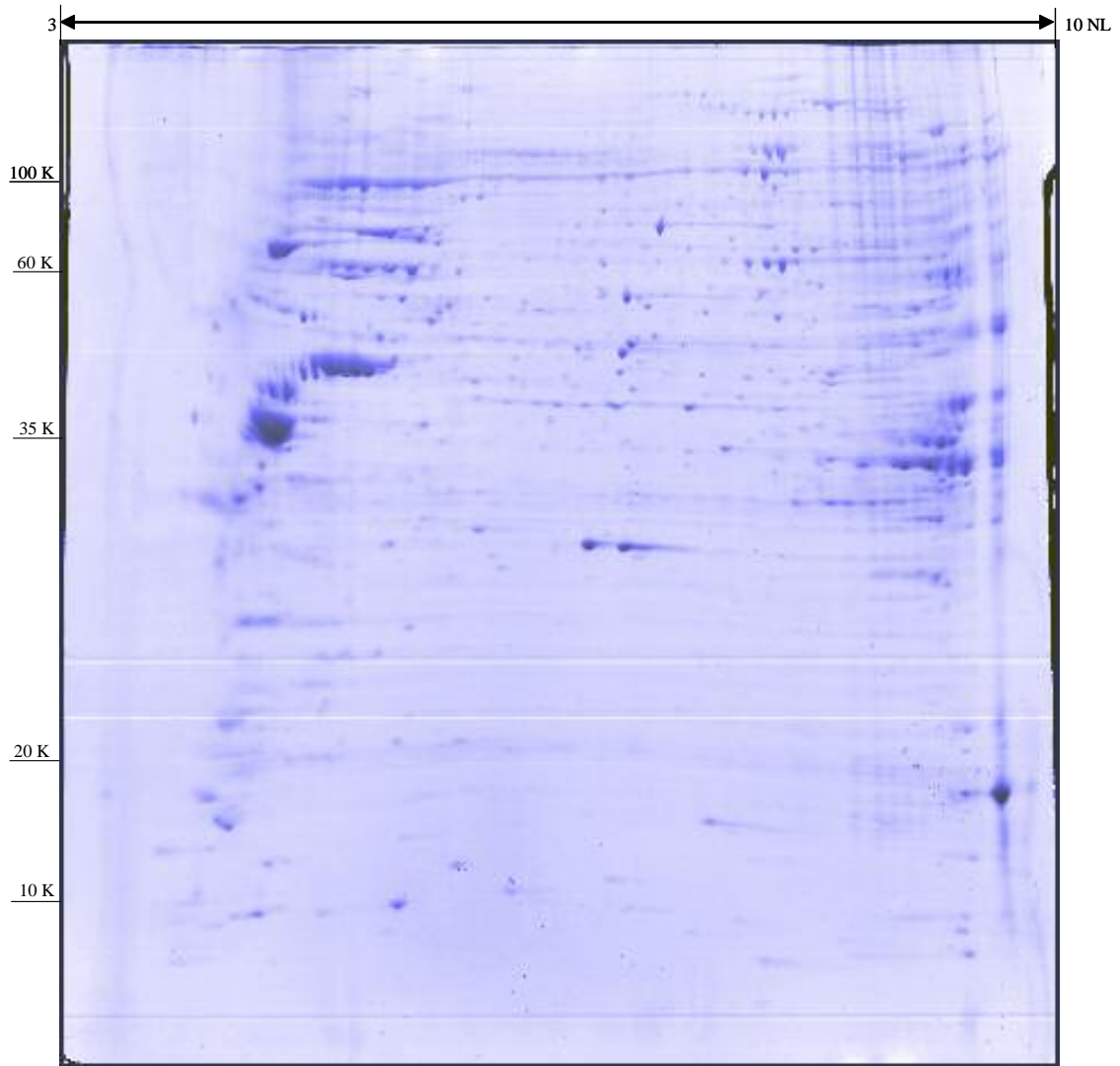


Figure 18: 2-D gel map of nuclear proteins of MCF-7/VP cells and labeled control MCF-7 cells.

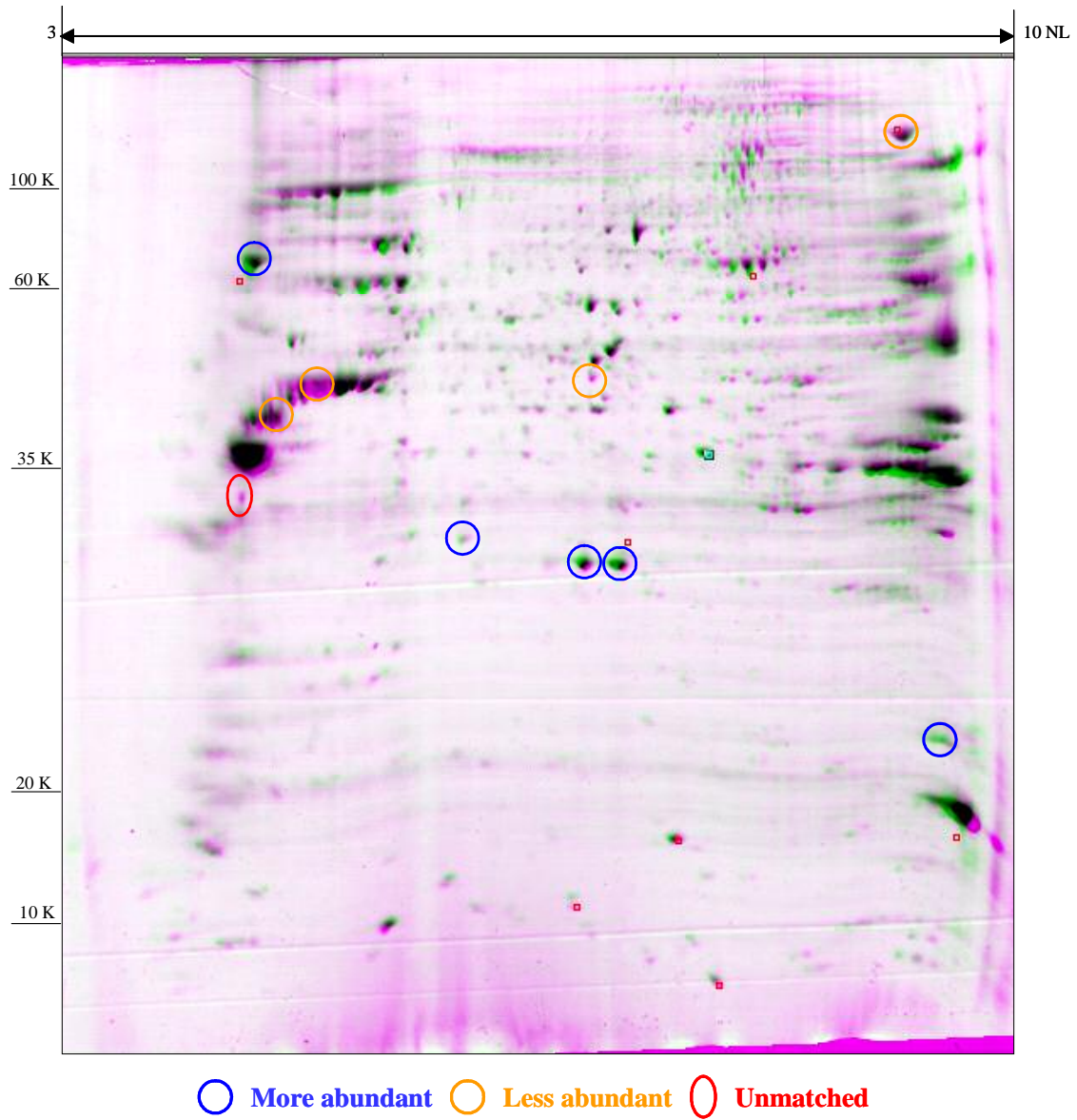
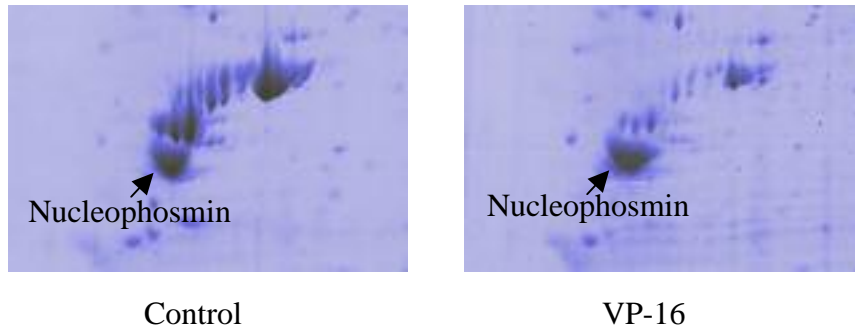
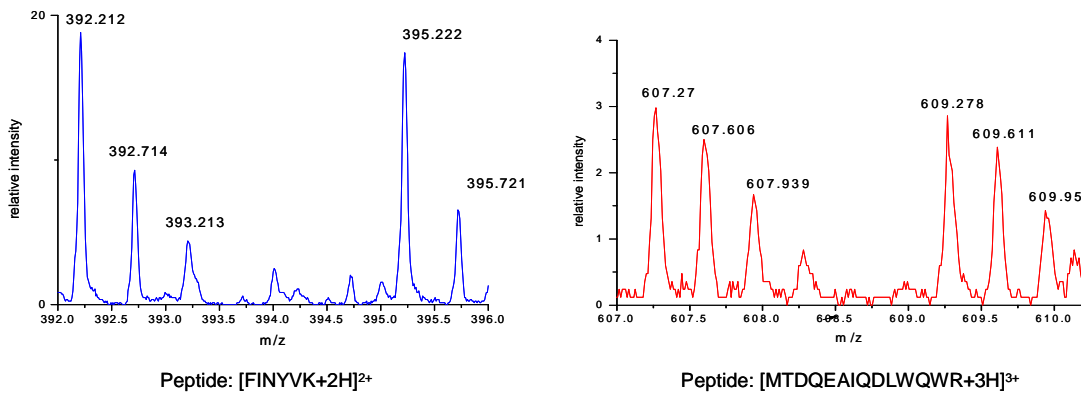


Figure 19: Densitometric comparison of 2-D gels of nuclear proteins: control vs. MCF-7/VP cells.

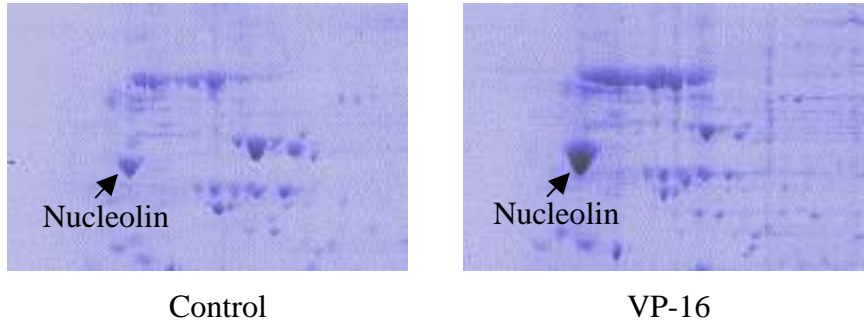


A: Enlarged images showing nucleophosmin with equal abundance

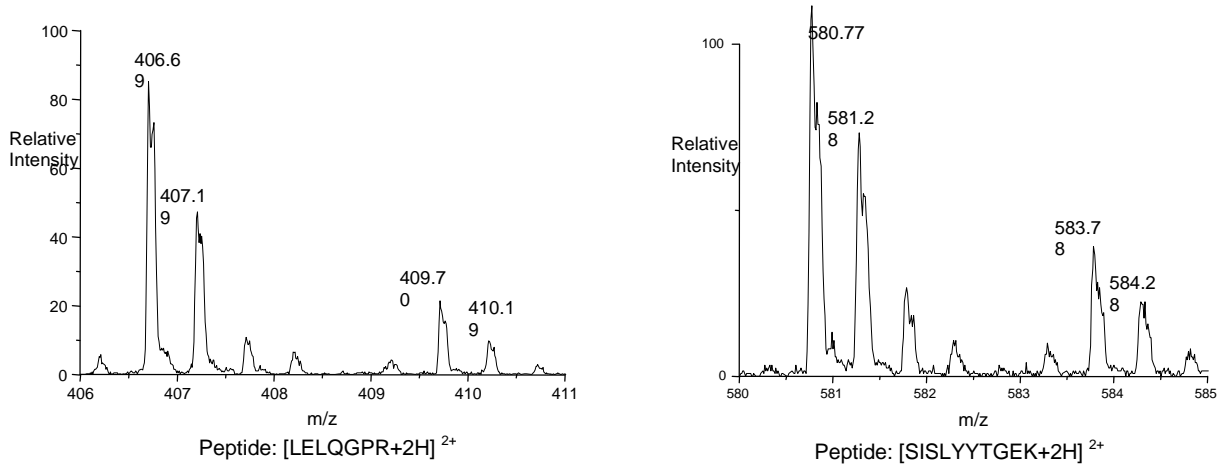


B: Metabolic labeling showing nucleophosmin with equal abundance

Figure 20: Nucleophosmin has no change in abundance in MCF-7/VP cells.

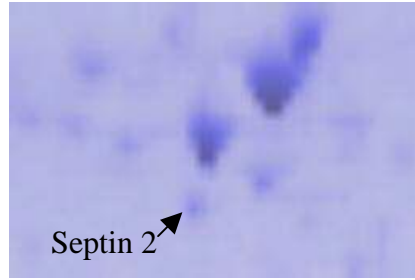
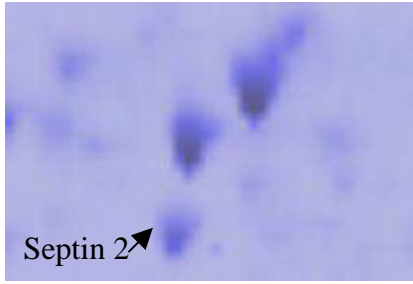


A: Enlarged images showing nucleolin with higher abundance

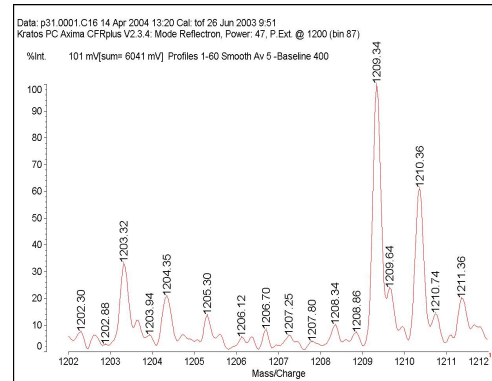
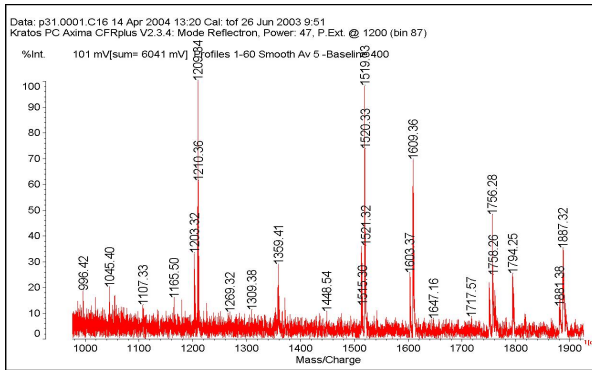


B: Metabolic labeling showing nucleolin with higher abundance

Figure 21: Nucleolin has a higher abundance in MCF-7/VP cells.



A: Enlarged images showing septin 2 with lower abundance



MALDI-TOF spectra of septin 2 in Isotope mixture

Peptide: [YLHDESGGLNR+H]<sup>+</sup>

B: Metabolic labeling showing septin 2 with lower abundance

Figure 22: Septin 2 has a lower abundance in MCF-7/VP cells.



Table 2: Relative abundance of nuclear proteins from MCF-7/VP cells.

<b>Protein ID</b>	<b>Ratio by comparative densitometry (VP-16/Control)</b>	<b>Ratio by stable isotope labeling (VP-16/Control)</b>
Nucleolin (76K)	2.78 ±0.23	3.15 ±0.26
40 S ribosomal protein SA	1.72 ±0.28	2.25 ± 0.28
Cyclophilin B	2.04 ±0.14	2.12 ±0.11
HMG-1	2.1 ±0.18	2.1 ± 0.18
Nucleolin (100K)	2.08 ±0.39	1.87±0.14
NHP-2 like protein 1	1.62 ±0.20	1.82±0.23
PP1A	1.88 ±0.19	1.79±0.22
HAT type B subunit	1.94 ±.016	1.71 ± 0.36
Guanine nucleotide-binding protein beta	1.05 ±0.12	1.60 ± 0.28
Structure maintainance of chromosome 1	1.3 ±0.13	1.56 ± 0.24
HMG-4L	1.44 ±0.16	1.56±0.08
Splicing factor 3A subunit 3	0.94 ±0.21	1.55 ± 0.28
snRNP-G	1.41 ±0.16	1.55 ± 0.40
Enhancer of rudimentaryhomolog	1.12±0.32	1.52±0.23
Breast carcinoma amplified sequence 2	1.38 ±0.23	1.51 ± 0.24
40S ribosomal protein S12	0.91 ±0.12	1.51±0.31
Single-stranded DNA-binding protein	1.04 ±0.15	1.5 ± 0.31
40S ribosomal protein S7	1.48 ±0.4	1.48 ± 0.26
THO complex subunit 3	1.23 ±0.18	1.44±0.21
ATP synthase alpha chain	1.06 ±0.02	1.44 ± 0.26
DEK oncogene	1.15 ±0.06	1.43±0.23
Annexin IV	1.14 ±0.15	1.41±0.15
Nuclear matrix pro 200	0.91 ±0.07	1.36 ± 0.31
HLA-B associated transcript-1	1.31 ±0.12	1.35 ± 0.25
NIF3L1BP1 protein	1.18 ±0.18	1.34 ± 0.23
ATP-dependent helicase DDX1	1.2±0.15	1.34 ± 0.10
U2 small nuclear ribonucleoprotein A'	0.91 ±0.10	1.33 ± 0.23
S100 calcium-binding protein A13	0.95 ±0.09	1.33 ± 0.31
U6 snRNA-associated Sm-like protein LSm7	1.1 ±0.09	1.32±0.11
hnRNP A2/B1	0.88 ±0.09	1.30 ± 0.24
Cleavage stimulation factor	0.8 ±0.09	1.30 ± 0.25

hnRNP Do	1.05 ±0.12	1.29±0.23
HSP 27	1.35 ±0.21	1.26 ± 0.12
Structure maintaince of chromosome 3	1.2 ±0.24	1.26 ± 0.09
Splicing factor PQ	0.78 ±0.16	1.26 ± 0.58
Set Protein	2.84 ±0.22	1.25±0.19
hnRNP Q	1.21±0.09	1.25±0.12
60 Sacidic ribosomal protein P2	0.7 ±0.09	1.25 ± 0.24
Elongation initiation factor 4A-1	1.17 ±0.13	1.24 ± 0.36
Prohibitin	1.72 ±0.12	1.24 ± 0.12
Stress-70 protein	1.18 ±0.15	1.23±0.13
Elongaton factor 1-gamma	1.04 ±0.17	1.23 ± 0.36
EF-2	1.3 ±0.21	1.2±0.15
BAF 53	1.17 ±0.12	1.20 ± 0.36
RuvB-like 1	0.63 ±0.06	1.17 ± 0.10
Ubiquitin	0.79 ±0.11	1.14 ± 0.19
hnRNP K (truncated)	0.68 ±0.07	1.14± 0.24
hnRNP L	0.89 ±0.09	1.13 ± 0.19
ATP-depedent DNA helicase II, 80kDa subunit	1.08 ±0.09	1.13±0.14
Stress-induced-phosphoprotein 1	0.98 ±0.06	1.09±0.12
SRP 54	1.0 ±0.08	1.09±0.05
S100 calcium-binding protein A16	0.61 ±0.19	1.09 ± 0.09
hnRNPA3	1.29 ±0.09	1.08 ± 0.36
Atp-depedent DNA helicase II, 70kDa subunit	0.99±0.12	1.08 ± 0.10
hnRNP K	1.1 ±0.06	1.07 ± 0.12
EF-1-beta	1.02±0.08	1.06±0.12
Annexin II	0.79±0.10	1.06 ± 0.24
Regulator of chromosome condensation	0.97 ±0.09	1.05±0.06
Elongation factor 1-alpha 1	1.66 ±0.15	1.05 ± 0.21
Aspartyl-tRNA synthetase	0.98 ±0.07	1.05 ± 0.05
Annexin V	0.21 ±0.04	1.05±0.21
60 S acidic ribosomal protein p0	0.79 ±0.12	1.02±0.03
RUV-like 2	1.56 ±0.21	1.00 ± 0.21
Proliferation-association pro 2G4	1.28 ±0.11	1.00 ± 0.16
Mitotic checkpoint protein BUB 3	1.22 ±0.13	1.00 ± 0.11
hnRNP A1	0.96±0.13	1.00 ± 0.22

ATP synthase beta chain	1.06 ±0.12	1.00 ± 0.16
Transcription factor NF-AT 45K chain	1.1 ±0.13	0.99 ± 0.30
Phenylanyl-tRNA synthetase beta chain	1.13±.015	0.99±0.12
CAF-1 subunit	0.88 ±0.12	0.98 ± 0.11
Signal recognition particle 9Kd Pro	0.87 ±0.09	0.97 ± 0.30
Heat shock cognate 71 kDa	0.57 ±0.10	0.96 ± 0.05
eIF-3 beta 2	0.85 ±0.13	0.96±0.30
Calcium-binding transporter	1.0 ±0.06	0.96±0.05
Nucleophosmin	0.96 ±0.12	0.95 ± 0.04
Copine III	1.39 ±0.16	0.95 ± 0.26
hnRNP A/B	0.98 ±0.16	0.94 ± 0.26
eIF4E	1.92 ±0.21	0.93 ± 0.09
Guanine Nucleotide -binding protein	0.81 ±0.20	0.87±0.05
Creatine kinase	1.68±0.26	0.86 ± 0.20
Actin gamma	1.32 ±0.16	0.85 ± 0.31
Splicing factor SC35	0.87 ±0.12	0.83 ± 0.20
Glutamate dehydrogenase 1	1.03 ±0.09	0.81 ± 0.12
U6 snRNA-associated Sm-like protein LSm2	0.69 ±0.10	0.77 ± 0.10
T-complex protein 1, beta	0.72 ±0.10	0.77 ± 0.23
snRNP-F	1.1 ±0.07	0.76±0.10
C1-THF synthase	0.64 ±0.13	0.74 ± 0.13
54 kDa DNA- and RNA-binding Protein	1.43 ±0.13	0.74 ± 0.18
HMG 2	0.61±0.05	0.72±0.12
Actin beta	0.79 ±0.14	0.69 ± 0.10
Delta coat protein	0.31 ±0.06	0.68 ± 0.09
HSP 70-1	0.47 ±0.12	0.67±0.07
Septin 7	0.81 ±0.11	0.64 ± 0.13
Annexin VI	0.53 ±0.07	0.62±0.07
Cytokeratin 8 (truncated)	0.47 ±0.10	0.45 ± 0.15
hnRNP H3	0.65 ±0.11	0.44 ± 0.10
Cytokeratin 19	0.58±0.09	0.43 ± 0.06
PARP-1	0.62 ±0.10	0.4 ±0.06
Septin 2	0.44 ±0.04	0.26±0.04
Alpha tropomyosin	unamtched	0.11±0.03

### **Nuclear protein expression profile of MCF-7/MX cells**

The nuclear proteins from mitoxantrone resistant MCF-7 cells were analyzed by both densitometric comparison and metabolic labeling methods. However, a limited number of spots were analyzed by the metabolic labeling method guided by the results of densitometric comparisons. Prohibitin, 78K glucose-regulated protein (GRP78), HMG-1, 40S ribosomal protein SA, and nucleolin were found to be significantly more abundant (more than 2 fold). Cytokeratin19, cytokeparin 8, septin 2, PARP-1 and alpha tropomyosin were found to be less abundant. Figure 23 shows a 2-D gel map of nuclear proteins from MCF-7/MX cells. Figure 24 shows a 2-D gel map of mixture of nuclear proteins from MCF-7/MX cells and isotope labeled control MCF-7 cells. Figure 25 shows the results of the densitometric comparison of a pair of 2-D gel arrays of nuclear proteins from control and MCF-7/MX cells made using Compugen software. Identified proteins with significant changes in abundance are circled. GRP78 was not shown in the annotated 2-D gel map of nuclear proteins from control MCF-7 cells because it was not checked initially. Retrospective inspections indicated that there was a weak spot on its position in 2-D gel of control sample. Table 3 provides results for proteins analyzed with both methods.

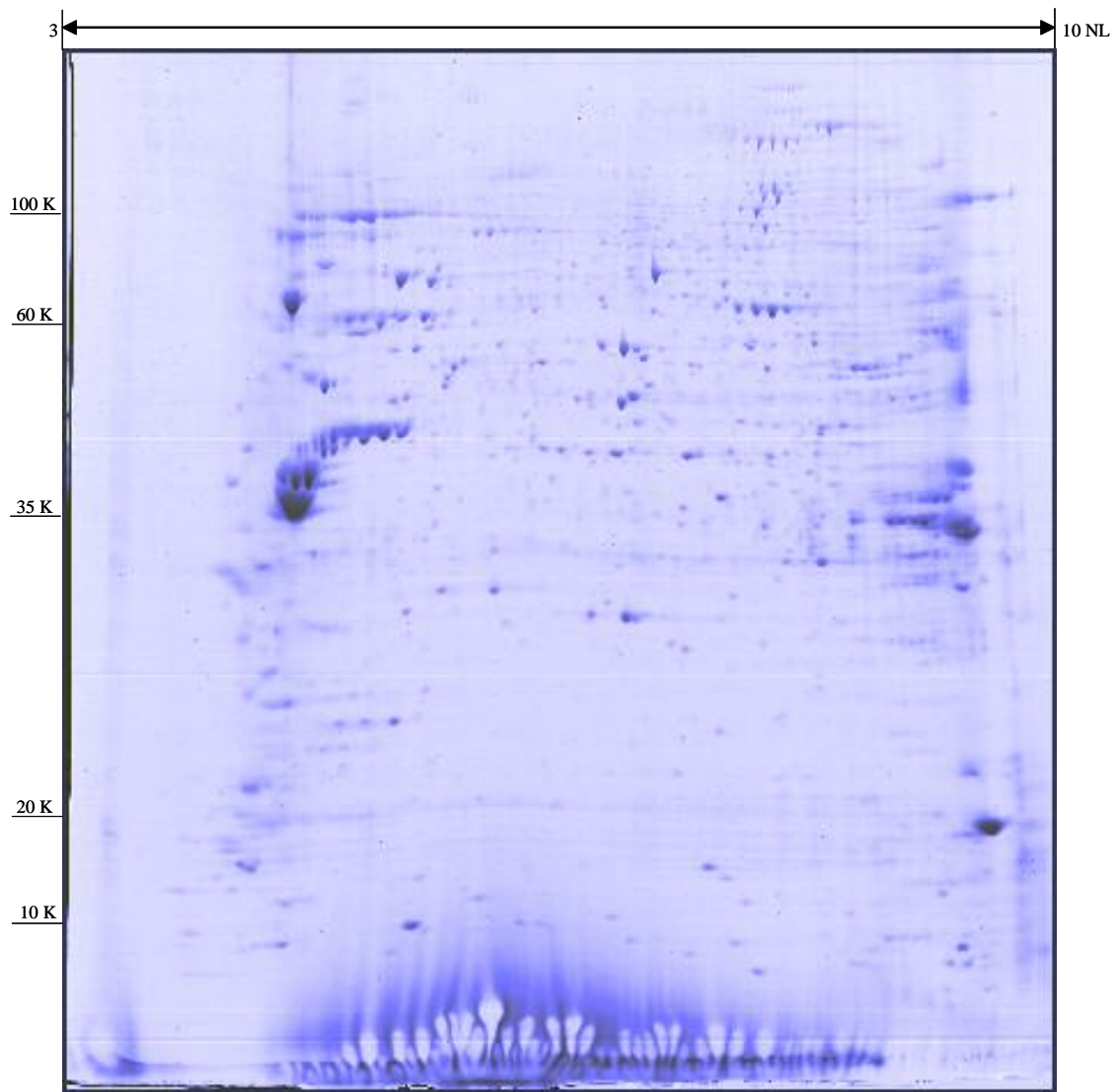


Figure 23: 2-D gel map of nuclear proteins from MCF-7/MX cells.

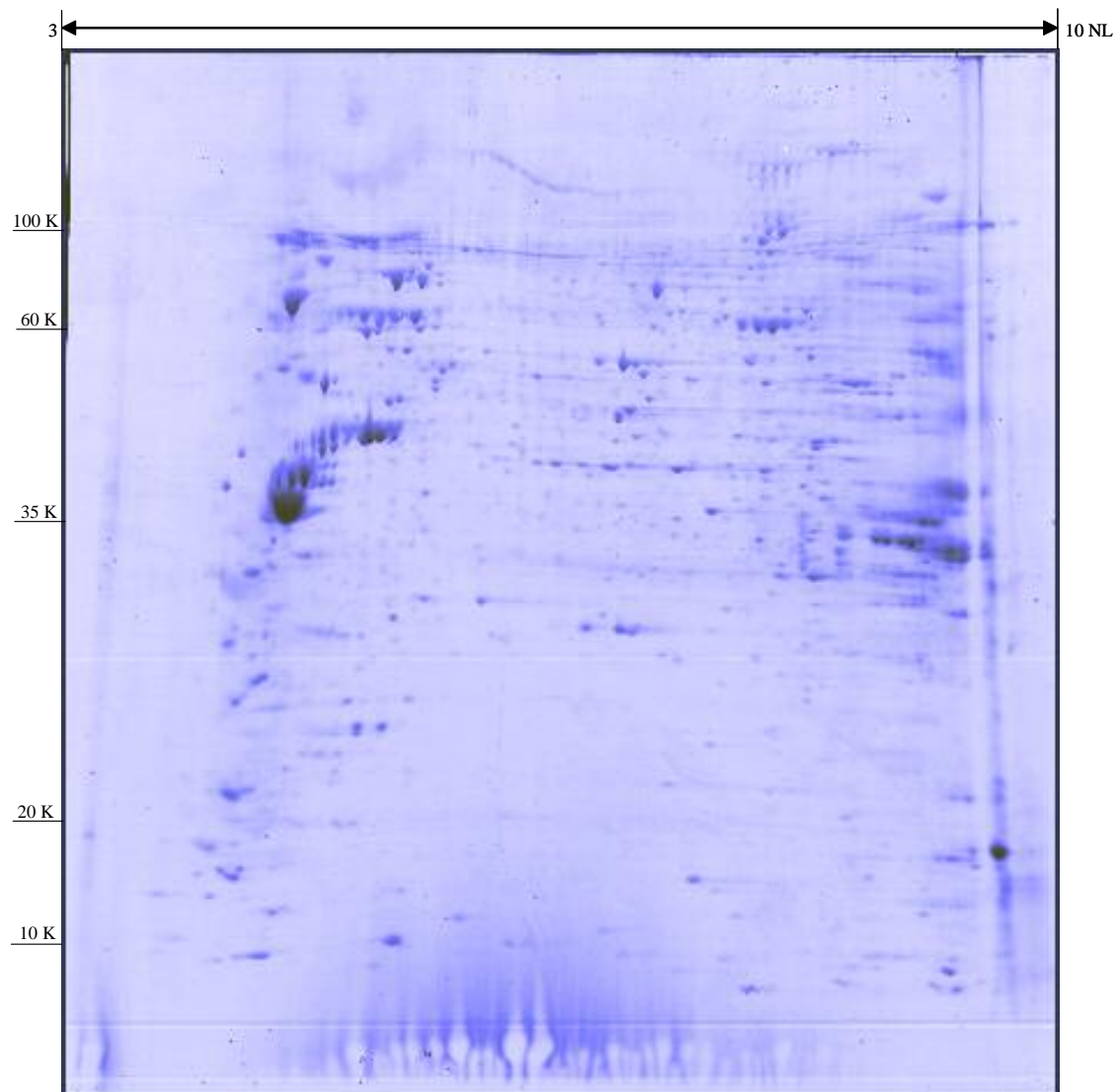


Figure 24: 2-D gel map of nuclear proteins from MCF-7/MX cells and isotope labeled control MCF-7 cell mixture.

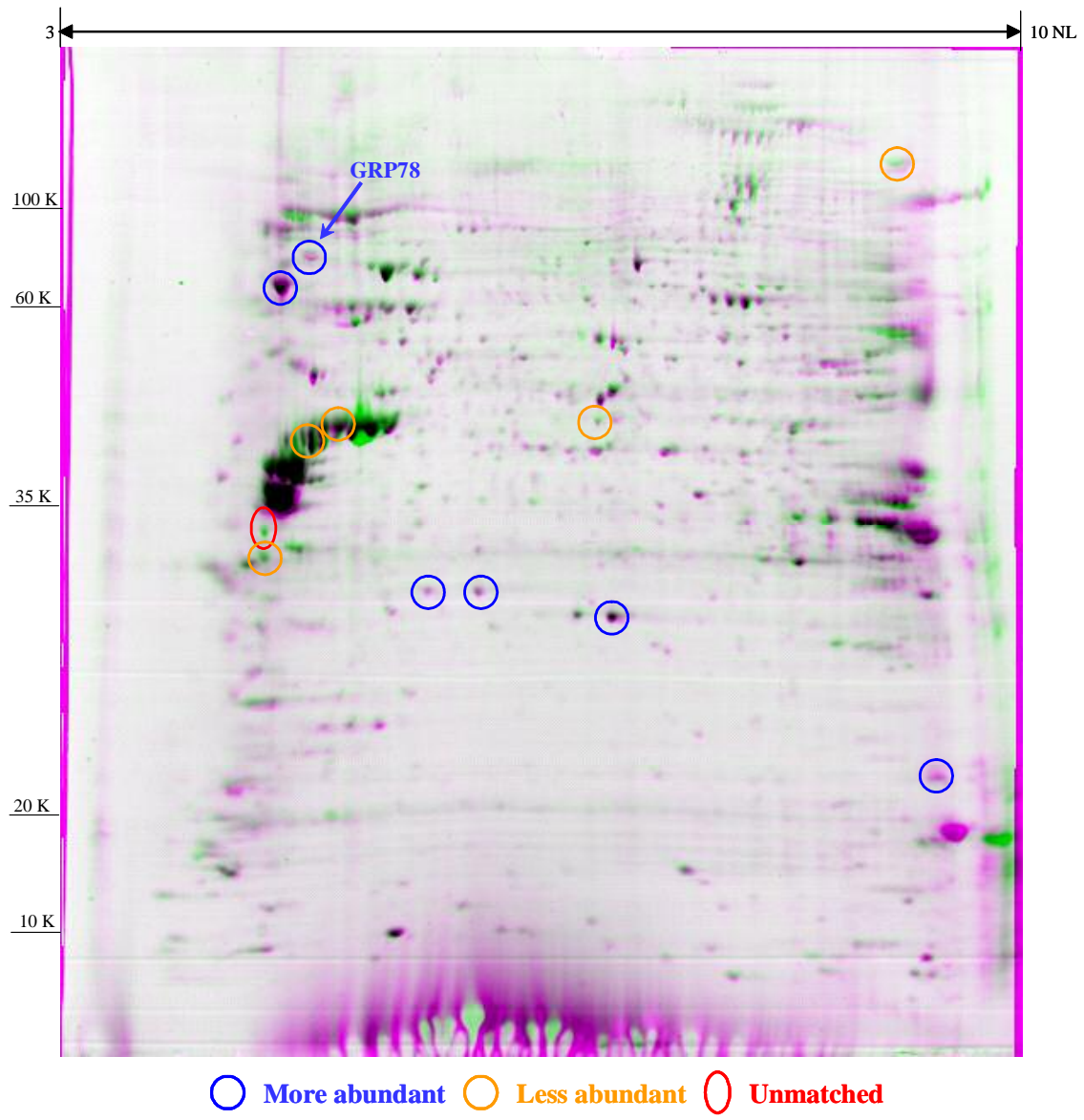


Figure 25: Densitometric comparison of 2-D gels of nuclear proteins: control vs. MCF-7/MX cells.

Table 3: Relative abundance of nuclear proteins from MCF-7/MX cells.

<b>Protein ID</b>	<b>Ratio by comparative densitometry (MTX/Control)</b>	<b>Ratio by stable isotope labeling (MTX/Control)</b>
78kGlucose-regulated protein	5.53±0.69	4.91±0.46
Prohibitin	2.81±0.31	3.69±0.33
HMG-1	1.52±0.16	2.56±0.18
40 S ribosomal protein SA	1.74±0.19	2.35±0.15
Cyclophilin B	1.66±0.45	2.22±0.16
Nucleolin(70K)	1.98±0.24	2.18±0.16
hnRNP Do	1.60±0.17	1.82±0.13
Nuclear matrix protein 200	1.47±0.40	1.75±0.20
Cleavage stimulation factor	1.49±0.26	1.46±0.14
Mitotic checkpoint protein BUB 3	1.68±0.32	1.42±0.11
Proliferation-association pro 2G4	1.58±0.14	1.42±0.13
Stress-70 protein	1.42±0.16	1.34±0.13
HSP 27	0.82±0.17	1.31±0.23
Elongaton factor 1-gamma	0.85±0.23	1.31±0.11
Cleavage stimulation factor	1.89±0.12	1.26±0.21
Atp-depedent DNA helicase II, 70kDa subunit	1.21±0.21	1.25±0.15
Enhancer of rudimentary homolog	1.02±0.11	1.2±0.14
hnRNPA3	1.33±0.17	1.13±0.26
hnRNP L	1.11±0.19	1.09±0.12
Nucleophosmin	0.88±0.18	1.02±0.17
Set Protein	1.55±0.22	0.99±0.22
Septin 7	1.2±0.19	0.97±0.16
Guanine nucleotide-binding protein beta	1.0±0.16	0.95±0.11
Heat shock cognate 71 kDa	0.68±0.23	0.92±0.10
Breast carcinoma amplified sequence 2	1.23±0.31	0.91±0.12
CAF-1 subunit	0.76±0.24	0.81±0.15
Actin beta	0.69±0.10	0.66±0.20
Cytokeratin 19	0.58±0.14	0.53±0.09
Cytokeratin 8 (truncated)	0.43±0.06	0.49±0.05
PARP-1	0.30±0.13	0.46±0.06
EF-1-beta	0.28±0.09	0.36±0.06
Septin 2	0.22±0.03	0.11±0.03
Alpha tropomyosin	unmatched	0.10±0.02



### **Nuclear protein expression profile of MCF-7/AdrVp cells**

The nuclear proteins from MCF-7/AdrVp were also analyzed by both densitometric comparison and isotope labeling methods. Mitotic checkpoint protein BUB 3 and cyclophilin B were found more abundant. Septin2, septin7, cytokeatin19, cytokeatin 8 and alpha tropomyosin were found to be less abundant. Figure 26 shows a 2-D gel map of nuclear proteins from MCF-7/AdrVp cells. Figure 27 shows a 2-D gel map of nuclear proteins from control isotope labeled MCF-7 cells and MCF-7/AdrVp cells. Figure 28 shows the results of densitometric comparison of a pair of 2-D gel arrays of nuclear proteins from control and MCF-7/AdrVp cells made using Compugen software. Identified proteins with significant abundance change are circled. Table 4 provides relative abundances of some nuclear proteins in MCF-7/AdrVp cells.

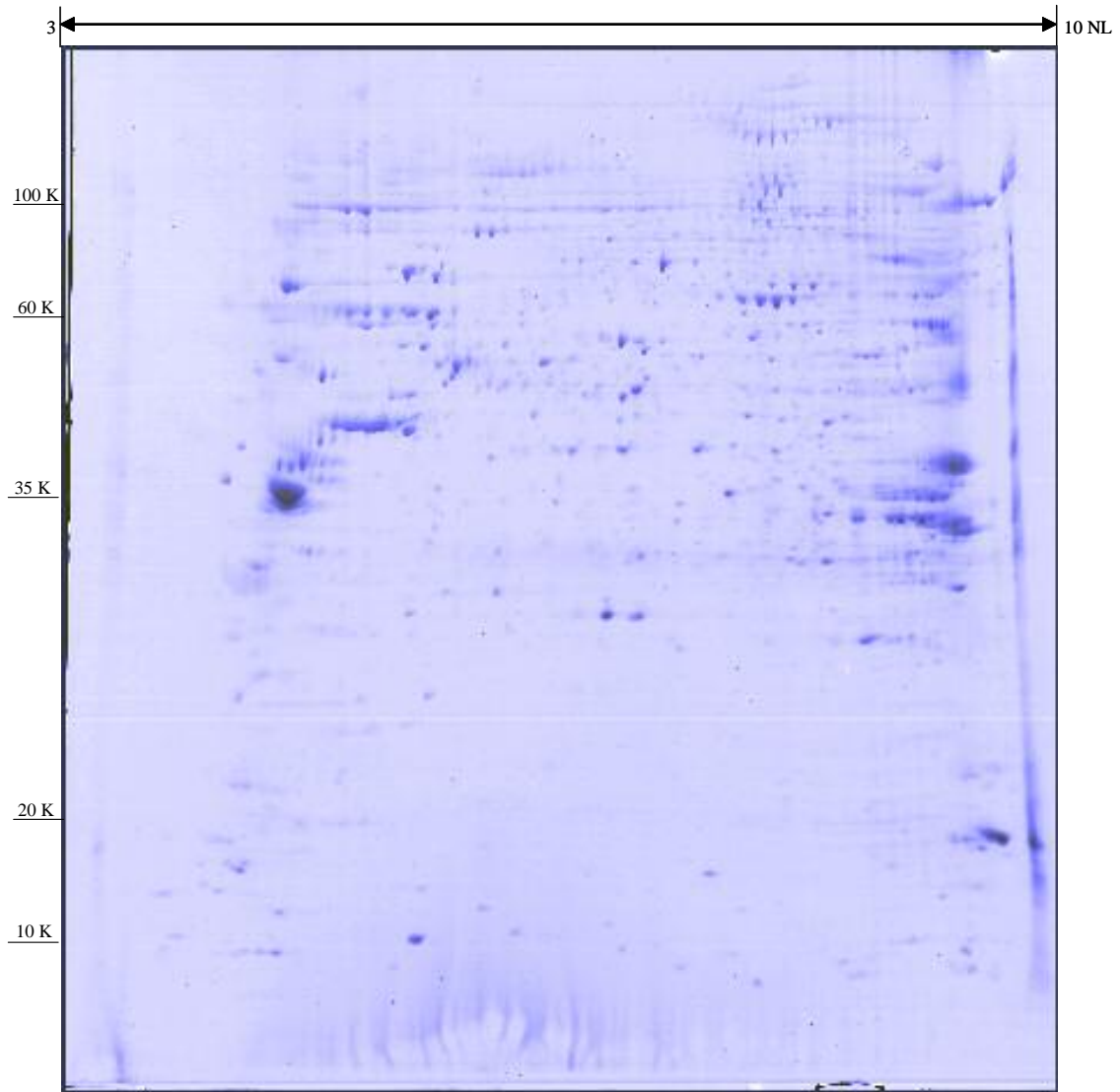


Figure 26: 2-D gel map of nuclear proteins from MCF-7/AdrVp cells.

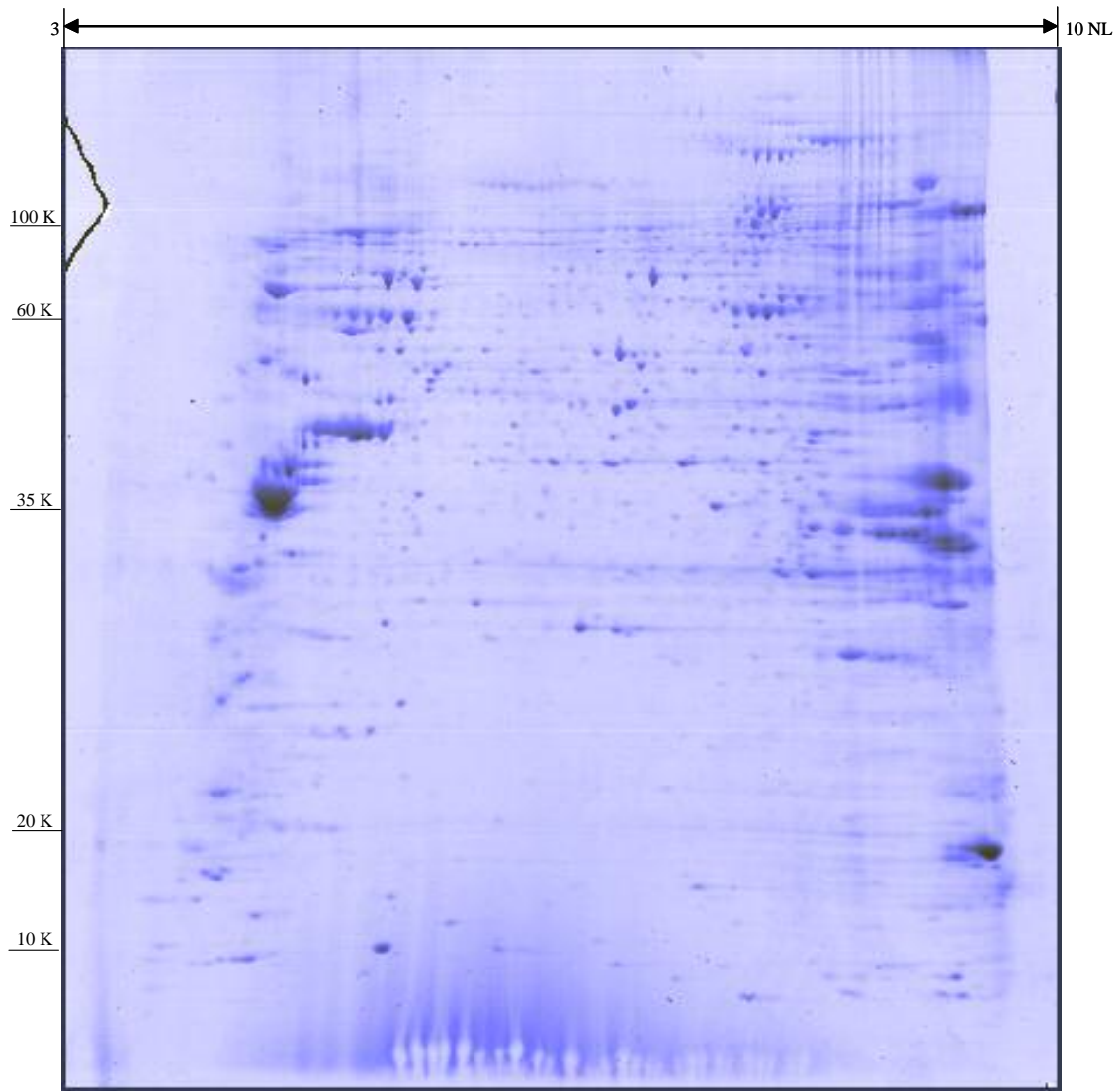


Figure 27: 2-D gel map of nuclear proteins from MCF-7/AdrVp cells and isotope labeled control MCF-7 cell mixture.

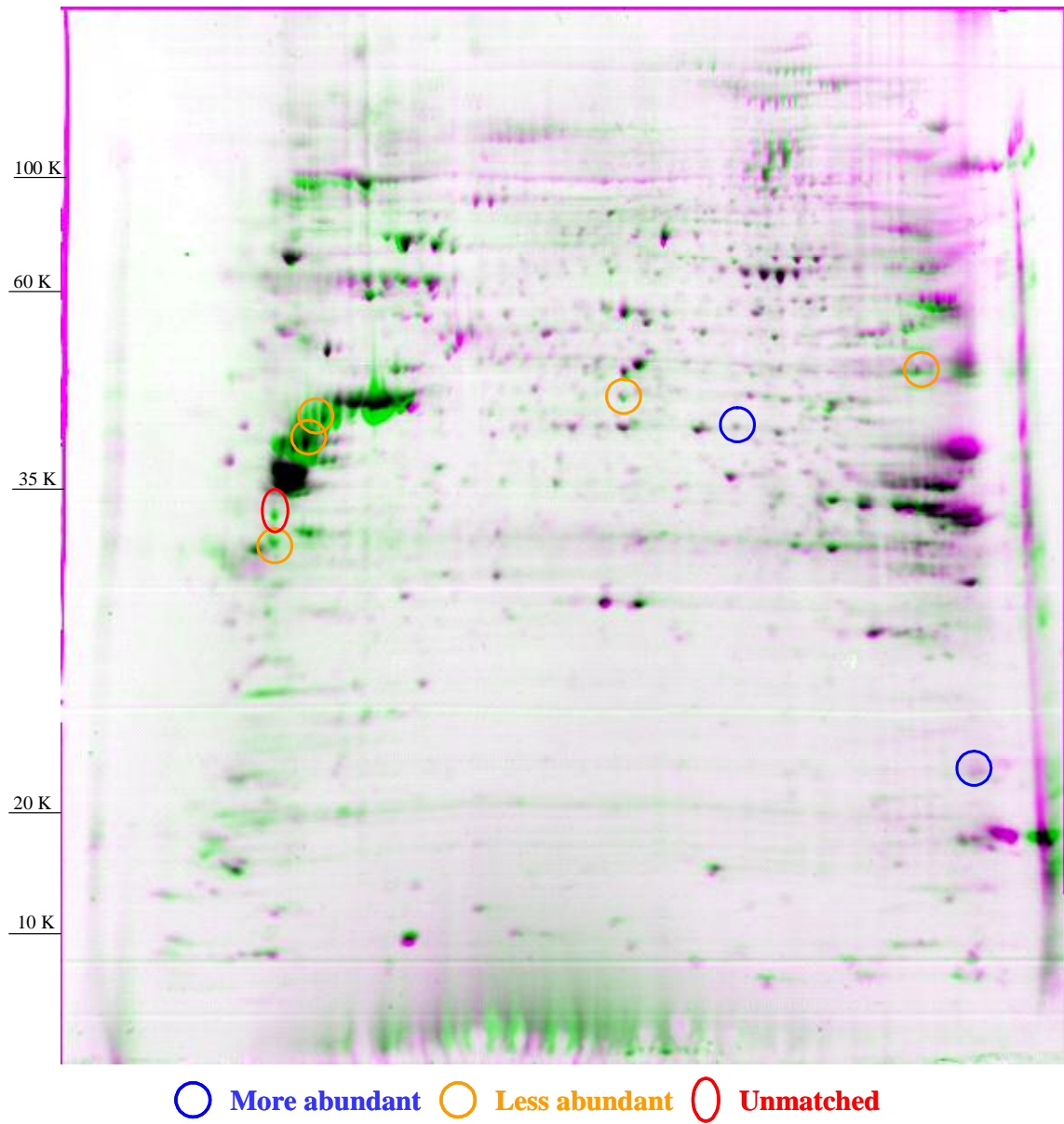


Figure 28: Densitometric comparison of 2-D gels of nuclear proteins: control vs. MCF-7/AdrVp cells.

Table 4: Relative abundance of nuclear proteins from MCF-7/AdrVp cells.

<b>Protein ID</b>	<b>Ratio by comparative densitometry (AdrVp/Control)</b>	<b>Ratio by stable isotope labeling (AdrVp/Control)</b>
Cyclophilin B	1.92±0.22	2.32±0.16
Mitotic checkpoint protein BUB 3	2.01±0.19	2.23±0.13
hnRNP K (truncated)	1.75±0.21	1.56±0.35
HMG 2	1.66±0.24	1.66±0.34
Creatine kinase	1.65±0.27	0.82±0.16
Regulator of chromosome condensation	0.84±0.14	1.42±0.23
RuvB-like 1	1.35±0.19	1.42±0.21
ATP synthase beta chain	1.53±0.16	1.35±0.16
40 S ribosomal protein SA	1.33±0.25	1.34±0.20
snRNP-G	1.23±0.17	1.32±0.19
HMG-1	1.68±0.30	1.28±0.13
hnRNP A1	0.64±0.16	1.25±0.24
Elongation initiation factor 4A-1	1.21±0.14	1.25±0.14
Nuclear matrix pro 200	1.12±0.14	1.25±0.16
EF-2	1.43±0.27	1.25±0.16
HLA-B associated transcript-1	1.04± 0.19	1.24±0.16
Splicing factor PQ	0.92±0.09	1.21±0.14
ATP-depedent DNA helicase II, 70kDa subunit	1.01±0.19	1.11±0.17
HSP 27	1.27±0.16	1.09±0.25
C1-THF synthase	1.03±0.21	1.06±0.10
Enhancer of rudimentaryhomolog	1.31±0.16	1.02±0.13
Breast carcinoma amplified sequence 2	0.83±0.24	1.02±0.19
ATP-dependent helicase DDX1	0.87±0.21	1.02±0.12
hnRNP A/B	0.89±0.16	0.99±0.12
Splicing factor 3A subunit 3	0.66 ±0.14	0.98±0.07
eIF4E	1.03±0.19	0.96±0.14
BAF 53	1.31± 0.16	0.96±0.10
CAF-1 subunit	1.38±0.22	0.95±0.12
Prohibitin	0.77±0.13	0.87±0.14
40S ribosomal protein S12	0.66±0.11	0.86±0.09
54 kDa DNA- and RNA-binding Protein	0.84 ±0.16	0.86±0.21

S100 calcium-binding protein A16	0.91±0.17	0.85±0.14
hnRNP L	1.03±0.16	0.83±0.09
40S ribosomal protein S7	0.91±0.23	0.82±0.08
Annexin II	0.59±0.06	0.82±0.09
hnRNP A2/B1	0.86±0.18	0.82±0.10
Elongation factor 1-alpha 1	1.14±0.22	0.82±0.20
Cleavage stimulation factor	1.23±0.16	0.82±0.14
RUV-like 2	0.93 ±0.21	0.82±0.14
Nucleolin(76K)	0.69±0.16	0.81±0.16
Nucleolin(100K)	0.79 ±0.21	0.79±0.11
S100 calcium-binding protein A13	0.69±0.24	0.76±0.14
Aspartyl-tRNA synthetase	0.68±0.22	0.76±0.12
Nucleophosmin	1.1±0.21	0.74±0.15
U6 snRNA-associated Sm-like protein LSM7	1.21±0.13	0.7±0.09
P10 protein	0.66±0.09	0.69±0.09
PARP-1	0.93±0.29	0.65±0.10
Actin beta	0.68±0.15	0.65±0.09
Proliferation-association pro 2G4	0.84±0.26	0.58±0.07
Glutamate dehydrogenase 1	0.65±0.14	0.58±0.06
HMG-4L	0.75±0.16	0.57±0.06
Septin 2	0.65±0.21	0.49±0.04
Septin 7	0.36±0.10	0.32±0.07
Cytokeratin 19	0.33±0.10	0.25±0.03
Cytokeratin 8 (truncated)	0.37±0.15	0.25±0.04
EF-1-beta	0.19±0.05	0.14±0.03
Alpha tropomyosin	unmatched	0.09±0.01

### **Nuclear protein expression profile of MCF-7/Adr cells**

The nuclear proteins from MCF-7/Adr were analyzed only with densitometric comparison method. The expression profile of nuclear proteins from MCF-7/Adr was found to be dramatically different from that of control MCF-7 cells as expected. Figure 29 shows a 2-D gel map of nuclear proteins from MCF-7/Adr cells. Figure 30 shows the results of densitometric comparison of a pair of 2-D gel arrays of nuclear proteins from control and MCF-7/AdrVp cells made using Compugen software. About 1/5 of the visible proteins that are expressed in control MCF-7 cells are not detected in MCF-7/Adr cells. There are also spots that are not detected from control MCF-7 cells detected from mcf-7/Adr. These spots are marked as “unmatched”.

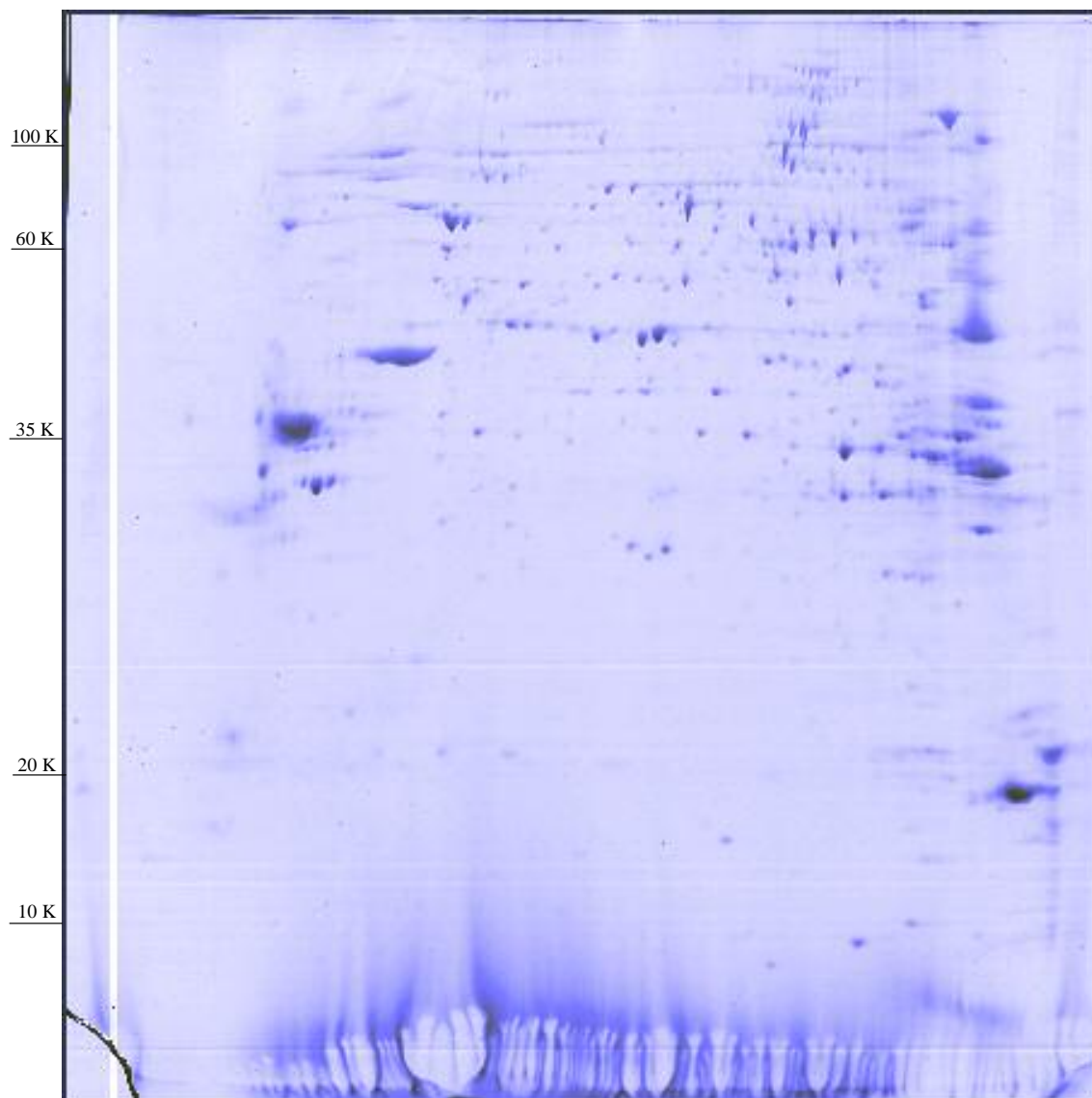


Figure 29: 2-D gel map of nuclear proteins from MCF-7/Adr cells.



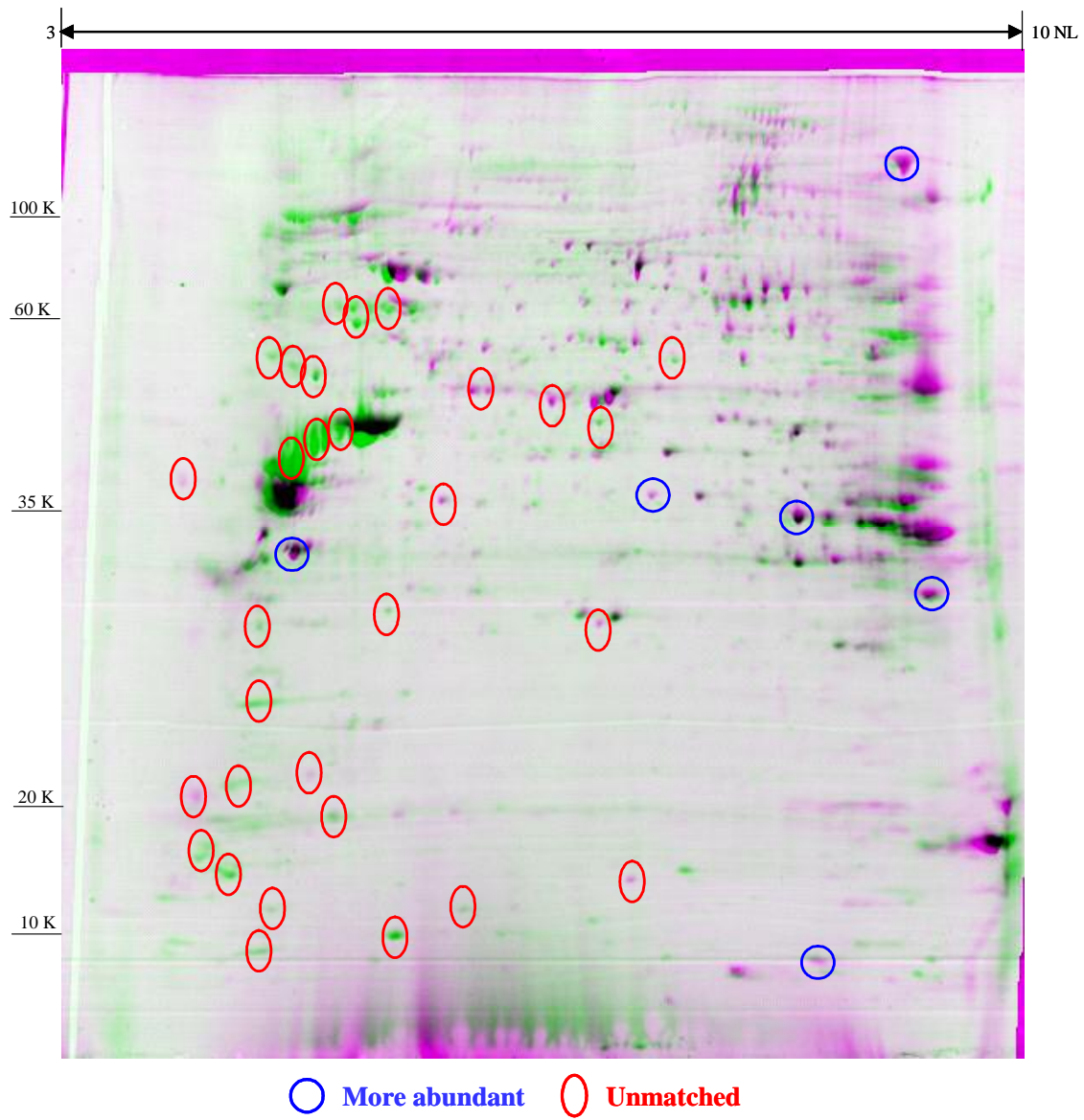


Figure 30: Densitometric comparison of 2-D gels of nuclear proteins: control vs. MCF-7/Adr cells.

Table 5: Nuclear proteins having abundance changes in MCF-7/Adr cells.

<b>Protein ID</b>	<b>Ratio by comparative densitometry (Adr/Control)</b>
Annexin IV	2.76±0.54
Annexin V	2.62±0.41
FK506-binding protein 3	3.12±0.44
hnRNP H3	3.65±0.51
P10 protein	2.64±0.34
PARP-1	3.46±0.61
40S ribosomal protein S12	um
60 Sacidic ribosomal protein P2	um
ATP synthase beta chain	um
Breast carcinoma amplified sequence 2	um
CAF-1 subunit	um
Cytokeratin 19	um
Cytokeratin 8 (trunk)	um
DEK oncogene	um
Enhancer of rudimentary homolog	um
HAT type B subunit	um
hnRNP C	um
hnRNP K	um
S100 calcium-binding protein A13	um
Septin 2	um
Septin 6	um
Set Protein	um
snRNP-F	um
U6 snRNA-associated Sm-like protein LSm3	um
U6 snRNA-associated Sm-like protein LSm7	um

um - Unmatched

## Chapter 5: Discussion

### 2-D gel electrophoresis and protein identification

We have developed a method to isolate nuclei and extract soluble nuclear proteins from MCF-7 cells. The nuclear proteins were subjected to 2-D gel electrophoresis. Many of the protein spots were identified by peptide mass fingerprinting and microsequencing. More than 90% of these proteins are classically cataloged as nuclear proteins or proteins that may present in the nucleus. Some of the non-nuclear proteins have also been found in other researchers' nuclear protein preparation (119-121). For example, ATP synthase beta chain (spot 104) is classified as a mitochondrial protein, it has also been found in directed proteomics analysis of human nucleolus by Anderson et al (2002). This may indicate that this protein is closely associated with the nucleus. It needs to be pointed out that further purification often causes low recovery of samples in organellar proteomics (122-123). A balance must be found between sample purity and recovery. Our samples contained highly enriched soluble nuclear proteins. A 2-D gel map of soluble nuclear proteins has been obtained in this research. It can be used for further study of soluble nuclear proteins in MCF-7 cells.

### Densitometry vs. isotope labeling

We used densitometric comparisons and isotope labeling methods to analyze differentially abundant soluble nuclear proteins in drug resistant and susceptible MCF-7 cells. The results by the two methods are consistent (Table 2, 3, 4) in most cases. Two-dimensional gel electrophoresis remains the technique of choice for proteomics studies. It

can separate and provide a global view of many proteins in a gel. After the gel images are digitized, they can be compared conveniently with a very low cost. For densitometric comparison, the reproducibility of the sample preparations is crucial. The poor quality of isoelectric focusing of extremely basic proteins poses a special problem for determining relative abundances. For a protein with extremely high abundance, computer software sometimes can not properly recognize its spot as a single protein. This may also cause comparison errors. The densitometric comparison also can not deal well with a spot containing more than one protein. Isotope labeling methods can minimize process variations. The relative abundances of several proteins in one spot can be differentiated. However, the high cost of isotopes is a disadvantage. It is only applicable to cultured cells.

### **Biological implications of abundance changes**

We have identified about a dozen proteins whose abundance is changed in each of the resistant MCF-7 cell lines resistant to etoposide, mitoxantrone, and adriamycin in the presence of verapamil. Table 6 summarizes the abundance changes in the three drug resistant cell lines. Those proteins may play important roles in conferring drug resistance in MCF-7 cancer cells. Their biological functions and potential implications are discussed in the following paragraphs. In contrast, expression profile of soluble nuclear proteins from MCF-7/Adr cells is dramatically different from that of control MCF-7 cells. About 20 proteins identified in control MCF-7 cells are not detected in MCF-7/Adr cells (unmatched spots). Profiling of cytosolic proteins in our lab has also led to the suggestion that the cell line has an uncertain identity (69). Thus the results from this cell line are excluded from further consideration.

Table 6: Summary of abundance changes in three drug resistant MCF-7 cell lines\*.

Protein	Cell line	MCF-7/VP	MCF-7/MX	MCF-7/AdrVp
	78 k glucose -regulated protein ↑		nd	4.91±0.46
prohibitin ↑		1.24±0.12	3.69±0.33	0.95±0.11
HMG-1 ↑		2.1±0.18	2.56±0.18	1.28±0.13
40S ribosomal protein SA ↑		2.25±0.28	2.35±0.18	1.34±0.14
Cyclophilin B ↑		2.12±0.11	2.22±0.16	2.32±0.16
Nucleolin(76K) ↑		3.15±0.26	2.18±0.16	0.81±0.16
Nucleolin (100K) ↑		1.87±0.14	1.58±0.18	0.79±0.11
Mitotic checkpoint protein BUB 3 ↑		1.00±0.11	1.42±0.11	2.23±0.13
Cytokeratin 19 ↓		0.45±0.15	0.53±0.09	0.25±0.03
Cytokeratin 8 ↓		0.43±0.06	0.49±0.05	0.25±0.04
Septin 2 ↓		0.26±0.04	0.11±0.03	0.49±0.04
EF-1-beta ↓		1.06±0.12	0.36±0.06	0.14±0.03
Alpha tropomyosin ↓		0.11±0.03	0.10±0.02	0.09±0.01
Septin 7 ↓		0.64±0.11	0.97±0.11	0.32±0.07
PARP-1 ↓		0.40±0.06	0.46±0.06	0.65±0.10

Higher abundance ↑      Lower abundance ↓

\*Based on metabolic labeling    nd: not determined

### **Lower abundance of poly [ADP-ribose] polymerase (PARP)-1**

PARP-1 (spot 151) was found to be significantly less abundant in MCF-7/VP, MCF-7/MX than in control MCF-7 cells, with ratios of  $0.40 \pm 0.06$  and  $0.46 \pm 0.06$ , respectively. It also has a lower abundance in MCF-7/AdrVp ( $0.65 \pm 0.10$ ), but does not meet the 2-fold threshold that we set as a significant change.

PARP-1 is a 114 kDa nuclear zinc-finger enzyme, catalyzing the attachment of ADP-ribose units to target proteins. It targets proteins directly involved in DNA metabolism and regulation of chromatin structure, such as topoisomerases, DNA ligases, or DNA polymerases (124). PARP-1 activity increases substantially in response to genotoxic stress. It has been found to be involved in DNA repair (125-127). PARP-1 acts as a sensor of DNA damage, and forms a functional complex with XRCC1 protein in base excision repair (126). It also provides ATP for the DNA ligation step (127).

It has also been shown that PARP-1 is involved in cell death (129-134). PARP-1 seems to signal a p53-independent cell death pathway (130). Chirugi and Yu et al (2002) have proposed a PARP-1-dependent signaling pathway in apoptosis (131-132). This pathway starts with activation of PARP-1 after genotoxic stimuli. PARP-1 activation leads to massive synthesis of poly [ADP-ribose], which subsequently causes  $\text{NAD}^+$  depletion. Poly [ADP-ribose] formation and  $\text{NAD}^+$  depletion trigger mitochondrial depolarization and release of a mitochondrial apoptosis-inducing factor (AIF) that promotes programmed cell death through a caspase-independent pathway. It is controversial whether this is necrosis or apoptosis (132). However, the result of the process is cell death. Recent studies show DNA-damaging agents selectively induce

tumor death through this pathway independent of p-53 or Bcl-2 family proteins (133-134). In addition, independent research has shown that PARP-1 is up-regulated at the early stage of apoptosis induced by UV irradiation (135). Mouse cells lacking PARP-1 has been observed to have increased resistance to anticancer therapy (136).

Overproduction of PARP-1 has been implicated in the molecular pathway leading to cell death by energy depletion following stress (137). In the present research, lower abundance of PARP-1 is closely correlated with drug resistance in MCF-7 cells. It is potentially responsible for drug resistance conferred by MCF-7 cells by repressing cell death through this signaling pathway. It is likely that the low level of PARP-1 can not fulfill the requirement of PARP-1 activation at the first step.

### **Lower abundance of cytoskeletal proteins**

Cytoskeletal proteins, including alpha tropomyosin (spot 45), cytokeratin 19 (spot 61-63), cytokeratin 8 (spot 66-68) and septin 2 (spot 88), were found to be less abundant in MCF-7/VP, MCF-7/MX, and MCF-7/AdrVp cells than in control MCF-7 cells. Septin 7 was found to be less abundant in MCF-7/AdrVp only. Cytoskeletal functions range from cellular architecture to signal transduction and apoptosis (138-141). Cytokeratins are common contaminants from human fingers, in our experiments, the finding of isotope labeled cytokeratins ruled out the possibility of contamination. Several papers have linked differential expression of those proteins to drug resistance (142-144). Cytokeratins and alpha tropomyosin have been reported to be up- and down-regulated in breast cancer cells than normal breast cells (145). Tropomyosin was found to be down-regulated in drug resistant SNU 638 gastric cancer cells compared to their parental cells (144). However, the nucleus is not the major subcellular location of the proteins. The results

from this research may indirectly reflect the abundance of the proteins in the whole cells. Analysis of whole cell lysate can give more conclusive results.

### **Higher abundance of nucleolin**

Nucleolin is a multifunctional nuclear protein with high abundance. Two forms of nucleolin, differing in the amino acid composition with N-terminal domain, 100 K Da and 76K Da (Spot126, spot 159), were found in 2-D gel map from MCF-7 Cells. Nucleolin of 76K Da was found to have significantly higher abundance in MCF-7/VP and MCF-7/MX cells, accompanied by moderately higher abundance of 100 KDa nucleolin.

Nucleolin is a highly abundant nuclear protein. It can interact with DNA or RNA or proteins. Nucleolin exhibits intrinsic self-cleaving, DNA helicase, RNA helicase and DNA-dependent ATPase activities (146-148). Nucleolin also acts as a sequence-specific RNA binding protein, an autoantigen (149), and as the component of a B cell specific transcription factor (150). Its activities are regulated by proteolysis, methylation, ADP-ribosylation, and phosphorylation (147). It has been implicated to be involved directly or indirectly in apoptosis, chromatin structure, DNA replication, recombination, repair, ribosome biogenesis and maturation, nucleolar-cytoplasmic transport, cytokinesis, embryogenesis, nucleogenesis, cell proliferation and growth, and transcriptional repression (135,149-156). It is fundamental to the survival and proliferation of cells. The regulation of all these functions of a single protein is a challenging puzzle. As its contribution to drug resistance in cancer cells, we focus on its functions in apoptosis and DNA repair.



Apoptosis in U937 leukemia cells is accompanied by lower level and localization alteration of nucleolin within the nucleus (135). It is suggested that apoptosis in HL-60 cells induced by taxol and okadaic acid treatment is through a process that involves down-regulation of nucleolin and destabilization of bcl-2 mRNA. Nucleolin was identified as an AU-rich element binding protein involved in stabilization of mRNA of bcl-2, a known apoptosis inhibitor (152). Nucleolin has also been identified as a genotoxic stress-responsive protein. Nucleolin expression levels were found to be increased in Chinese hamster ovary (CHO) cells after UV or ionizing radiation exposure (149). It has been reported to form a complex with replication protein A after cell stress to prevent initiation of DNA replication and mobilize DNA repair (155). The C-terminal domain of nucleolin accelerates nucleic acid annealing. Its ability to promote homologous DNA pairing in vitro may also indicate it has similar function in vivo (151). It has been demonstrated that nucleolin interacts with topoisomerase I. It is not known if nucleolin interacts with topoisomerase II, which is the target of the VP-16 and mitoxantrone (156-157). Taken together, the up-regulation of nucleolin may inhibit apoptosis and enhance DNA repair in drug resistant MCF-7 cells.

### **Higher abundance of high mobility group protein-1(HMG-1)**

HMG-1(also called HMGB-1) (spot29, 30) was found more abundant in MCF-7/VP and MCF-7/MX cells. HMG1 is a non-histone chromosomal protein encoded by HMGB1 gene (158). It binds DNA without sequence specificity, but has a high affinity for bent or distorted DNA, and bends linear DNA. It seems to play an architectural role in the assembly of nuclear protein complex in a variety of biological processes, such as DNA

replication, transcription, recombination, and repair, but the mechanism of these processes is not clear(159). It has been suggested that HMGB1 is involved in chromatin structural modulation in global nuclear events through its interaction with a multiprotein complex in mammalian cells (160). It was found to inhibit cell death in yeast and mammalian cells and to be abundantly expressed in human breast carcinoma (161). The higher abundance of HMGB1 may contribute to drug resistance to VP-16 and mitoxantrone by enhancing DNA repair, or modulating chromatin structure, thus interfering with drug action.

### **Higher abundance of 40S ribosomal protein SA**

40S ribosomal protein SA (spot33) was found to have a higher abundance in MCF-7/VP and MCF-7/MX cells. It is a 33k Da protein which has been reported to be associated with drug resistance (162-165). It is also called multidrug resistance-associated protein MGr1-Ag (162). It was originally thought to be a laminin receptor (163). It was found to be essential for 40S ribosomal unit maturation (166). It was suggested to play a role in the regulation of cellular attachment to basement membranes via laminin. It was identified as a genotoxic responsive protein (167). Its expression level in L929 cells was elevated 3 fold after X-irradiation. How this protein might function in cancer drug resistance is not clear and needs further investigation.

### **Higher abundance of prohibitin**

Prohibitin (spot 34) was found to be more abundant in MCF-7/MX cell than control MCF-7 cells. Prohibitin is a 30 kDa protein, evolutionarily conserved in a variety of organisms (168). It is mainly located in the inner membrane of mitochondria, and is

recruited into nucleus in response to genotoxic stress (169-170). Mutations of prohibitin have been found in breast cancer cells (168). Prohibitin has also been reported to play a protective role in breast cancer cell lines treated with chemotherapeutic agents.

Comparing the parental UMSCC10b head and neck carcinoma cell line and the 5.9-fold cisplatin-resistant subline, UMSCC10b/Pt-S15, by mRNA levels, prohibitin has been shown to be up-regulated in association with cisplatin resistance (171). It has also been shown stable over-expression of prohibitin in a human B cell line blocks apoptosis induced by the topoisomerase I inhibitor camptothecin(172). It appears to play an important role in determining the chemosensitivity of the cells. How prohibitin interacts with the established cell death pathway to regulate response to chemotherapeutic drugs is not clear. It may be a cell survival or anti-apoptotic factor (173-174).

### **Higher abundance of mitotic checkpoint protein BUB 3**

Mitotic checkpoint protein BUB 3 (spot 77) is more abundant in MCF-7/AdrVp than in control MCF-7 cells. Its abundance in MCF-7/VP, MCF-7/MX is the same as that in control MCF-7 cells. Mitotic checkpoint protein BUB3 plays an important role in mitotic spindle checkpoint, “a signal transduction based surveillance mechanism that ensures the fidelity of cell division by preventing the premature advance of cells from metaphase to anaphase prior to the successful attachment of kinetochores to spindle microtubules (spindle assembly)” (175). This control functions to ensure the chromosomes are intact and that crucial steps of the cell cycle are completed before the following step is initiated. Improper spindle formation causes M arrest until the defect is fixed. Mitotic checkpoint 3, together with two other checkpoint proteins BUB1 and BUB2, has been observed to be

overexpressed in gastric cancer. For MCF-7 cancer cells under genotoxic stress caused by chemotherapeutic agents, the higher abundance of mitotic protein BUB 3 may mean enhancement of this checkpoint in cell cycle, allowing enough time for DNA repair and cytoskeleton assembly, resulting in the fixation of the defects caused by the drug.

### **Higher abundance of the 70 kDa glucose-regulated protein (GRP78)**

GRP78 is found to be more abundant only in MCF-7/MX cells than in control MCF-7 cells ( $4.91 \pm 0.46$ ). It is a member of heat shock protein 70 (HSP70) family (178). It is a molecular chaperon localized in ER lumen (179). The presence of GRP78 in nucleus is mostly likely due to translocation after genotoxic stress (180). Interestingly, overexpression of GRP has been reported to be in association with drug resistance to chemotherapeutic drugs, such as adriamycin and etoposide(181-182). Its overexpression is also in association with the malignance of human breast tumors (183). It is well accepted that GRP78 is antiapoptotic, but how it interfere with apoptosis still needs further investigation (184-185).

### **Higher abundance of cyclophilin B**

Cyclophilin B (spot22) is found to be more abundant in the three drug resistant cell lines. It binds to a potent immunosuppressive drug, cyclosporine A (186). It is a ubiquitous intracellular protein (187). It has been identified as a chaperone facilitating nuclear retrotransport (188). Further investigation is needed to study its role in drug resistance.

Overall, in the present research, we have found that MCF-7/VP, MCF-7/MX, MCF-7/AdrVp cell lines have similar patterns of abundance changes in nuclear proteins with important differences. They all have lower abundances of cytoskeletal proteins. Besides this, MCF-7/VP and MCF-7/MX share more similarities. For example, changes in nucleolin and PARP-1 seem to be very important to deal with genotoxic stress and resisting cell death, and similar changes are observed in the two cell lines. Nucleolin level in MCF-7/AdrVp cells is about the same as those in control MCF-7 cells. PARP level in MCF-7/AdrVp is lower than that in control MCF-7 cells, but does not exceed the threshold of 2-fold that we set as significant change. An important cell cycle regulation protein, mitotic checkpoint protein BUB 3 is found to be more abundant only in MCF-7/AdrVp. MCF-7/MX cells have been found to be cross-resistant to etoposide and adriamycin (10-fold). It should be pointed out that etoposide and mitoxantrone are both topoisomerase II poisons, sharing similar mechanisms of action to kill cancer cells. The cells resistant to these drugs, MCF-7/VP and MCF-7/MX cells have more similarities in nuclear abundance changes.

### **Summary and prospectus**

Our objective is to contribute to the understanding of the mechanisms of drug resistance in cancer cells. Proteomics allows analysis of many proteins at once and narrows the targets for further investigation. Using proteomics approach, we have been able to identify some proteins whose changes of abundance correlate with drug resistance in MCF-7 breast cancer cells. These proteins are actively involved in chromatin structure, DNA repair, cell cycle regulation and protein folding. This is the first indication that most of them are related to drug resistance. The results support the hypothesis that drug

resistance in cancer cells is a multifactorial process. Many proteins are involved, although one or a few proteins may play a dominant role. Different sets of proteins may be involved to deal with different genotoxic assaults.

The present research has laid a foundation for further study of nuclear proteins in MCF-7 cells. A new method of protein pre-fractionation, liquid isoelectrofocusing, is being developed and implemented in our lab. This will enable us to analyze low-abundant nuclear proteins in MCF-7 cells. In combination with other biology techniques, such as chromatin immunoprecipitation, more nuclear proteins which are involved in drug resistance can be revealed.

The proteins which alter in abundance in drug resistant cells need to be further investigated. Over-expression or gene silencing can be used to test their roles in drug resistance. Once their roles are confirmed, they can be exploited as biomarkers for diagnosis of development of drug resistance. New strategies may be developed to kill the cancer cells using these proteins as novel drug targets.

## References

1. <http://www.nlm.nih.gov/medlineplus/breastcancer.html> (Access in May 2004).
2. Salmon SE and Sartorelli AC. **Cancer chemotherapy, in basic and clinical pharmacology.** (Katzung BG, ed) Appleton-Lange, Pp. 881-911 (1996).
3. Hait WN (Ed) Kluwer. **Drug resistance.** Academic Publishers, Boston (1996).
4. Roninson IB (Ed). **Molecular and cellular biology of multidrug resistance in tumor cells.** Plenum Press, New York (1991).
5. Gupta S Tsuruo, T (Eds). **Multidrug resistance in cancer cells: molecular, biochemical and biological aspects.** John Wiley and sons, England (1996).
6. Bates S. **Drug resistance: still on the learning curve.** Clin Cancer Res 1999, 5: 3346-3348.
7. Endicott JA, Ling V. **The Biochemistry of P-glycoprotein-mediated multidrug resistance.** Annu Rev Biochem 1989, 58:137-171.
8. Dyle LA, Yang W, Abruzzo LV, Krogmann T, Gao Y, Rishi AK, Ross DD. **A multidrug resistance transporter from human MCF-7 breast cancer cells.** Proc Natl Acad Sci USA 1992, 95: 15665-15670.
9. Politi PM, Arnold ST, Felsted RL, and Sinha BK. **P-glycoprotein –independent mechanism of drug resistance to VP-16 in multidrug –resistance tumor cell lines: pharmacokinetic and photoaffinity labeling studies.** Mol Pharmacol 1990, 37: 790-796. 23.
10. Gottesman MM, Fojo T, Bates SE. **Multidrug resistance in cancer: role of ATP-dependent transporters.** Nat Rev Cancer 2002, 2 (1): 48-58.
11. Litman T, Brangi M, Hudson E, Fetsch P, Abati A, Ross DD, Miyake K, Resau JH, Bates SE. **The multidrug-resistant phenotype associated with overexpression of the new ABC half-transporter, MXR (ABCG2).** J Cell Sci 2000 113 ( Pt 11): 2011-2016.
12. Colvin OM, Freidman HS, Gamesik MP and Fenselau C. **Role of Glutathione in cellular resistance to alkylating agents,** in **Advances in enzyme regulation** (Weber G, ed), Pergamon Press, New York, NY 33: 19-2615.

13. O'Brien ML and Tew KD. **Gluthathione and related enzymes in multidrug resistance.** Eur J Cancer 1996, 32A: 967-978.
14. Kelley SL, Basu A, Teicher BA, Hacker MP, Hamer DH, Lazo JS. **Overexpression of metallothionein confer resistance to anticancer drugs.** Science 1985, 241: 1813-1815.
15. He T, Wei D, Fabris and Fenselau C. **Intracellular sequestration of antitumor drugs by metallothionein.** Cellular and Molecular Biol 2000, 40: 383-392.
16. Wang ZM, Chen ZP, Xu ZY, Christodoulopoulos G, Bello V, Mohr V, Aloyz R, and Panasci LC. **In vitro evidence for homologous recombinational repair in resistance to melphalan.** J Natl Cancer Inst 2001, 93: 1473-1478.
17. Fojo T. **Cancer, DNA repair mechanisms, and resistance to chemotherapy.** J. Natl. Cancer Inst 2001, 93 (19): 1434-1436.
18. Fink D, Nebel S, Aebi S, Zheng H, Cenni B, Nehme A, Christen RD and Howell SB. **The role of mispair repair in drug resistance.** Cancer Res 1996, 56: 4881-4886.
19. Soengas MS, Lowe SW. **Apoptosis and melanoma chemoresistance.** Oncogene 2003, 19; 22 (20): 3138-3151.
20. Cheng Q, Lee HH, Li Y, Parks TP, Cheng G. **Upregulation of Bcl-x and Bfl-1 as a potential mechanism of chemoresistance, which can be overcome by NF-kappaB inhibition.** Oncogene 2000, 5; 19 (42): 4936-4940.
21. Thomas H, Coley HM. **Overcoming multidrug resistance in cancer: an update on the clinical strategy of inhibiting p-glycoprotein.** Cancer Control 2003, 10 (2): 159-165.
22. Gottesman MM. **Mechanisms of drug resistance.** Annu Rev Med 2002, 53:615-627.
23. Gutierrez PL and Desai TT. **Chemotherapy and drug resistance.** BioMedicina 1999, 2(5): 235-240.
24. Simon SM and Schindler M. **Cell biological mechanisms of multidrug resistance in tumors.** Proc Natl Acad Sci 1994, 91: 3497-3504.
25. Harris A and Hochhauser D. **Mechanisms of drug resistance in cancer treatment.** Acta Oncologica 1992, 31: 205-213.
26. Hayes JD and Wolf CR. **Molecular mechanisms of drug resistance.** Biochem J 1990, 272: 281-295.



27. Kastan MB. **Molecular determinants of sensitivity to antitumor agents.** Biochemica et Biophysics Acta 1999, 1424: R37-R42.
28. Leonard GD, Polgar O, Bates SE. **ABC transporters and inhibitors: new targets, new agents.** Curr Opin Investig Drugs 2002, 3 (11): 1652-9.
29. Ohi Y, Kim T, Toge T. **Overcoming of multidrug resistance by introducing the apoptosis gene, bcl-Xs, into MRP-overexpressing drug resistant cells.** Int J Oncol 2000, 16: 959-969.
30. Stein WD, Bates SE, Fojo T. **Intractable cancers: the many faces of multidrug resistance and the many targets it presents for therapeutic attack.** Curr Drug Targets 2004, 5 (4): 333-46.
31. Leonard GD, Fojo T, Bates SE. **The role of ABC transporters in clinical practice.** Oncologist 2003, 8 (5): 411-424.
32. Litman T, Druley TE, Stein WD, Bates SE. **From MDR to MXR: new understanding of multidrug resistance systems, their properties and clinical significance.** Cell Mol Life Sci 2001, 58 (7): 931-59.
33. International human genome sequence Consortium. Nature 2001, 409: 860-921.
34. Venter JC, et al. **The sequence of the human genome.** Science 2001, 291: 1304-1351.
35. Pandey A and Mann M. **Proteomics to study genes and genomes.** Nature 2000, 405: 837-846.
36. Anderson NL, Anderson NG. **Proteome and proteomics: new technologies, new concepts, and new words.** Electrophoresis 1998, 19: 1852-1861.
37. Wulfkuhle JD, McLean KC, Paweletz CP, Sgroi DC, Trock BJ, Steeg PS, and Petricoin III EF. **New approaches to proteomics analysis of breast cancer.** Proteomics 2001, 1: 1205-1215.
38. Hutter G, Sinha P. **Proteomics for studying cancer cells and the development of chemoresistance.** Proteomics 2001, 1: 1233-1248.
39. Lamond AI and Earnshaw WC. **Structure and function in the nucleus.** Science 1998, 280: 547-553.
40. Newport JW and Forbes DJ. **The nucleus: structure, function and dynamics.** Ann. Rev. Biochem 1987, 56: 535-565.

41. Roix J and Misteli T. **Genome, proteomes, and dynamic networks in the cell nucleus.** *Histochem Cell Biol* 2002, 118: 105-116.
42. Swedlow JR, and Lamond A. **Nuclear dynamics: where genes are and how they got there.** *Geno Biol* 2001, 2: Reviews0002.1-0002.7 .
43. Trotta RF, Brown ML, Terrell JC, and Geyer JA. **Defective DNA repair as a potential Mechanism for the rapid development of drug resistance in plasmodium falciparum.** *Biochemistry* 2004, 43(17): 4885-4891.
44. Soule HD, Vazquez J, and Brennan M. **A cell line from a pleural effusion derived from a breast carcinoma.** *J Natl Cancer Inst* 1973, 51: 1409-1416.
45. Schneider E, Horton JK, Yang CH, Nakagawa M, Cowan KH. **Multidrug resistance-associated protein gene overexpression and reduced drug sensitivity of topoisomerase II in a human breast carcinoma MCF7 cell line selected for etoposide resistance.** *Cancer Res* 1994, 54: 152-158.
46. Cory AH and Cory JG. **Comparison of the properties of human breast cancer cells: MCF-7 and MCF-7 cells selected for resistance to etoposide.** *Advan. Enzyme Regul* 2001. 41(1): 177-188.
47. Nakagawa M, Schneider E, Dixon KH, Horton JK, Kelley K, Morrow C, and Cowan KH. **Reduced intracellular drug accumulation in the absence of P-glycoprotein(mdr 1) overexpression in the mitoxantrone-resistant human breast cancer cells.** *Cancer Res* 1992, 52: 6175-6181.
48. Yang CHJ, Horton JK, Cowan KH and Schneider E. **Reselection of a mitoxantrone-resistant breast carcinoma cell line with mitoxantrone results in a parallel increase in cross-resistant to camptothecin analogues[abstract].** *Proc Am Assoc Cancer Res* 1996, 37: 308.
49. Yang CHJ, Cowan KH, and Schneider E. **Cross-resistance to camptothecin analogues in a mitoxantrone-resistant human breast carcinoma cell line is not due to DNA topoisomerase I alterations.** *Cancer Res* 1995, 55: 4004-4009.
50. Lee JS, Scala S, Matsumoto Y, Dickstein B, Robey R, Zhan Z, et al. **Reduced drug accumulation and multidrug resistance in human breast cancer cells without associated P-glycoprotein or MRP overexpression.** *J Cell Biochem* 1997, 65: 513-26.
51. Volk EL, Rohde K, Rhee M, McGuire JJ, Doyle LA, Ross DD, and Schneider E. **Methotrexate cross-resistance in a mitoxantrone-selected multidrug-resistant MCF7 breast cancer cell line is attributable to enhanced energy-dependent drug efflux.** *Cancer Res* 2000, 60: 3514-3521.

52. Volk EL, Farley KM, Wu Y, Li F, Robey RW and Schneider E. **Overexpression of wild-type breast cancer resistance protein mediates methotrexate resistance.** *Cancer Res* 2002, 62: 5035-5040.
53. Volk EL, and Schneider E. **Wild-type breast cancer resistance protein (BCRP/ABCG2) is a methotrexate polyglutamate transporter.** *Cancer Res* 2003, 63 (17): 5538 - 5543. 47.
54. Ross DD, Yang W, Abruzzo LV, Dalton WS, Schneider E, Lage H, Dietel M, Greenberger L, Cole SP, Doyle LA. **Atypical multidrug resistance: breast cancer resistance protein messenger RNA expression in mitoxantrone-selected cell lines.** *J Natl Cancer Inst* 1999, 91 (5): 429-433.
55. Robey RW, Honjo Y, van de Laar A, Miyake K, Regis JT, Litman T, Bates SE. **A functional assay for detection of the mitoxantrone resistance protein, MXR (ABCG2).** *Biochim Biophys Acta* 2001, 1512 (2): 171-182.
56. Cole SP, Sparks KE, Fraser K, Loe DW, Grant CE, Wilson GM, et al. **Pharmacological characterization of multidrug resistant MRP-transfected human tumor cells.** *Cancer Res* 1994, 54: 5902-5910.
57. Taylor CW, Dalton WS, Parrish PR, Gleason MC, Bellamy WT, Thompson FH, et al. **Different mechanisms of decreased drug accumulation in doxorubicin and mitoxantrone resistant variants of the MCF7 human breast cancer cell line.** *Br J Cancer* 1991, 63: 923-929.
58. Futscher BW, Abbaszadegan MR, Domann F, Dalton WS. **Analysis of MRP mRNA in mitoxantrone-selected, multidrug-resistant human tumor cells.** *Biochem Pharmacol.* 1994, 47: 1601-1606.
59. Hazlehurst LA, Gros P, and Dalton R. **Chromosome mediated gene transfer of drug resistance to mitoxantrone.** *Anticancer Res* 1998, 18 (2A): 1005-1010.
60. Chen YN, Mickley LA, Schwartz AM, Acton EM, Hwang JL, Fojo AT. **Characterization of adriamycin-resistant human breast cancer cells which display overexpression of a novel resistance-related membrane protein.** *J Biol Chem* 1990, 265 (17): 10073-10080.
61. Doyle LA, Ross DD. **Multidrug resistance mediated by the breast cancer resistance protein BCRP (ABCG2).** *Oncogene* 2003, 22 (47): 7340-7358.
62. Batist G, Tulpule A, Sinha BK, Katki AG, Myers CE, Cowan KH. **Overexpression of novel anionic glutathione transferase in multidrug-resistant human breast cancer cells.** *J Biol Chem* 1986, 261: 15544-15549.

63. Fairchild CR, Ivy PS, Kao-Shan CS, Whang-Peng J, Rosen N, Israel MA, et al. **Isolation of amplified and overexpressed DNA sequences from adriamycin-resistant human breast cancer cells.** *Cancer Res* 1987, 47: 5141-5148.
64. Ross DT, Scherf U, Eisen MB, Perou CM, Rees P, et al. **System variation in gene expression patterns in human breast cancer cell lines.** *Nat Genet* 2000, 24:227-235.
65. Devarajan E, Chen J, Multani AS, Pathak S, Sahin AA, and Mehta K. **Human breast cancer MCF-7 cell line contains inherently drug-resistant subclones with distinct genotypic and phenotypic features.** *Int J Oncol* 2002, 20: 913-920.
66. Scudiero DA, Monks A, Sausville VA. **Cell line in the NCI anticancer screen [Letter].** *J Natl Cancer Inst* 1998, 90: 862.
67. Pirinia F, Breuleux M, Schneider E, Hochmeister M, Bates SE, Marti A, et al. **Unretain identity of doxorubicin-resistant MCF-7 cell lines expressing mutated p53.** *J Natl Cancer Inst* 2000, 92: 1535-1536.
68. Mehta K, Devarajan E, Chen J, Multani A, Pthak S. **Multidrug-resistant MCF-7 cells: an identity crisis.** *J Natl Cancer Inst* 2002, 94: 1652-1654.
69. Hathout Y, Gehrman ML, Chertov A, and Fenselau C. **Proteomic phenotyping: metastatic and invasive breast cancer.** *Cancer Lett* 2004, 210: 245-253.
70. Washinger VC. Washinger VC, Cordwell SJ, Cerpa-Poljak A, Yan JX, Gooley AA, Wilkins MR, et al. **Progress with gene-product mapping of the Mollicutes: Mycoplasma genitalium** *Electrophoresis* 1995; 16: 1090-4
71. Kahn P. **From genome to proteome: looking at a cell's proteins.** *Science* 1995, 270 (5235): 369-370.
72. O'Farrell PH. **High-resolution two dimensional electrophoresis of proteins.** *J Biol Chem* 1975, 250: 4007-4021.
73. Klose J. **Protein mapping by combined isoelectric focusing and electrophoresis of mouse tissues. A novel approach to testing for induced point mutations in mammals.** *HUMANGENETIK* 1975, 26 (3): 231-243.
74. Gygi SP, Corthals GL, Zhang Y. **Evaluation of two-dimensional gel electrophoresis-based proteome analysis technology.** *Proc Natl Acad Sci USA* 2000, 97: 9390-9395.
75. Gorg A, Obermaier C, Boguth G, et al. **The current status of two-dimensional electrophoresis with immobilized pH gradients.** *Electrophoresis* 2000, 21: 1037-1053.

76. Wilkins MR, Sanchez JC, Gooley AA, Appel RD, Humphery-smith I, Hochstrasser DF, Willams KL. **Progress with proteome projects: why all proteins expressed by a genome should be identified and how to do it.** *Biotechnol Genet Eng Rev* 1996, 13: 19-50.
77. Hochstrasser DF. **Proteome in perspective.** *Clin Chem Lab Med* 1998, 36 (11): 825-836.
78. Ducret A, Desponts C, Desmarais S, Gresser MJ, Ramachandran C. **A general method for the rapid characterization of tyrosine-phosphorylated proteins by mini two-dimensional gel electrophoresis.** *Electrophoresis* 2000, 21: 2196-2208.
79. Oda Y, Nagasu T & Chait BT. **Enrichment analysis of phosphorylated proteins as a tool for probing the phosphoproteome.** *Nat Biotech* 2001, 19: 379-382.
80. Charlwood J, Skehel JM, Camilleri P. **Analysis of N-linked oligosaccharides released from glycoproteins separated by two-dimensional gel electrophoresis.** *Anal Biochem* 2000, 284 (1): 49-59.
81. Anderson L, Seihamer J. **A comparison of selected mRNA and protein abundances in human liver.** *Electrophoresis* 1997, 18: 533-537.
82. Gygi SP, Rochon Y, Franza BR & Aebersold R. **Correlation between protein and mRNA abundance in yeast.** *Mol Cell Biol* 1999, 19: 1720-1730.
83. Celis JE, Kruhoffer M, Gromova I, Frederiksen C, Qstergaard M, Thykjaer T, Gromov P, Yu JS, Pálsdóttir H, Magnusson N and Orntoft TF. **Gene expression profiling: monitoring transcription and translation products using DNA microarrays and proteomics.** *FEBS Lett* 2000, 480: 2-16.
84. Blackstock WP and Weir MP. **Proteomics: quantitative and physical mapping of cellular proteins.** *Trends Biotechnol* 1999, 17: 121-127.
85. Chang J, Van Remmen H, Cornell J, Richardson A, Ward WF. **Comparative proteomics: characterization of a two-dimensional gel electrophoresis system to study the effect of aging on mitochondrial proteins.** *Mech. Ageing Dev* 2003, 124 (1): 33-41.
86. Righetti PG, Bossi A. **Isoelectric focusing in immobilized pH gradients: an update.** *J Chromatogr B Biomed Sci Appl* 1997, 10, 699(1-2):77-89 (abstract).
87. Nawrocki A, Larsen MR, Podtelejnikov AV, Jensen ON, Mann M, Roepstorff P, Gorg A, Fey SJ, Larsen M. **Correlation of acidic and basic carrier ampholyte and immobilized pH gradient two-dimensional gel electrophoresis patterns based on mass spectrometric protein identification.** *Electrophoresis* 1998, 19 (6):1024-1035.

88. Norbeck J, Blomberg A. **Two-dimensional electrophoretic separation of yeast proteins using a non-linear wide range (pH 3-10) immobilized pH gradient in the first dimension; reproducibility and evidence for isoelectric focusing of alkaline (pI > 7) proteins.** *Yeast* 1997, 13 (16): 1519-1534.
89. Gorg A, Obermaier C, Boguth G, Csordas A, Diaz JJ, Madjar JJ. **Very alkaline immobilized pH gradients for two-dimensional electrophoresis of ribosomal and nuclear proteins.** *Electrophoresis* 1997, 18: 328-337.
90. Glasson MJ, Molloy MP, Walsh BJ, Willcox MD, Morris CA, Williams KL. **Development of mini-gel technology in two-dimensional electrophoresis for mass-screening of samples: application to tears.** *Electrophoresis* 1998, 19 (5): 852-855.
91. Sanchez JC, Rouge V, Pisteur M, Ravier F, Tonella L, Moosmayer M, Wilkins MR. **Hochstrasser DF Improved and simplified in-gel sample application using reswelling of dry immobilized pH gradients.** *Electrophoresis* 1997, 18 (3-4): 324-327 (abstract).
92. Cordwell SJ, Basseal DJ, Bjellqvist B, Shaw DC, Humphery-Smith I. **Characterisation of basic proteins from spiroplasma melliferum using novel immobilised pH gradients.** *Electrophoresis* 1997, 18 (8): 1393-1398.
93. Blomberg A, Blomberg L, Norbeck J, Fey S, Larsen, PM., Larsen MR, Roepstorff P, Degand H, Boutry M, Posch A and Görg A. **Interlaboratory reproducibility of yeast protein patterns analyzed by immobilized pH gradient two gel electrophoresis.** *Electrophoresis* 1995, 16: 1935-1945.
94. Aebersold R, Goodlett DR. **Mass spectrometry in proteomics.** *Chem Rev* 2000, 101 (2): 69-296.
95. Patterson SD. **Mass spectrometry and proteomics.** *Physiol Genomics* 2000, 2: 59-65.
96. Yates JR.III. **Mass Spectrometry and the Age of the Proteome.** *J Mass Spectrom* 1998, 65: 972A.
97. Takana K, Waki H, Ido Y, Akita S, Yoshida T. **Protein and polymer analyses up to m/z 100 000 by laser ionization time-of flight mass spectrometry.** *Rapid Commun Mass Spectrom* 1988, 2: 151-153.
98. Karas M, Hillenkamp F. **Laser desorption/ionization of proteins with molecular masses exceeding 100,000 daltons.** *Anal Chem* 1988, 60: 2299-2301.
99. Fenn B, Mann M, Meng CK, Wong SF and Whitehouse CM. **Electrospray ionization for mass spectrometry of large biomolecules.** *Science* 1989, 246: 64 -67.

100. McIver RT, Li Y and Hunter RL. **Matrix-assisted laser desorption/ionization with an external ion source fourier-transform mass spectrometer.** Rapid Commun Mass Spectrom 1994, 8: 237-241.
101. Fenselau C. **MALDI-MS and Strategies for Protein Analysis.** Anal Chem 1997, 69: 661A.
102. Costello CE. **Time, life ... and mass spectrometry. New techniques to address biological questions.** Biophys Chem. 1997, 68 (1-3): 173-188.
103. Wilm M, Mann M. **Analytical properties of the nanoelectrospray ion source.** Anal. Chem 1996, 1, 68 (1): 1-8, 1996, 68: 1-8.
104. Abian J, Oosterkamp AJ, Gelpi E. **Comparison of conventional, narrow-bore and capillary liquid chromatography mass spectrometry for electrospray ionization mass spectrometry: practical considerations.** J. Mass Spectrom 1999, 34: 244-254 (nonospray).
105. Figeys D, Ducret A, Yates JR 3<sup>rd</sup>, Aebersold R. **Protein identification by solid phase microextraction-capillary zone electrophoresis-microspray-tandem-mass spectrometry.** Nat Biotechnol 1996, 14 (11): 1579-1583.
106. Gygi SP, Aebersold R. **Mass spectrometry and Proteomics.** Curr Opin Chem Biol 2000, 4: 489-494.
107. Henzel WJ, Billeci TM, Stults JT, Wong SC, Grimley C, Watanabe C. **Identifying proteins from two-dimensional gels by molecular mass searching of peptide fragments in protein sequence databases.** Proc Natl Acad Sci USA 1993, 90: 5011-5015.
108. Cleveland DW, Fischer SG, Kirschner MW, Laemmli UK. **Peptide mapping by limited proteolysis in sodium dodecyl sulfate and analysis by gel electrophoresis.** J Biol Chem, 1977, 252: 1102-1106.
109. Yates J R 3<sup>rd</sup>, Speicher S, Griffin PR, Hunkapiller T. **Peptide mass maps: a highly informative approach to protein identification.** Anal Biochem 1993, 214: 397-408.
110. Shevchenko A, Jensen ON, Podtelejnikov AV, Sagliocco F, Wilm M, Vorm O, Mortensen P, Boucherie H, Mann M. **Linking genome and proteome by mass spectrometry: large-scale identification of yeast proteins from two dimensional gels.** Proc Natl Acad Sci USA 1996, 93: 14440-14445.
111. Yates JR. **Database searching using mass spectrometry data.** Electrophoresis 1998, 19: 893-890.

112. Mann M, Hojrup P, Roepstorff P. **Use of mass spectrometric molecular weight information to identify proteins in sequence databases.** Biol Mass Spectrom 1993, 22: 338-345.
113. Mann M, Wilm M. **Error-tolerant identification of peptides in sequence databases by peptide sequence tags.** Anal Chem 1994, 66: 4390-4399.
114. Ong SE, Blagoec B, Kratchmarova I, Kristensen DB, Steen H, Pandey A, and Mann M. **Stable isotope labeling by amino acids in cell culture, SALIC, as a simple and accurate approach to expression proteomics.** Mol Cell Proteomics 2002, 1: 376-386.
115. Regnier FE, Riggs L, Zhang R, Xiong Li, Liu P, Chakraborty A, Seeley E, Sioma C, and Thompsin RA. **Comparative proteomics based on stable isotope labeling and affinity selection.** J Mass Spectrom 2002, 37: 133-145.
116. Blobel G, Potter VR. **Nuclei from rat liver: Isolation method that combines purity and high yield.** Science 1996, 154: 1662-1665.
117. Jensen ON, Wilm M, Shevchenko A, Mann M. **Sample preparation methods for mass spectrometric peptide Mapping directly from 2-DE gels in: Methods in molecular biology.** Link AJ (Ed), Human Press, Totowa, New Jersey, 1999, 112: 513-530.
118. Soskic V, Godovac-Zimmermann J. **Improvedment of an in-gel tryptic digestion method for matrix-assisted laser desorption/ionization-time of -flight mass spectrometry peptide mapping by using of volatile solublizing agents.** Proteomics 2001, 1: 1364-1367.
119. Dreger M, Bengtsson L, Schoneberg T, Otto H, and Hucho F. **Nuclear envelope proteomics: Novel integral membrane proteins of the inner nuclear membrane.** Natl Acad Sci USA., 2001, 98 (21): 11943-11948.
120. Andersen JS, Lyon CE, Fox AH, Leung AK, Lam YW, Steen H, Mann M., & Lamond, AI. **Directed proteomic analysis of the human nucleolus.** Curr Biol. 2002,12: 1-11
121. Scherl A, Couté Y, Déon C, Aleth Callé A, Kindbeiter K, Sanchez JC, Greco A, Hochstrasser D, and Diaz JJ. **Functional Proteomic Analysis of Human Nucleolus.** Mol Biol Cell 2002, 13 (11): 4100-4109
122. Jung E, Heller M, Sanchez JC, Hochstrasser DF. **Proteomics meets cell biology: The establishment of subcellular proteomes.** Electrophoresis 2000, 21: 3369-3377.
123. Schirmer EC, and Gerace L. **Organelar proteomics: the prize and pitfall of opening the nuclear envelop.** Geno Biol 2002, 1008: 1-4.



124. D'Amours D, Desnoyers D, D' Silva I, and Poirier G G. **Poly(ADP-ribosylation) reactions in the regulation of nuclear functions.** Biochem J 1999, 342: 249–268,
125. Ivana Scovassi A, Diederich M. **Modulation of poly(ADP-ribosylation) in apoptotic cells.** Biochem Pharmacol 2004, 68(6):1041-7.
126. Durkacz BW, Omidiji O, Gray DA and Shall S. **(ADP-ribose)<sub>n</sub> participates in DNA excision repair.** Nature 1980, 283:593–596.
127. Masson M, Niedergang C, Schreiber V, Muller S, Menissier de Murcia J, de Murcia G. **XRCC1 is specifically associated with poly(ADP-ribose) polymerase and negatively regulates its activity following DNA damage.** Mol Cell Biol 18: 3563-3571, 1998
128. Oei SL and Ziegler M, **ATP for the DNA ligation step in base excision repair is generated from poly(ADP-ribose).** J Biol Chem 2000, 275:23234–23239.
129. Kaufmann S H, Desnoyers S, Ottaviano Y, Davidson N E, Poirier G G. **Specific proteolytic cleavage of poly(ADP-ribose) polymerase: an early marker of chemotherapy-induced apoptosis.** Cancer Res 1993, 53: 3976-3985.
130. Wasierka-Gadek J, Bugajska-Schretter A, Löw-Baselli A, Grasl-Kraupp B. **Cleavage of poly(ADP-ribose) transferase during p53-independent apoptosis in rat liver after treatment with N-nitrosomorpholine and cyproterone acetate.** Mol Carcinog 1999, 24: 263-275.
131. Chiarugi A and Moskowitz WA. **PARP-1—a perpetrator of apoptotic cell death?** Science 2002, 297: 200-201. Published debate responses: **PARP-1 and AIF produce cellular necrosis, not apoptosis.** Denson G. Fujikawa (29 July 2002)
132. Yu SW, Wang H, Poitras MF, Coombs C, Bowers WJ, Federoff HJ, Poirier GG, Dawson TM, and Dawson VL. **Mediation of poly(ADP-Ribose) polymerase-1-dependent cell death by apoptosis-inducing factor.** Science 2002, 259-263.
133. Pettitt AR, Sherrington PD, Cawley JC. **Role of poly(ADP-ribosylation) in the killing of chronic lymphocytic leukemia cells by purine analogues.** Cancer Res 2000, 1, 60 (15): 4187-4193.
134. Zong WX, Ditsworth D, Bauer DE, Wang ZQ, Thompson CB. **Alkylation DNA damage stimulates a regulated form of necrotic cell death.** Genes Dev 2004, 1; 18(11):1272-1282
135. Mi YC, Thomas SD, Xu XH, Casson LK, Miller DM, and Bates PJ. **Apoptosis in leukemia cells is accompanied by alteration in the levels and localization of nucleolin.** J Biol Chem 2003, 278 (10): 8572-8579.

136. Wurzer G, Herceg, Z and Wsierska-Gadek J .**Increased Resistance to Anticancer Therapy of Mouse Cells Lacking the Poly(ADP-ribose) Polymerase Attributable to Up-Regulation of the Multidrug Resistance Gene Product P-Glycoprotein** Cancer Res 2000 60: 4238-4244.
137. Drazen DL, Bilu D, Edwards N, and Nelson RJ. **Disruption of poly(ADP-ribose) polymerase (PARP) protects against stress-evoked immunocompromise.** Mol Med 2001, 7: 761-766.
138. Drubin,DG and Nelson,WJ. **Origins of cell polarity.** Cell 1996, 84:335-344.
139. Hanrahan J and Snyder M. **Cytoskeleton activation of checkpoint kinase.** Mol Cell 2003, 12:663-673
140. Caulín C, Salvesen GS, Oshima RG **Caspase cleavage of keratin 18 and reorganization of intermediate filaments during epithelial cell apoptosis** J Cell Biol 1997, 138(6):1379-1394
141. Pankov R, Simcha I, Zoller M, Oshima R, and Ben-Ze'ev A.**Contrasting effects of K8 and K18 on stabilizing K19 expression, cell motility and tumorigenicity in the BSp73 adenocarcinoma.** J Cell Sci 1997; 110(8): 965 - 974.
142. *Bauman PA, Dalton WS, Anderson JM and Cress AE. Expression of Cytokeratin Confers Multiple Drug Resistance.* Proc Natl Acad Sci USA 1994 91: 5311-5314.
143. Bichat F., Mouawad R., Solis-Recendez G., Khayat D., Bastian G. **Cytoskeleton alteration in MCF7R cells, a multidrug resistant human breast cancer cell line.** Anticancer Res 17: 3393-3401, 1997
144. Yoo BC, Ku JL, Hong SH, Shin YK, Park SY, Kim HK, Park JG. **Decreased pyruvate kinase M2 activity linked to cisplatin resistance in human gastric carcinoma cell lines.** Int J Cancer 2004, 10; 108(4):532-9.
145. Hondermarck H, Vercoutter-Edouart AS, Révillion F, Lemoine J, Belkoura IE, Nurcombe V, and Peyrat JP. **Proteomics of breast cancer for marker discovery and signal pathway profiling.** Proteomics 2001, 1(10):1216-1232.
146. Ginisty H, Sicard H, Roger B, Bouvet P. **Structure and functions of nucleolin.** J. Cell Sci., 1999, 112 ( Pt 6): 761-72 Review.
147. Tuteja R, Tuteja N. **Nucleolin: a multifunctional major nucleolar phosphoprotein.** Crit. Rev. Biochem Mol Biol 1998, 33 (6): 407-436.
148. Srivastava M, Pollard HB. **Molecular dissection of nucleolin's role in growth and cell proliferation: new insights.** FASEB J 1999, 13 (14): 1911-1922.

149. Yang C et al. **Identification of nucleolin and nucleophosmin as genotoxic stress responsive RNA-binding proteins.** *Nucleic Acids Res* 2002, 30 (10): 2251-2260.
150. Yang TH, Tsai WH, Lee YM, Lei HY, Lai MY, Chen DS, Yeh NH, Lee SC. **Purification and characterization of nucleolin and its identification as a transcription repressor.** *Mol Cell Biol* 1994, 14 (9): 6068-6074.
151. Thyagarajan B et al. **Nucleolin promotes homologous DNA pairing in vitro.** *Somat Cell Mol Genet* 1998, 24 (5): 263-272.
152. Sengupta TK, Bandyopadhyay S, Fernandes DJ, Spicer EK. **Identification of nucleolin as an AU-rich element binding protein involved in bcl-2 mRNA stabilization.** *J Biol Chem* 2004, 279 (12): 10855-10863.
153. Roger B, Moisan A, Amalric F, Bouvet P. **Nucleolin provides a link between RNA polymerase I transcription and pre-ribosome assembly.** *Chromosoma* 2003, 111 (6): 399-407.
154. Galande S. **Chromatin (dis)organization and cancer: BUR-binding proteins as biomarkers for cancer.** *Curr Drug Targets* 2002, 2 (2): 157-190.
155. Daniely Y, Dimitrova DD, Borowiec JA. **Stress-dependent nucleolin mobilization mediated by p53-nucleolin complex formation.** *Mol Cell Biol* 2002, 22 (16): 6014-6022.
156. Edwards TK, Saleem A, Shaman JA, Dennis T, Gerigk C, Oliveros E, Gartenberg MR, Rubin EH. **Role for nucleolin/Nsr1 in the cellular localization of topoisomerase I.** *J Biol Chem* 2000, 275 (46): 36181-36188.
157. Guichard SM, Danks MK. **Topoisomerase enzymes as drug targets.** *Curr Opin Oncol* 1999, 11 (6): 482-489 Review.
158. Thomas JO. **HMG1 and 2: architectural DNA-binding proteins.** *Biochem. Soc T* 2001, 29 (4): 395-401.
159. Bustin M. **Regulation of DNA dependent activity by the functional motifs of the high-mobility-group chromosomal proteins.** *Mol Cell Biol* 1999, 19 (8): 5237-5246.
160. Brezniceanu ML et al. **HMGB1 inhibit cell death in yeast and mammalian cells and is abundantly expressed in human breast carcinoma.** *FASEB J* 2003, 17 (10): 1295-1297.
161. Kawahara N et al. **Enhanced coexpression of thioredoxin and high mobility group protein1 genes in human hepatocellular carcinoma and the possible association with decreased sensitivity to cisplatin.** *Cancer Res* 1996, 56 (23): 53.

162. Yow H, Wong JM, Chen HS, Lee C, Steele GD Jr., Chen LB. **Increased mRNA expression of a laminin-binding protein in human colon carcinoma: complete sequence of a full-length cDNA encoding the protein.** Proc Natl Acad Sci USA 1998, 85: 6394-6398.
163. Wewer UM, Liotta LA, Jaye M, Ricca GA, Drohan WN, Claysmith AP, Rao CN, Wirth P, Coligan JE, Albrechtsen R, Mudryj M, Sobel ME. **Altered levels of laminin receptor mRNA in various human carcinoma cells that have different abilities to bind laminin.** Proc Natl Acad Sci USA 1986, 83: 7137-7141.
164. Pogo BG-T, Melana SM, Holland JF, Mandeli JF, Pilotti S, Casalini P, and Menard S. **Sequences homologous to the mouse mammary tumor virus env gene in human breast carcinoma correlate with overexpression of laminin receptor.** Clin Cancer Res 1999, 5 (8): 2108 - 2111.
165. Ozaki I, Yamamoto K, Mizuta T, Kajihara S, Fukushima N, Setoguchi Y, Morito F, and Sakai T. **Differential expression of laminin receptors in human hepatocellular carcinoma.** Gut 1998, 43 (6): 837 - 842.
166. Demianova M, Formosa TG, and Ellis SR. **Yeast Proteins Related to the p40/Laminin Receptor Precursor Are Essential Components of the 40 S Ribosomal Subunit.** J Biol Chem 1996, 271 (19): 11383-11391.
167. Szkanderova S, Hernychova L, Kasalova I, Vavrova J, Stulik J, Abend M, van Beuningen D. **Proteomic analysis of radiation-induced alterations in L929 cells.** Folia Biol (Praha) 2003, 49 (1): 15-25.
168. Sato T, Saito H, Swensen J, Olifant A, Wood C, Danner D, Sakamoto T, Takita K, Kasumi F, Miki Y, et al. **The human prohibitin gene located on chromosome 17q21 is mutated in sporadic breast cancer.** Cancer Res 1992, 52: 1643-1646.
169. Nijtmans LG, de Jong L, Artal Sanz M, Coates PJ, Berden JA, Back JW, Muijsers AO, van der Spek H, Grivell LA. **Prohibitins act as a membrane-bound chaperone for the stabilization of mitochondrial proteins.** EMBO J 2000, 19 (11):2444-51.
170. Steglich G, Neupert W, Langer T. **Prohibitins regulate membrane protein degradation by the m-AAA protease in mitochondria.** Mol Cell Biol 1999, 19(5):3435-42.
171. Johnsson A, Zeelenberg I, Min Y, Hilinski J, Berry C, Howell SB, and Los G. **Identification of genes differentially expressed in association with acquired cisplatin resistance.** Brit J Cancer 2000, 83 (8): 1047-1054.
172. Fusaro G, Wang S, Chellappan S. **Differential regulation of Rb family proteins and prohibitin during camptothecin-induced apoptosis.** Oncogene 2002, 21: 4539-4548.

173. McClung JK, Jupe ER, Liu XT, Dell'Orco RT. **Prohibitin: potential role in senescence, development, and tumor suppression.** *Exp Gerontol* 1995, 30(2):99-124.
174. Fraser M, Leung B, Jahani-Asl A, Yan XJ, Thompson WE, and Tsang BK. **Chemoresistance in human ovarian cancer: the role of apoptotic regulators.** *Reprod Biol Endocrin* 2003, 1: 66-78.
175. Planas-Silva MD, and Weinberg RA. **The restriction point and control of cell proliferation.** *Curr Opin Cell Biol* 1997, 9: 768-772.
176. Sherr C J. **Cancer cell cycles.** *Science* 1996, 274: 1672-1677.
177. Grabsch H, Takeno S, Parsons WJ, Pomjanski N, Boecking A, Gabbert HE, Mueller W. **Overexpression of the mitotic checkpoint genes BUB1, BUBR1, and BUB3 in gastric cancer—association with tumour cell proliferation.** *J Pathol* 2003, 200 (1): 16-22.
178. Feige U, Polla BS. **Heat shock proteins: the hsp70 family.** *Experientia* 1994, 50:979-976
179. Haas IG. **GRP78, an essential hspresident protein in the endoplasmic reticulum.** *Experientia* 1994, 1012-1020.
180. Moreno-Flores MT, Olazabal UE, Kreutzberg GW. **Axotomy increases the expression of glucose-regulated protein 78 kDa in rat facial nucleus.** *Exp Neurol* 1997, 146(1):10-6.
181. Shen J, Hughes C, Gessner T, Subjeck. **Coinduction of glucose-regulated proteins and doxorubicin resistance in Chinese hamster cells.** *Proc. Natl Acad Sci USA.* 1989, 4452-4459.
182. Chatterjee S, Cheng MF, Berger RB, Berger SJ, and Berger NA. **Effect of inhibitors of poly(ADP-ribose) polymerase on the induction of GRP78 and subsequent development of resistance to etoposide.** *Cancer Res* 1995 55: 868-873
183. Fernandez PM, Tabbara SO, Jacobs LK, Manning FC, Tsangaris TN, Schwartz AM, Kennedy KA, Patierno SR. **Overexpression of the glucose-regulated stress gene GRP78 in malignant but not benign human breast lesions.** *Breast Cancer Res Treat* 2000, 59(1):15-26.
184. Vladimir L. Gabai, Anatoli B. Meriin, Julia A. Yaglom, Vladimir Z. Volloch and Michael Y. Sherman. **Role of Hsp70 in regulation of stress-kinase JNK: implications in apoptosis and aging,** *FEBS Letters* 1998, 30: 1-4

185. Kiang JG, Gist ID, Tsokos GC. **Cytoprotection and regulation of heat shock proteins induced by heat shock in human breast cancer T47-D cells: role of [Ca<sup>2+</sup>]<sub>i</sub> and protein kinases.** FASEB J 1998, 12(14):1571-9.

186. Price ER, Zydowsky LD, Jin MJ, Baker CH, McKeon FD, Walsh CT. **Human cyclophilin B: a second cyclophilin gene encodes a peptidyl-prolyl isomerase with a signal sequence.** Proc Natl Acad Sci USA. 1991, 1; 88(5):1903-1907.

187. Le Hir M, Su Q, Weber L, Woerly G, Granelli-Piperno A, Ryffel B. **In situ detection of cyclosporin A: evidence for nuclear localization of cyclosporine and cyclophilins.** Lab Invest 1995, 73 (5):727-33.

188. Rycyzyn MA, Reilly SC, O'Malley K and Clevenger CV. **Role of Cyclophilin B in Prolactin Signal Transduction and Nuclear Retrotranslocation** Mol Endocrinol 2000, 14 (8): 1175-1186